IDENTIFICATION AND CHARACTERIZATION OF *AGROBACTERIUM TUMEFACIENS* VirD2-BINDING PROTEINS

GUO MINLIANG

NATIONAL UNIVERSITY OF SINGAPORE

2005

IDENTIFICATION AND CHARACTERIZATION OF *AGROBACTERIUM TUMEFACIENS* VirD2-BINDING PROTEINS

GUO MINLIANG

(M. Sc.)

A THESIS SUBMITTED

FOR THE DEDREE OF DOCTOR OF PHILOSOPHY

DEPARTMENT OF BIOLOGICAL SCIENCES

NATIONAL UNIVERSITY OF SINGAPORE

2005

Acknowledgements

First of all, my deepest gratitude goes to my supervisors, Professor Hew Choy Leong and Associate Professor Pan Shen Quan, not only for giving me the opportunity to undertake this interesting project but also for their patience, encouragement, practical and professional guidance throughout my Ph. D candidature. I sincerely thank my thesis committee members for their comments and suggestions during my thesis research.

Secondly, I would like to express my heartfelt gratitude to Dr Li Qingsong and Ms Wang Xianhui for their technical guidance in using mass spectrometry facility. I also thank Professor Charles Rosenberg, Laboratoire de Biologie Moleculaire des Relations Plantes-Microorganismes, C.N.R.S.-I.N.R.A., Groupement Scientifique Microbiologie Toulouse, France, for generously providing *Agrobacterium tumefaciens* GMI9017 strain and Associate Professor Jin Shouguang, University of Florida, USA, for the donation of plasmid pEX18Tc.

I would also like to thank the following laboratory members who have helped me in different ways: Tan Lu Wee, Chang Limei, Hou Qingming, Tang Hock Chun, Li Xiaobo, Qian Zhuolei, Sun Deying, Alan Lowton, Zhang Li, Tu Haitao and Seng Eng Khuan. I want to thank the friends from other laboratories who once helped me in a way or other.

Moreover, I must thank my wife and daughter for their enduring the hardships of family separation for four years.

Finally, I gratefully acknowledge the financial support provided by the National University of Singapore.

Contents

Manuscripts Related to This Study

1) Guo M.L., Hou Q.M., Hew C.L., and Pan S.Q. (2005) *Agrobacterium* VirD2-binding protein is encoded by three functionally redundant homologs and involved in tumorigenesis. *Journal of Bacteriology* (Submitted).

2) Guo M.L., Hew C.L., and Pan S.Q. (2005) Recruiting protein for conjugal DNA transfer: *Agrobacterium* VirD2-binding protein VBP recruits nucleoprotein substrate to type IV secretion system. *Science* (Submitted).

List of Figures

List of Tables

List of Abbreviations

Amp	ampicillin
AS	acetosyringone
bp	base pair(s)
BSA	bovine serum albumin
DMF	N,N-dimethylformamide
DMSO	dimethylsulfoxide
dsDNA	double-stranded DNA
Dtr	DNA transfer and replication system
DTT	dithiothreitol
EB	ethidium bromide
EDTA	ethylenediaminetetraacetic acid
g	grams or gravitational force, according to the intended meaning
GUS	β-D-glucuronidase
h	hour(s)
His-VBP	His-tagged VBP fusion protein
HRP	horseradish peroxidase
IPTG	isopropyl-β-D-thiogalactoside
kDa	kilodalton(s)
Km	kanamycin
MALDI	matrix-assisted laser desorption/ionization
MBP	maltose-binding protein
MBP-C-VirD2	MBP-VirD2 C-terminus fusion protein
MCS	multiple cloning site(s)
MES	2-[N-morpholino] ethanesulfonic acid
MOWSE	molecular weight search
Mpf	mating pair formation system
MS	mass spectrometer
NCBI	National Center for Biotechnology Information
NLS	nuclear localization signal
ORF	open reading frame
PAGE	polyacrylamide gel electrophoresis
PMSF	phenylmethylsulfonyl fluoride
Q-TOF	quadrupole-time of flight
R	resistant/resistance
RNase	ribonuclease
rpm	revolutions per minute
s	sensitive/sensitivity
SDS	sodium dodecyl sulfate
ssDNA	single-stranded DNA
T4SS	type IV secretion system
T-DNA	transferred DNA
TOF	time of flight
Tra	conjugal transfer system
UV	ultraviolet
VBP	VirD2-binding protein
vir	virulence
V/V	volume per volume
w/v	weight per volume

Summary

Agrobacterium tumefaciens uses a mechanism similar to plasmid conjugation to transfer its oncogenic T-DNA to a plant cell. During *Agrobacterium*-mediated T-DNA transfer to plant cells, VirD2 plays an important role in guiding the transfer of T-complex composed of single-stranded T-DNA, VirD2 and VirE2. We used the VirD2 protein as an affinity ligand to isolate VirD2-binding protein(s). By using pull down assay and peptide-mass-fingerprinting match, we identified an *A. tumefaciens* protein that can specifically bind VirD2. This VirD2-binding protein is designated VBP1.

Genome-wide sequence analysis showed that *A. tumefaciens* has two additional genes highly homologous to *vbp1*; they are designated *vbp2* and *vbp3*. Like VBP1 both VBP2 and VBP3 could bind VirD2 specifically. Mutational analysis of *vbp* genes demonstrated that the three *vbp* genes could functionally complement each other. Consequently, only inactivation of all three *vbp* genes highly attenuated the bacterial ability to cause tumors on plants. All the VBP proteins possessed a putative nucleotidyltransferase motif in their N-termini and a putative higher eukaryotes and prokaryotes nucleotide-binding (HEPN) domain in their C-termini. The predicted amino acid numbers of three VBP proteins are 313, 311 and 308, respectively. Although *vbp1* is harbored on the cryptic plasmid AT, *vbp2* and *vbp3* reside on the linear chromosome. The loci of *vbp2* and *vbp3* on the linear chromosome are close to each other.

The interaction between VBP1 and VirD2 was shown to be specific and strong. The presumable VirD2-T-strand-VirE2 complex could be pulled down by VBP1 from AS-induced *A. tumefaciens* cell extract. By using co-immunoprecipitation, we confirmed that

the presumable VirD2-T-strand-VirE2 complex exists in the *A. tumefaciens* cell extract. To gain an insight into VBP biochemical function, we analyzed the functions of genes adjacent to *vbp2* and *vbp3*. It was found that the gene organization of the region between *vbp2* and *vbp3* is similar to a DNA transfer and replication (Dtr) system. VBP proteins are most likely auxiliary proteins of T-DNA processing nucleoprotein complex, which is also known as relaxosome. The redundancy of three homologs for the VirD2-binding protein indicates a conserved function that is important for the gene transfer.

On the other hand, the T-complex is exported out of the bacterial cell by a type IV secretion system (T4SS) composed of VirB proteins. VBP proteins were used to pull down the T4SS components. Both the pull-down and co-immunoprecipitation experiments showed that VBP1 interacts with VirD4, VirB4 and VirB11. VBP proteins were demonstrated to be cytoplasmic proteins. VBP proteins can bind both T-complex and T4SS transporter specifically; and the *vbp* triple mutant has a highly attenuated ability to cause tumors on plants. This suggests that VBP recruits the T-complex to the transport site, thus coupling the two events in the conjugal transfer. It was shown that VBP protein is also involved in the conjugation of some plasmids. Therefore, our work defined VBP proteins as a new class of proteins that are responsible for recruiting proteins that can in turn recruit the cytoplasmic DNA transfer intermediate to the membrane transporter.

Chapter 1 Literature Review

1.1. Introduction

1.1.1. Chronicle and importance of *Agrobacterium tumefaciens* research

Agrobacterium tumefaciens is a soil phytopathogen. It causes the crown gall disease of dicotyledonous plants, which is characterized by a tumorous phenotype. The first paper that identified *A. tumefaciens* as the causal agent of crown gall disease was published in 1907 (Smith and Townsend, 1907). This organism is capable of inducing tumors at wound sites on the stems, crowns and roots of hundreds of dicotyledonous plants. At the beginning of the last century, crown gall disease was considered a major problem in horticultural production. This disease caused significant reduction of crop yield in many perennial horticultural crops (Kennedy, 1980), such as grape (Schroth *et al.*, 1988), apple (Ricker *et al.*, 1959), and cherry (Lopatin, 1939). All these horticultural crops are woody species and propagated by grafting scions onto rootstocks. The grafting causes wounds that are usually covered by soil and thus provides an excellent infection point for *A. tumefaciens* cells. In 1941, White and Braun demonstrated that crown gall tumor tissue could be permanently transformed by only transient exposure to the pathogen of *A. tumefaciens* (White and Braun, 1941). Thereafter, they proposed that a 'tumor-inducing capacity' was transmitted from *A. tumefaciens* to plant tissue (Braun, 1947; Braun and Mandle, 1948). However, the transformation principle remained elusive until the advent of molecular techniques that provided the first evidence that crown gall tumors, cultured axenically, contained DNA of *A. tumefaciens* origin (Schilperoort *et al.*, 1967). In 1974, the tumor-inducing (Ti) plasmid was identified to be essential for the

crown gall-inducing ability (Van Larebeke *et al*., 1974; Zaenen *et al*., 1974). Southern hybridization turned out to prove that the bacterial DNA, which encodes genes responsible for both the tumor formation and the opine production, originates from the Ti plasmid and ultimately resulted in the discovery of T-DNA (transferred DNA), specific segments transferred from *A. tumefaciens* to plant cells (Chilton *et al*., 1977; Chilton *et al*., 1978; Depicker *et al*., 1978). The T-DNA is referred to as the T-region when located on the Ti-plasmid. The T-region is delimited by 25-bp directly repeated sequences, which are called T-DNA border sequences. The T-DNAs, when transferred to plant cells, encode enzymes for the synthesis of the plant hormones auxin and cytokinin and strain-specific low molecular weight amino acid and sugar phosphate derivatives called opines. The massive accumulation of auxin and cytokinin in transformed plant cells causes uncontrolled cell proliferation and the synthesis of nutritive opines that can be metabolized specifically by the infecting *A. tumefaciens* strain. Thus, the opine-producing tumor effectively creates an ecological niche specifically suited to the infecting *A. tumefaciens* strain (for reviews see Escobar and Dandekar, 2003; Hooykaas and Schilperoort, 1992). Besides the T-DNAs, Ti-plasmid also contains most of the genes that are required for the transfer of the T-DNAs from *A. tumefaciens* to the plant cell.

Initial study of these plant tumors was intended to reveal the molecular mechanism that may be relevant to animal neoplasia. Although no relationship was found between animal and plant tumors, *A. tumefaciens* and plant tumor were proved to be of intrinsic interest because the tumorous growth was shown to result from the transfer of T-DNA from bacterial Ti-plasmid to the plant cell and the stable integration of the T-DNA to plant genome. The demonstration that wild-type T-DNA coding region can be replaced

by any DNA sequence without any effect on its transfer from *A. tumefaciens* to the plant inspired the promise that *A. tumefaciens* might be used as gene vector to deliver genetic material into plants. In the early of 1980's, two events about *A. tumefaciens* mediated T-DNA transfer signaled the beginning of the era of plant genetic engineering. First, the Ti-plasmid in *A. tumefaciens* was used as a gene vector system to produce the first transgenic plant (Zambryski *et al*., 1983). The healthy transgenic plants had the ability to transmit the disarmed T-DNA, including the foreign genes, to their progeny. Second, non-plant antibiotic-resistance genes, for example, a bacterial kanamycin-resistance gene, could be driven by a plant-active promotor to function efficiently in plant cells. This enabled accurate selection of transformed plant cells (Beven, 1984). The eventual success of using *A. tumefaciens* as a gene vector to create transgenic plants was viewed as a prospect and a "wish". The future of *A. tumefaciens* as a gene vector for crop improvement began to look bright. During the 1990's, maize, a monocot plant species that was thought to be outside the *A. tumefaciens* "normal host range", was successfully transformed by *A. tumefaciens* (Chilton, 1993). Today, many agronomically and horticulturally important plant species are routinely transformed using *A. tumefaciens*, and the list of plant species that can be genetically transformed by *A. tumefaciens* seems to grow daily (for review see Gelvin, 2003). At present, many economically important crops, such as corn, soybeans, cotton, canola, potatoes, and tomatoes, were improved by *A. tumefaciens*–mediated genetic transformation and their transgenic varieties are growing worldwide (Valentine, 2003). Recently, the species that is susceptible to *A. tumefaciens*–mediated transformation was broadened to yeast (Piers *et al*., 1996), fungi (Groot *et al*., 1998), and mammalian cells (Kunik *et al*., 2001).

In addition to the technical application as a gene vector to create transgenic plants, *A. tumefaciens* also provides a fascinating model system to study the wide variety of biological processes, including bacterial detection of host signaling chemicals (Winans, 1992), intercellular transfer of macromolecules (Christie, 2001), importing of nucleoprotein into plant nuclei (Ziemienowicz *et al*., 2001), and interbacterial chemical signaling via autoinducer-type quorum sensing (Newton and Fray, 2004).

1.1.2. Basic process of *A. tumefaciens*–mediated T-DNA transfer

The process of *A. tumefaciens*–mediated T-DNA transfer consists of several critical steps: (1) Sensing of plant chemical signals and inducing of virulence (vir) proteins. The chemical signals released by wounded plant are perceived by a VirA/VirG two-component system of *A. tumefaciens*, which leads to the transcription of virulence (vir) gene promoters and thus the expression of vir proteins. (2) T-DNA processing. T-DNA is nicked by VirD2/VirD1 from the T-region of Ti plasmid and forms a single-stranded linear T-strand by strand displacement; the T-strand is coated by VirE2 molecules along the entire T-strand length and forms a T-complex. (3) Attaching of *A. tumefaciens* to plant and transferring of T-complex to plant cell. *A. tumefaciens* cell attaches to plant and transfers the T-complex from *A. tumefaciens* to plant cell by a VirD4/B T4SS transport system. (4) Targeting of T-complex to plant cell nucleus and integrating of T-DNA into plant genome. The T-complex is transported into the nucleoplasm under the assistance of some host proteins and then integrated into plant genomic DNA. (5) Expressing of T-DNA in plant cell and inducing of plant tumor. The T-DNA genes encode phytohormone synthases that lead to the uncontrolled proliferation of plant cell and opine synthases that

provide nutritive compounds to infecting bacteria. The basic steps of *A. tumefaciens*-mediated T-DNA transfer are summarized in Fig. 1.1.

1.2. Sensing of Plant Signal Molecules and *vir* Gene Induction

1.2.1. Chemotaxis of *A. tumefaciens*

A. tumefaciens is a motile organism with peritrichous flagellae and possesses a highly sensitive chemotaxis system. It could respond to a range of sugars and amino acids and was attracted to these sugars and amino acids (Loake *et al*., 1988). *A. tumefaciens* mutants deficient in motility and in chemotaxis were fully virulent when inoculated directly, but when used to inoculate soil, which was air-dried and then to used to grow plants, these mutants were completely avirulent, indicating that the motility and chemotaxis is critical to *A. tumefaciens* infection under natural conditions (Hawes and Smith, 1989). Wild-type *A. tumefaciens* strains both containing and lacking Ti plasmid exhibited chemotaxis toward excised root tips from all plant species tested and toward root cap cells of pea and maize, suggesting that the majority of chemotactic responses in *A. tumefaciens* appear to be chromosomally encoded (Loake *et al*., 1988; Parke *et al*., 1987). However, the chemotactic response to some phenolic compounds, for example acetosyringone, which were identified as strong *vir* gene inducers, is controversial. Some reports showed that chemotaxis toward acetosyringone requires the presence of a Ti plasmid, specifically the regulatory genes *virA* and *virG*, and occurs with a threshold sensitivity of $< 10^{-8}$ M, 1000-fold below the maximal *vir*-inducing concentration (Ashby *et al*., 1988; Shaw *et al*., 1989). Whereas, reports from other groups indicated that acetosyringone did not elicit chemotaxis at any concentrations (Hawes and Smith, 1989)

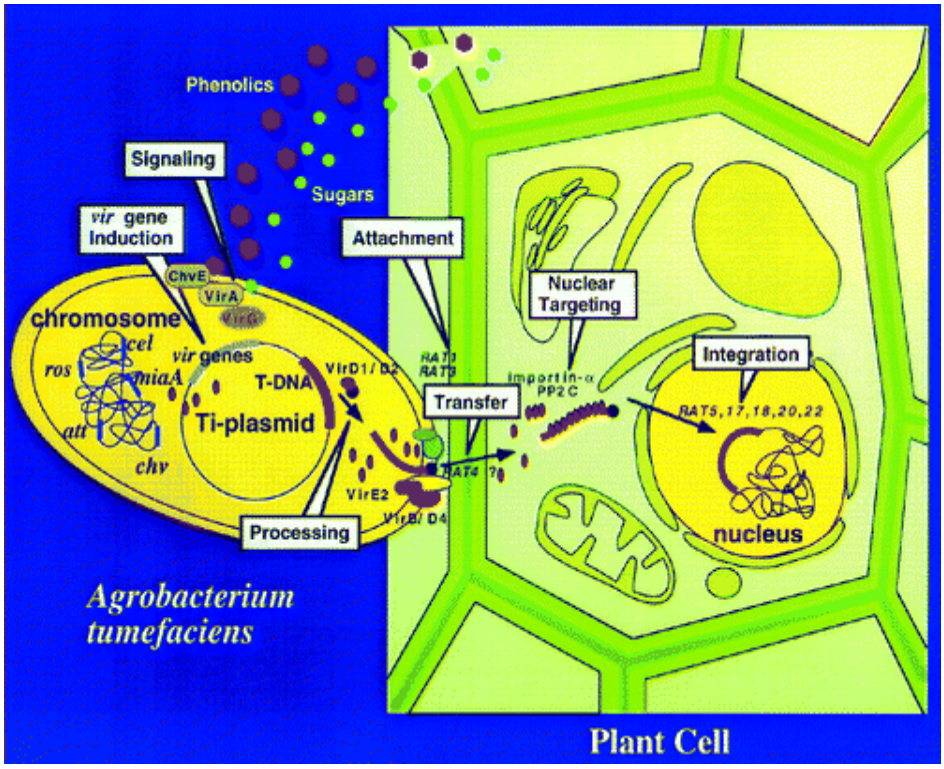

Fig. 1.1. Basic steps of the *Agrobacterium* infection process. Critical steps that occur to or within the bacterium (chemical signaling, *vir* gene induction, and T-DNA processing) and within the plant cell (bacterial attachment, T-DNA transfer, nuclear targeting, and T-DNA integration) are highlighted, along with genes and/or proteins known to mediate these events (Cited from Gelvin, 2000).

and chemotaxis toward related compounds did not require the Ti plasmid (Park *et al*., 1987). So, it does seem difficult to rationalize a role for acetosyringone and the regulatory genes *virA* and *virG* in chemotaxis.

1.2.2. *vir* gene induction

Many genes are involved in *A. tumefaciens*-mediated T-DNA transfer, but most of the genes required for T-DNA transfer are found on the *vir* region of Ti plasmid. This *vir* region comprises at least six essential operons (*virA*, *virB*, *virC*, *virD*, *virE*, and *virG*,) and two non-essential operons (*virF* and *virH*) encoding approximate 25 proteins. These proteins are termed virulence (vir) proteins and required for the sensing of plant signal molecules as well as the processing, transfer, nuclear localization, and perhaps integration of T-DNA into the plant genome. The protein number encoded by each operon differs, *virA*, *virG* and *virF* encode only one protein; *virE*, *virC*, and *virH* encode two proteins; *virD* encodes four proteins and *virB* encodes eleven proteins. Only *virA* and *virG* are constitutively expressed. The transcription of all other *vir* operons is coordinately induced during infection by a family of host-released phenolic compounds in combination with some monosaccharides and extracellular acidity in the range of pH 5.0 to 5.8. Virtually all of the genes in the *vir* region are tightly regulated by two proteins VirA and VirG encoded by *virA* operon and *virG* operon.

The inducible expression of *vir* operons was first found by using the cocultivation of *A. tumerfaciens* with mesophyll protoplasts, isolated plant cells or cultured tissues (Stachel *et al*., 1986). In vegetatively growing bacteria, only *virA* and *virG* are expressed at significant level. However, when *Agrobacteria* are cocultivated with the susceptible

plant cells, the expression of *virB*, *virC*, *virD*, *virE* and *virG* becomes induced to high levels (Engstrom *et al*., 1987). The partially purified extracts of conditioned media that are from root cultures can also induce the expression of *vir* operons, demonstrating that the *vir*-inducing factors are some diffusible plant cell metabolites. By screening 40 plant-derived chemicals, Bolton *et al* (1986) identified seven simple plant phenolic compounds that possess the *vir*-inducing activity. Most of these *vir*-inducing phenolic compounds are needed to make lignin, a plant cell wall polymer. The best characterized and most effective *vir* gene inducers are acetosyringone (AS) and hydroxy-acetosyringone from tobacco cells or roots (Stachel *et al*., 1985). The specific composition of phenolic compounds secreted by wounded plants is thought to underlie the host specificity of some *Agrobacterium* strains (Sheng and Citovsky, 1996).

When plant phenolic compounds are absent or present in low concentrations, specific monosaccharides, such as glucose, arabinose, galactose, xylose and fucose, may play a central role in *vir* gene induction. All these sugars significantly increase *vir* gene expression when acetosyringone (AS) is limited or absent. Some nonmetabolizable sugars, for example 2-deoxy-D-glucose and 6-deoxy-D-glucose, can also upregulate *vir* gene expression, demonstrating that the enhancement of *vir* gene expression does not result from nutritional benefits to *Agrobacterium*. Indeed, the regulatory pathway for *vir* gene induction by sugars is different from the pathway for induction by phenolics. This process is mediated by a chromosomal gene encoding the protein ChvE, a homolog of the *Escherichia coli* sugar-binding proteins (Cangelosi *et al*., 1990). The subsequent studies showed that most of the *vir*-inducing sugars are monomers of plant cell wall polysaccharides and were therefore postulated to be exuded from a wide variety of plant

wounds. The most potent sugar inducers are the acidic sugars D-glucuronic acid and D-galacturonic acid.

The induction of *vir* genes also depends on external factors such as pH and temperature. Acidic pH is thought to be a third environmental signal of central importance in *vir* gene induction. The induction requires extremely low pHs, a range of 5.0 to 5.5, and does not occur at neutral pH. The underlying mechanism by which pH regulates the *vir* gene induction remains unclear. One hypothesis is that acidic pH may protonate phenolic compounds, which would increase their membrane permeability. The *vir* genes cannot be induced at temperatures higher than 32 ºC because high temperature may induce the conformational change of VirA and thus inactivates its regulating properties (Jin *et al*., 1993).

1.2.3. Regulation of *vir* gene induction

The regulatory pathway for *vir* gene induction by phenolic compounds is mediated by the VirA/VirG two-component system, which has structural and functional similarities to other already described for other cellular mechanisms (Bourret *et al*., 1991; Nixon *et al*., 1986). The presence of acidic environment and phenolic compounds at a plant wound site may directly or indirectly induce autophosphorylation of VirA. VirA is a transmembrane receptor kinase. The phosphorylated VirA can transfer its phosphate to the cytoplasmic VirG to activate VirG. The activated VirG binds to sequences called *vir* box enhancer elements that are found in the promoters of the *virA*, *virB*, *virC*, *virD*, *virE* and *virG* operons, and then upregulates the transcription of these operons (Winans 1992).

Octopine-type Ti plasmid encoded VirA protein has 829 amino acids. Based on protein sequence similarities, VirA is a member of the histidine protein kinase class. VirA has been proved to be a kinase and able to autophosphorylate. When VirA autophosphorylates *in vitro*, the phosphate was found to bind to histidine residue 474, a histidine residue that is absolutely conserved among homologous proteins (Jin *et al*., 1990). VirA protein can be structurally divided into a number of domains. In an order from N-terminus to C-terminus, these domains are defined as transmembrane domain 1 (TM1), periplasmic domain, transmembrane domain 2 (TM2), linker domain, kinase domain and receiver domain (Lee *et al*., 1996). Two transmenbrane domains TM1 and TM2 serve to anchor VirA protein into the cytoplasmic membrane. TM1 and TM2 are supposed to play a role in maintaining the conformation of the periplasmic domain. The periplasmic domain is required for the interaction with ChvE, the sugar-binding protein that responds to the *vir*-inducing sugars. The linker domain is located on the region of amino acid 280~414. This region was supposed to interact with the *vir* gene inducing phenolic compounds. The evidence that deleting the periplasmic domain still allowed *vir* gene induction by phenolic compounds whereas the deletion of the linker domain eliminated the induction by this class of chemical confirmed the central role of the linker domain in detecting phenolic inducers (Chang and Winans 1992). A highly amphipathic helix sequence of 11 amino acids was identified in the region of amino acid 278-288. This amphipathic sequence is highly conserved in a large number of chemoreceptor proteins and thus was supposed to be the receptor site for phenolic inducers (Turk *et al*., 1994). However, it is unclear whether the phenolic inducers interact with VirA directly or indirectly. The kinase domain is a highly conserved domain that presents in the family of

the sensor proteins and contains the conserved histidine residue 474 that is the autophosphorylation site. Site-directing mutation of this His 474 results in avirulence and the lost of *vir* gene inducing expression in the presence of plant signal moleculaes (Jin *et al*., 1990). The receiver domain shows an unusual feature that is homologous to a region of VirG. Similar receiver domains are present in a small number of homologous histidine protein kinases, but the function of this domain is unclear.

VirG is a cytoplasmic protein of 241 amino acid residues, which is homologous over its entire length to a family of regulatory proteins (Miller *et al*., 1989). It is now known that VirG is a transcriptional activator. VirG is composed of two main domains, N-terminal domain and C-terminal domain. The aspartic acid 52 in the N-terminal domain of VirG can be phosphorylated by the phosphorylated VirA. The phosphorylation of N-terminal domain is thought to induce the conformation change of C-terminal domain. The C-terminal domain of VirG possesses the DNA-binding function. VirG can specifically bind to the *vir* box sequence that is found within 80 nucleotides upstream from the transcription initiation sites of *vir* genes. Phosphorylation is required for the transcriptional activation function of VirG, but how phosphorylation modulates the properties of VirG is unknown. Some models suggested that phosphorylation might increase the affinity of VirG to its binding sites or promote the ability of VirG to contact RNA polymerase.

1.3. T-DNA Processing

1.3.1. T-region in Ti plasmid

The activation of *vir* genes initiates a cascade of events. Following the expression of *vir* genes, some Vir proteins produce the transfer intermediate, a linear single stranded (ss) DNA called T-DNA or T-strand. The T-strand is derived from the bottom (coding) strand of the T-region of the Ti plasmid and is found at approximately one copy per induced *Agrobacterium* cell (Stachel *et al*., 1986b). The T-strand production is believed to initiate at the right T-DNA border and elongate in a 5′ to 3′ direction (Sheng and Citovsky, 1996). The right T-DNA border is required for efficient tumorigenesis and acts in a polar fashion, directing the transfer of sequences to its left (Shaw *et al*., 1984; Wang *et al*., 1984), whereas, the left T-DNA border is dispensable for tumor formation (Joos *et al*., 1983). An enhancer (or overdrive) sequence is found to present near many T-DNA right borders, but not left borders. Overdrive sequences enhance the transfer efficiency (Peralta *et al*., 1986; Peralta and Ream, 1985). The shift of overdrive sequences within 5 kb of the right border and the inversion of its orientation do not disrupt its function (Wang *et al*., 1987).

1.3.2. Roles of VirD2/VirD1 in T-DNA processing

The T-strand is produced by the cleavage of VirD2/VirD1 on the bottom strand of T-region at identical positions between bp 3 and 4 from the left end of each border (Albrigt *et al*., 1987; Jayaswal *et al*., 1987; Wang *et al*., 1987b). Double-stranded breaks have also been observed at this position although these breaks may result from the shearing of nicked DNA during isolation (Steck *et al*., 1989; Veluthambi *et al*., 1987). *In vitro*, purified VirD2 alone can cleave a single-stranded T-DNA border sequence (Jasper *et al*., 1994; Pansegrau *et al*., 1993), indicating that VirD2 possesses nickase activity. For the cleavage of double-stranded border sequences, research data obtained both *in vivo*

(Filichkin and Gelvin 1993; Yanofsky *et al*., 1986) and *in vitro* (Scheiffele *et al*., 1995) revealed that both VirD1 and VirD2 are required. After cleavage of T-DNA border sequence, VirD2 remains associated with the 5′-end of the ssT-strand covalently. The excised ssT-strand is removed, and the resulting single-stranded gap in the T-region is repaired, which is most likely replaced by a newly synthesizing DNA strand. The association of VirD2 with the 5′-end of the ssT-strand is believed to prevent the exonucleolytic attack to the 5′-end of the ssT-strand (Durrenberger *et al*., 1989) and to distinguish the 5′-end as the leading end of the T-DNA complex during transfer. The VirD2-catalyzed cleavage of T-DNA border sequence is dependent on the presence of Mg^{2+}. The oligonucleotide cleavage catalyzed by VirD2 is an equilibrium reaction that allows specific linkage of cleavage products. VirD2 site-direct mutations indicated that the tyrosine 29 is required for the association of VirD2 with the 5′-end of T-strand (Vogel and Das, 1992).

One report indicated that VirD1 possesses a topoisomerase-like activity (Ghai and Das, 1989). VirD1 appears to be a type I DNA topoisomerase that do not require ATP for activity. However, another study (Scheiffele *et al*., 1995) contradicted this conclusion. The VirD1 protein purified by Scheiffele *et al* (1995) never showed any topoisomerase activity. It was speculated that the topoisomerase activity observed by Ghai and Das (1989) might originate from VirD2. Mutational study of VirD1 showed that a region from amino acids 45~60 is important for VirD1 activity (Vogel and Das, 1994). Sequence comparison of this fragment with the functionally analogous proteins of conjugatable bacterial plasmids showed that this region is a potential DNA-binding domain (Vogel and Das, 1994).

The nopaline Ti plasmid encoded VirD2 consists of 447 amino acids with a molecular weight of 49.7 kDa. Deletion analysis of VirD2 demonstrated that the C-terminal 50% of VirD2 could be deleted or replaced without affecting its endonuclease activity. Sequence comparison of VirD2 from different *Agrobacterium* species shows that the N-terminus is highly conserved with 90% homology, whereas only 26% homology is found in the C-terminus (Wang *et al*., 1990). A sequence comparison of VirD2 protein with its functionally homologous proteins in bacterial conjugation and in rolling circle replication revealed that a conserved 14-residue motif lies in the residues 126~139 of VirD2. This motif contains the consensus sequence HxDxD(H/N)uHuHuuuN (invariant residues in capital letters; x, any amino acid; u, hydrophobic residue) (Ilyina and Koonin, 1992). Mutational analysis indicated that all the invariant residues except for the last asparagine (N) in this motif are important for the endonuclease activity of VirD2. The second aspartic acid (D) and three nonconserved residues in this motif are also essential for the endonuclease activity of VirD2 (Vogel *et al*., 1995). This motif is believed to coordinate the essential cofactor Mg^{2+} by the two histidines in the hydrophobic region of the motif (Ilyina and Koonin, 1992). The poorly conserved C-terminal halves of VirD2 from different *Agrobacterium* species displayed a very similar hydropathy profile (Wang *et al*., 1990). The C-terminal domain of VirD2 is thought to guide the T-complex to the plant nucleus. The sequence characterization and function of this region of VirD2 will be discussed in a late section of this chapter.

1.3.3. Roles of VirC1 and VirC2 in T-DNA processing

Besides VirD2 and VirD1, two additional virulence (Vir) proteins VirC1 and VirC2 were also suggested to be involved in the T-DNA processing. VirC1 and VirC2 have

been shown to bind to the overdrive site of octopine-type Ti plasmid and were supposed to enhance T-DNA border cleavage by the VirD1/VirD2 endonuclease (Toro *et al*., 1989). Deletion of both VirC proteins does not abolish virulence, but attenuates virulence about 100-fold, which is about the same level attenuated by the deletion of overdrive sequence. It should be noted that a strain containing both a *virC* deletion and an overdrive deletion is no more deficient in tumor formation than a strain containing only one of these two deletions (Ji *et al*., 1988). However, some reports showed that mutation of both *virC1* and *virC2* genes resulted in the loss of virulence on many plant species, indicating that VirC proteins are important for virulence (Stachel and Nester, 1986). Several reports indicated that T-strand production of *Agrobacterium virC* mutant strains occurs at wild-type levels (Stachel *et al*., 1986b; Veluthambi *et al*., 1987), suggesting that the VirC proteins may play a role after T-DNA processing, possibly in T-DNA export (Zhu *et al*., 2000). No more virulence proteins are identified to be involved in the T-DNA production. Because so few plant-induced *Agrobacterium* proteins are necessary for T-DNA production, many reports speculated that some bacterial housekeeping proteins or enzymes of DNA repair and replication, such as helicase, may also be involved in this process (Jasper *et al*., 1994; Pansegrau *et al*., 1993; Scheiffele *et al*., 1995; Sheng and Citovsky, 1996).

1.3.4. VirE2 and its roles in protecting ssT-strand from nucleolytic degradation

Single-stranded T-DNA is believed to be susceptible to nucleases. The action of cellular nucleases will result in the nucleolytic degradation of T-strand and thus the loss of genetic information on the T-DNA. An effective way to protect the T-strand from nucleolytic degradation is to make it inaccessible to these nucleases. VirE2 is a single-stranded DNA-binding protein (Christie *et al*., 1988; Citovsky *et al*., 1988) that can bind

single-stranded DNA without sequence specificity; the binding is strong and co-operative, suggesting that VirE2 coats the T-strand along its length (Citovsky *et al*., 1989). Another possible function of VirE2 is to guide the nuclear import of T-DNA (Ziemienowicz *et al*., 1999; 2001). This will be discussed in the following section of this chapter. Induced *Agrobacterium* cell can produce sufficient VirE2 to bind all intracellular single-stranded T-DNA. When bound to single-stranded DNA, VirE2 can alter the ssDNA from a random-coil conformation to a telephone cord-like coiled structure and increases the relative rigidity (Citovsky *et al*., 1997). Initial hypothesis is that the protective role of VirE2 is required to function in both bacteria and plant cells. So, the prevailing view on the T-DNA transfer is that a packaged nucleoprotein complex, the T-complex, composed of the T-strand DNA containing the 5′-associated VirD2 and coated with VirE2 along its length, is the transfer intermediate (Howard and Citovsky, 1990; Zupan and Zambryski, 1995). This T-complex structure model implies that both VirD2 and VirE2 together with the T-strand are transported into plant cell at the same time. This idea makes biological sense because it is likely that VirE2 with a high affinity to ssDNA (Citovsky *et al*., 1989) may form a complex with the T-strand present inside *Agrobacterium* cell, especially if both VirE2 and the T-strand are transported through the same channel (Binns *et al*., 1995). Indeed, the T-complex, which contains T-strand, VirD2 and VirE2, was observed in the crude extracts from *vir*-induced *Agrobacterium* by using anti-VirE2 antibodies to co-immunoprecipitate both T-strand and VirE2 (Christie *et al*., 1988). A model for the formation of T-complex is shown in Fig. 1.2.

However, two kinds of evidence argued against that the protective role of VirE2 is required to function inside bacterial cells. The first is the observation that a strain

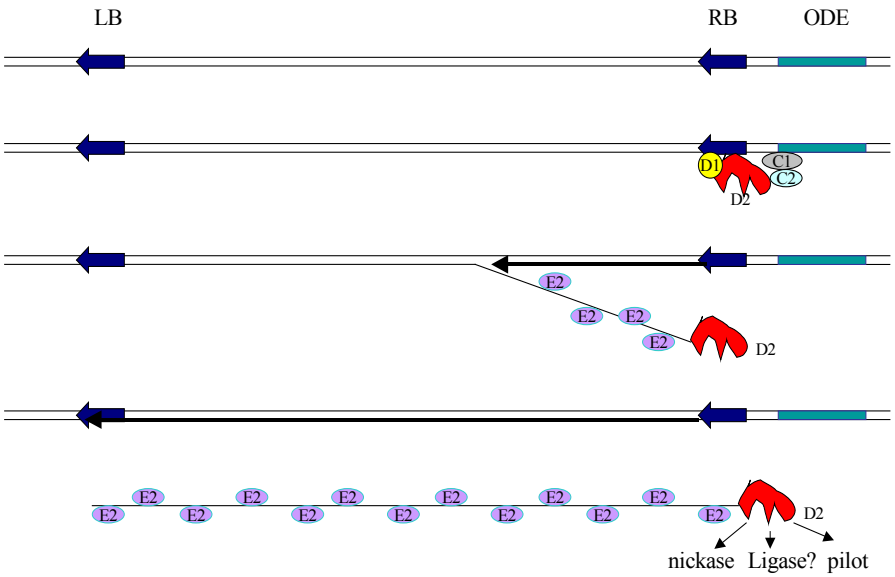

Fig. 1.2. Proposed mechanism of ssT-DNA processing and packaging. LB, RB, and ODE stand for the left border, right border, and overdrive sequences, respectively. Thick arrows indicate newly synthesized DNA that could displace the bottom strand of T-DNA. C1, C2, D1, D2, and E2 represent VirC1, VirC2, VirD1, VirD2, and VirE2 proteins, respectively.

expressing *virE2* but lacking T-DNA can complement a *virE2* mutant in a tumor formation assay (Otten *et al*., 1984) and the T-strand accumulates to wild-type levels in *virE2* mutants (Stachel *et al*., 1987; Veluthambi *et al*., 1988). The second kind of evidence is that *virE2* expression in transgenic tobacco plants restores the infectivity of a VirE2-deficient *Agrobacterium* strain (Citovsky et al., 1992). In addition, the observation that *virE2* mutants can transfer T-DNA into plant cells (Yusibov *et al*., 1994) also proved that VirE2 is not essential for the export of T-DNA. All these data appear to support that T-DNA may not be packaged by VirE2 in the bacterial cells, at least, the packaging of T-DNA inside bacterial cells by VirE2 is not necessary for the tumor formation. This question will be further discussed in the section of T-DNA transfer.

1.3.5. VirE1 may regulate the binding of VirE2 to T-strand

Another protein encoded by *virE* oporen is VirE1 with a molecular weight of 7 kDa. Protein sequence analysis of the VirE1 revealed that VirE1 shares a number of properties with molecular chaperones that are involved in the protein transport (Deng *et al*., 1999). VirE1 also possesses the structural characteristics of a molecular chaperone (Wattiau *et al*., 1996), being a small (7 kDa), acidic (pI = 5.0) protein with a dimerization domain (Deng *et al*., 1999; Vergunst *et al*., 2003). Mutational analysis of *virE1* showed that *virE1* is essential for the export of VirE2 to plant (Binns *et al*., 1995). A VirE1-deficient mutant having normal amounts of VirE2 and T-strand is not infectious, however, the VirE1-deficient mutant can be complemented by the coinfection with a strain producing both VirE1 and VirE2 but lacking T-DNA, indicating that the VirE1 assists the export of VirE2 but not of T-strands or VirE1 can be exported independently (Sundberg *et al*., 1996). *In vitro*, VirE1 can bind VirE2 strongly and prevent VirE2 from self-aggregation.

Analysis of various *virE2* deletions showed that the VirE1 binding domain of VirE2 overlaps the VirE2 self-interaction domain (Deng *et al*., 1999). The VirE1 binding domain of VirE2 is further proved to be the same domains that required for single-stranded DNA binding and cooperative interaction (Sundberg and Ream, 1999) implying that VirE1 can prevent VirE2 from binding to T-strand. The VirE1 binding domain of VirE2 lies in the N-terminal domain (Zhao *et al*., 2001). VirE1 interacts with VirE2 to form a VirE1-VirE2 complex with a predicted 2:1 stoichiometry (Zhao *et al*., 2001). Deletion of *virE1* did not affect transcription but decreased translation of *virE2*, indicating that *virE1* regulates efficient *virE2* translation in the context of expression from the native P_{virE} promoter (Zhao *et al*., 2001). Recent results show that VirE1 is not essential for the recognition of the translocation signal of ViE2 by the transport machinery and the subsequent translocation of VirE2 into plant cells, indicating that the role of VirE1 playing in the export process of VirE2 seems restricted to the stabilization of VirE2 by preventing VirE2 from the premature interactions in the bacterial cell before translocation into plant cells (Vergunst *et al*., 2003).

1.4. Attachment of *A. tumefaciens* to Plant

1.4.1. Bacterial genes involved in the attachment of *A. tumefaciens* to plant

For the transfer of T-complex into plant cells, *A. tumefaciens* must contact the plant and attach to the plant cells. The binding of *A. tumefaciens* to host plant cells seems to require the participation of specific receptors that may exist on the bacterial and plant cell surface because the binding of *A. tumefaciens* to host plant cells is saturable and unrelated bacteria fail to inhibit the binding of *A. tumefaciens* to host plant cells

(Lippincot and Lippincot, 1969). A number of *A. tumefaciens* mutants affecting the attachment of bacteria to plant cells have been isolated. Some related genes are identified and sequenced (Matthysse *et al*., 2000; Reuhs *et al*., 1997). However, it is surprising that a large number of genes are involved in the bacterial attachment to host cells and the actual functions of most genes are unclear (Matthysse *et al*., 2000). All the genes reported to affect the bacterial attachment to host cells are chromosomal genes.

The genes involved in the binding of bacteria to host plant cells are mainly located at two regions of the bacterial chromosome. The binding of bacteria to host cells is thought to be a two-step process (Matthysse and McMahan, 1998). The binding in the first step is loose and reversible because it is easy to wash the bound bacteria from the binding sites by shear forces, such as water washing or vortexing of tissue culture cells. Genes involved in this step are identified to locate on the *att* gene region (more than 20 kb in size) of the bacterial chromosome. Gene mutations in this region abolish virulence. The mutants in the *att* gene region can be divided into two groups. The first group can be restored to attachment and virulence by the addition of conditioned medium. This group appears to be altered in signal exchange between the bacterium and the host. Mutations in this group of mutants occur in the genes homologous to ABC transporters and transcriptional regulator as well as some closely linked downstream genes (Matthysse *et al*., 2000; Matthysse and McMahan, 1998; Reuhs *et al*., 1997).

The second group of mutants in the *att* gene region is not affected by the presence of conditioned medium. This mutant group appears to affect the synthesis of surface molecules, which may play a role in the bacterial attachment to the host. This group includes mutants in the genes homologous to transcriptional regulator and ATPase as

well as a number of biosynthetic genes, which include the transacetylase required for the formation of an acetylated capsular polysaccharide. The acetylated capsular polysaccharide is required for the bacterial attachment to some plants because the production of the acetylated capsular polysaccharide is correlated to the attachment of wild-type strain C58 to the host cells and the purified acetylated capsular polysaccharide from wild-type strains blocks the binding of the bacteria to some host cells (Matthysse *et al*., 2000; Matthysse and McMahan, 1998; 2001; Reuhs *et al*., 1997).

The second step in the bacterial attachment to the host results in tight binding of the bacteria to the plant cell surface because the bound bacteria can no longer be removed from the plant cell surface by shear forces. This step requires the synthesis of cellulose fibrils by the bacteria, which recruits larger numbers of bacteria to the wound sites. Cellulose-minus bacterial mutants show reduced virulence (Minnemeyer *et al*., 1991). The genes required for the synthesis of bacterial cellulose fibrils (*cel* genes) are identified to locate on the bacterial chromosome near, but not contiguous with the *att* gene region (Robertson *et al*., 1988).

Some other chromosomal virulence genes *chvA*, *chvB*, and *pscA* (*exoC*) are believed to be involved indirectly in bacterial attachment to host (Cangelosi *et al*., 1987; Douglas *et al*., 1982; O'Connell and Handelsman, 1989). These genes are involved in the synthesis, processing, and export of a cyclic β-1,2-glucan, which has been implicated in the bacterial binding to plant cells. Mutations in *chvA*, *chvB*, and *pscA* (*exoC*) cause a 10-fold decrease in binding of bacteria to zinnea mesophyll cells (Douglas *et al*., 1985) and strongly attenuate virulence (Douglas *et al*., 1985; Kamoun *et al*., 1989; Thomashow *et al*., 1987). ChvB is believed to be involved in the synthesis of the cyclic β-1,2-glucan

(Zorreguieta and Ugalde, 1986). ChvA is homologous to a family of membrane-bound ATPases and appears to be involved in the export of the cyclic β-1,2-glucan from the cytoplasm to the periplasm and extracellular fluid (Cangelosi *et al*., 1989; De Iannino and Ugalde, 1989). However, the virulence of *chvB* mutants is temperature sensitive (Banta *et al*., 1998). At lower temperature (16 ºC), *chvB* mutants became virulent and were able to attach to plant roots (Bash and Matthysse, 2002).

1.4.2. Plant factors involved in the attachment of *A. tumefaciens* to plant

In addition to bacterial factors, some plant factors are essential for the attachment of *A. tumefaciens* to plant cells. Two plant cell wall proteins: a vitronectin-like protein (Wagner and Matthysse, 1992) and a rhicadhesin-binding protein (Swart *et al*., 1994) have been proposed to mediate the bacterial attachment to plant cells. Vitronectin is an animal receptor that is specifically utilized by different pathogenic bacteria (Burridge *et al*., 1988). A plant vitronectin-like protein is reported to occur in several *A. tumefaciens* host plant (Sanders *et al*., 1991). Human vitronectin and antivitronectin antibodies were shown to inhibit the binding of *A. tumefaciens* to plant tissues. Nonattaching *A. tumefaciens* mutants, such as *chvB*, *pscA* and *att* mutants, showed a reduction in the ability to bind vitronectin. Therefore, the plant vitronectin-like protein was proposed to play a role in *A. tumefaciens* attachment to its host cells (Wagner and Matthysse, 1992).

Recently, some genetic studies showed that additional plant cell-surface proteins might play a role in *A. tumefaciens* attachment. Two *Arabidopsis* ecotypes, B1-1 and Petergof, which are highly recalcitrant to *Agrobacterium*-mediated transformation, were proposed to be blocked at an early step of the binding (Nam *et al*., 1997). Two

Arabidopsis T-DNA insertion mutants of the ecotype Ws, *rat1* and *rat3*, which are resistant to *Agrobacterium* transformation (*rat* mutants), are deficient in *A. tumefaciens* binding to cut root surfaces (Nam *et al*., 1999). DNA sequence analysis indicated that *rat1* and *rat3* mutations affect an arabinogalactan protein (AGP) and a potential cell-wall protein, respectively. AGPs were confirmed to be involved in *A. tumefaciens* transformation (Nam *et al*., 1999). Other two *rat* mutans, *rat*T8 and *rat*T9, were identified to be mutated in the genes coding for receptor-like protein kinases (Zhu *et al*., 2003).

1.5. T-DNA Transfer

1.5.1. T-DNA transfer models

T-DNA is transferred in the form of ssT-strand-protein complex. However, the controversy is where and when VirE2 binds to T-strand. In other word, whether T-DNA is transferred from *A. tumefaciens* to plant cell in the form of VirD2-ssT-strand complex or in the form of VirD2-ssT-strand-VirE2 complex is in the controversy (Zupan and Zambryski, 1997). Therefore, three models were proposed to envision the T-DNA transfer from *A. tumefaciens* to plant cell.

The most accepted model is that T-DNA is transferred in the form of VirD2-ssT-strand-VirE2 complex. In this model, VirE2 is believed to bind to the ssT-strand inside *A. tumefaciens* cell. The evidence supporting this model includes: (1) VirE2 accumulates in *A. tumefaciens* cell at the same time as T-strand and in stoichiometric amounts sufficient to bind the T-strand completely (Citovsky *et al*., 1988; 1989; Zambryski, 1992). (2) VirE2 can bind ssT-strand strongly and cooperatively and the cooperative association

extends the ssT-strand, which reduces the complex diameter to approximately 2 nm and makes the translocation through membrane channels easier (Citovsky *et al*., 1989; 1997). (3) The ssT-strand can be co-immunoprecipitated from an extract of induced *A. tumefaciens* cells by using anti-VirE2 antibodies (Christie *et al*., 1988).

However, more and more experimental evidences demonstrated that VirE2 could be exported independently (Atmakuri *et al*., 2003; Cascales and Christie, 2004; Chen *et al*., 2000; Deng *et al*., 1999; Schrammeijer *et al*., 2003; Simone *et al*., 2001; Vergunst *et al*., 2000) and that the transfer of VirE2 as part of the ssT-strand complex is not necessary for the tumorigenesis (Sundberg *et al*., 1996). In addition, *A. tumefaciens* was shown to be able to transfer naked T-srand to the plant cells although the transfer efficiency may be very low (Binns *et al*., 1995; Sundberg *et al*., 1996). Therefore, a second model was proposed to light for the ssT-strand complex transfer. In this model, the transferred ssT-strand complex is a naked ssT-strand with a VirD2 molecular covalently bound at its 5′-end, no VirE2 coated the ssT-strand. VirE2 is exported to the periplasm (and possibly secreted into the extracellular environment) independently of ssT-strand transfer and then transported to plant cells via VirB channel (Chen *et al*., 2000; Simone *et al*., 2001). Once the naked ssT-strand-VirD2 complex is transported into the plant cell, it will be coated by VirE2 (Binns *et al*., 1995; Lessl and Lanka, 1994). To explain why VirE2 can not access to the ssT-strand and not coat it inside the bacterial cytoplasm, it was suggested that *A. tumefaciens* may adopt a mechanism analogous to conjugal DNA transfer, in which the Ti plasmid is tightly associated with the export apparatus VirB channel so that the naked ssT-strand is exported as it is produced before VirE2 has the opportunity to bind (Sundberg *et al*., 1996). Recent results suggested that VirE1, as a specific molecular

chaperone, might play a role in preventing VirE2 from accessing to ssT-strand inside agrobacterial cytoplasm (Deng *et al*., 1999; Vergunst *et al*., 2003).

Although most of the recent data appear to support the second model, additional questions are still confounded by this model. (1) If T-DNA transfer evolved from plasmid conjugation (Lessl and Lanka, 1994), then *Agrobacterium* : plant contact would likely be maintained because the donor : recipient contact is required for ensuring that conjugal DNA transfer occurs with high efficiency. Thus, it is unlikely that VirE2 is exported into the environment. In addition, export of VirE2 outside of the bacterium would require a plant apparatus to import VirE2 across the plant plasma membrane, but no experimental evidence supports such a mechanism. (2) If the naked ssT-strand and VirE2 are exported by the same apparatus VirB channel independently (Atmakuri *et al*., 2003; Simone *et al*., 2001), the export apparatus must distinguish between VirE2 and the naked ssT-strand to regulate their independent export. (3) In order to maintain the VirE2 concentration in plant cytoplasm being high enough to favor the binding of VirE2 to ssT-strand, *A. tumefaciens* has to export an extremely large excess of VirE2 to plant cell cytoplasm because the volume of plant cell cytoplasm is so much greater than that of *A. tumefaciens*. For these reasons, an explanation may be acceptable that, in principle, the independent export of naked ssT-strand and VirE2 can occur, but this may not be the natural export mechanism in *A. tumefaciens* tumorigenesis (Zupan and Zambryski, 1997).

To incorporate the features of the first two models, an intermediate model for the T-DNA transfer was proposed. In this intermediate model, both naked ssT-strand and VirE2 are possibly localized near the export apparatus. The ssT-strand might be exported in a range of partially to completely VirE2-coated states. In the same time, free VirE2 could

also be exported in the same export apparatus and would be expected to bind the ssT-strand during the transit and entry into the plant cell so that the ssT-strand could be coated by VirE2 completely before the ssT-strand arrives in the plant cell cytoplasm. Any free VirE2 might also enter the plant cell cytoplasm. To compare these three models of T-complex transfer, a schematic diagram is shown in Fig.1.3.

1.5.2. T-DNA transfer apparatus is a type IV secretion system (T4SS)

A. tumefaciens uses type IV secretion system (T4SS) to transfer T-DNA and effector proteins, VirE2, VirF, and possibly VirE3 to its host cells (Cascales and Christie, 2003; 2004). The T4SS were initially defined to be a class of DNA transporters whose components are highly homologous to the conjugal transfer (tra) system of the conjugative IncN plasmid pKM101 and the *A. tumefaciens* T-DNA transfer system (Burns, 2003; Christie and Vogel, 2000). T4SS, also known as the mating pair formation (Mpf) apparatus, are cell envelope-spanning complexes (composed of 11-13 core proteins) that are believed to form a pore or channel through which DNA and/or protein is delivered from the donor cell to the recipient cell. Recently the members of T4SS have steady increased, with the identification of additional systems involved in DNA and protein translocation (Cascales and Christie, 2003; Christie and Vogel, 2000). However, the best-studied T4SS member is the VirB transporter of *A. tumefaciens*. In the past decade, much of the research on *Agrobacterium*-mediated T-DNA transfer has focused on the *vir*-specific T4SS, the T-complex transporter. Thus, the *A. tumefaciens* T-complex transporter has become a paradigm of T4SS (Cascales and Christie, 2003; Christie, 1997).

The T-complex transporter is assembled from 11 proteins (VirB1 to VirB11)

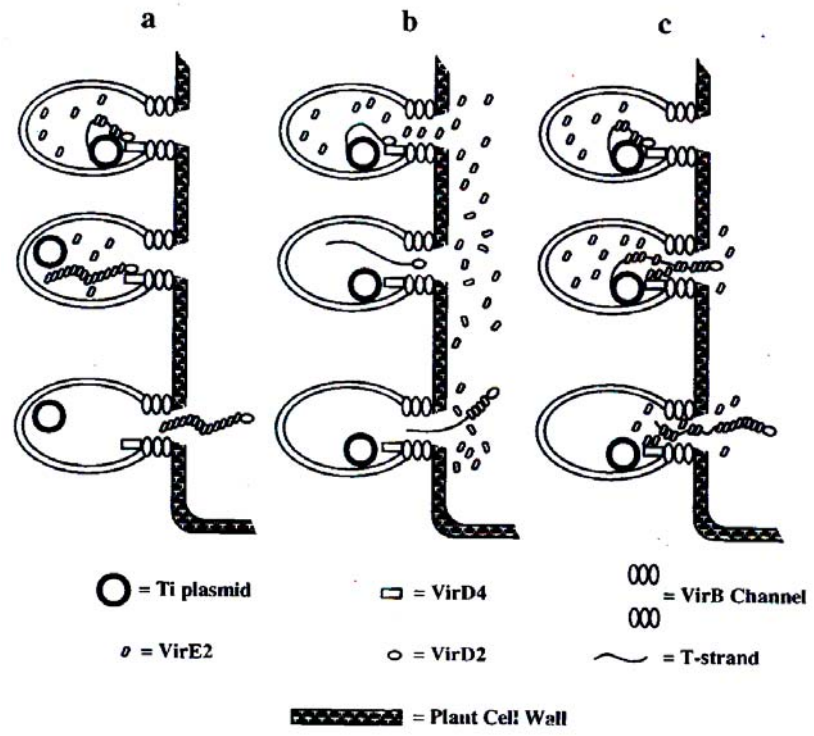

Fig. 1.3. Three models of T-complex formation and transfer. In each model, formation of the T-complex initiates with the nicking reaction at the border sequences and the subsequent covalent bonding of VirD2 to the 5′ end of the T-strand. (**a**) The T-strand is displaced from the Ti plasmid and coated with VirE2 inside the bacterial cell, followed by export of the entire complex. (**b**) T-strand and VirE2 are exported independently from the bacterial cell, and binding of VirE2 to the T-strand occurs in the plant cell cytoplasm. As shown here, VirE2 is exported first, followed by the T-strand. Sundberg *et al*. (1996) have suggested that the T-strand might be exported, as it is displaced and VirE2 is exported subsequently. (**c**) VirE2 primarily binds to the T-strand shortly after it is displaced inside the bacterial cell. Independent export of VirE2 ensures that the T-strand becomes completely coated during transit through the export apparatus (Cited from Zupan and Zambrysky, 1997).

encoded by the *virB* operon, and VirD4. At least 10 of the 11 VirB proteins are believed to be the structural subunits of the T-pilin and associated transport apparatus that spans from the cytoplasm of the cell, through the inner membrane, periplasmic space and outer membrane, to the outside of the cell. In the past few years, work in identifying the interactions among the VirB protein subunits and defining the steps in the transporter assembly pathway has extended our knowledge of the structure of the VirB transport apparatus. The subcellular localizations, protein-protein interactions and proposed functions of the VirB proteins are summarized in Table 1.1.

1.5.3. Characteristics of T4SS components

VirB1 has a motif found among lytic transglycosylases in its N-terminus and is postulated to have glycosidase activity (Mushegian *et al*., 1996). Such a lysozyme-like activity is believed to be important for the hydrolysis of peptidoglycan layer of bacterial membrane and the formation of a channel in the bacterial membrane so that the other VirB proteins can penetrate the peptidoglycan layer to assemble a multiprotein apparatus large enough to traffic nucleoprotein complexes. VirB1 is processed to release its C-terminal 73-residue peptide. This 73-residue peptide is designated as VirB1*. VirB1* is secreted to the exterior of *A. tumefaciens* cells and remains loosely associated with the exterior of the cell (Baron *et al*., 1997). VirB1* is not detected in purified T-pilus preparations, but chemically crosslinks with VirB9, and thus might mediate close contacts between donor and recipient cells (Llosa *et al*., 2000).

VirB2, as the pro-pilin, is translated as a 12.3 kDa protein with 121 amino acid residues. This 12.3 kDa protein is quickly processed into a 7.2 kDa protein, the T-pilin of

Table 1.1. [a] Molecular weights, subcellular localizations, protein-protein interactions and postulated functions of the VirB proteins [b]

Proteins	Size (kDa) [c]	Localization	Protein-protein contacts [d]		Proposed function
			Dihybrid screen	Biochemical assay	
Channel subunits					
VirB6	31.8	IM		B7, B9	Assembly factor; channel subunit
VirB8	26.4	IM	B1, B8, B9, B10	B8, B9, B10	Assembly factor; bridge between subcomplexes; IM & OM VirB channel subunit
VirB10	40.6	IM	B8, B9, B10	B8, B9, B10	Bridge between IM & OM subcomplexes; channel subunit
VirB3	11.6	OM			Unknown
VirB7	5.9, 4.5*	OM lipoprotein	B7, B9	B2, B6, B7, B9, B10	Stabilizes B9 by disulphide crosslink; B7-B9 dimer stabilizes other VirB proteins
VirB9	32.1	OM	B1, B7, B8, B9, B10, B11	B6, B7, B9, B10	OM pore?
Energetics					
VirB4	87.4	IM	B4, B8, B10, B11	B4	ATPase; energy for substrate export & pilus biogenesis; homomultimer
VirB11	38.1	IM	B4, B9	B11	ATPase; energy for substrate export & pilus biogenesis; homomultimer
Periplasmic factor					
VirB1	28.0, 12.0*	PP	B1, B4, B8, B9, B10	B1	Peptidoglycan hydrolase; channel assembly
T pilus					
VirB2	12.3, 7.2*	IM, EX	B2, B5, B7		Cyclized pilin subunit
VirB5	23.3	PP, EX	B2		Pilus subunit;chaperone?
VirB7	5.9, 4.5*	OM, EX		B2	Pilus assembly?

[a] Cited from Cascales and Christie, 2003; Lai and Kado, 2000.

[b] Abbreviations: IM, inner membrane; OM, outer membrane; PP, periplasm; EX, Exocellular.

[c] Processed proteins are indicated with an asterisk.

[d] Evidence for subunit-subunit contacts on the basis of results of yeast or bacterial dihybrid screen or biochemical assays. References are presented in the text.

74 amino acid residues (Jones *et al*., 1996). The N-terminus of the full-length VirB2 is removed by cleaving the peptide bound between Ala 47 and Gln 48. The resulting 74-residue T-pilin is ligated between its N-terminus (Gln 48) and C-terminus (Gly 121) by a head-to-tail peptide bond, forming a cyclic peptide, the cyclized T-pilin subunit (Eisenbrandt *et al*., 1999; Jones *et al*., 1996).

VirB3 and VirB4 show highly homologous to the IncF proteins TraC and TraL. These two IncF proteins were proved to be essential for pilus formation but not be pilus structural components. So, VirB3 and VirB4 were suggested to play a role in pilus assembly (Jones *et al*., 1994). VirB4 possesses a conserved Walker A nucleotide-binding motif and the purified VirB4 shows week ATPase activity (Christie, 1997). Cellular levels of VirB3 are reduced in *virB4* deletion mutant. The localization of VirB3 is also affected by the *virB4* deletion. In the *virB4* deletion mutant, VirB3 is localized to the inner membrane rather than both inner and outer membranes as in wild-type strains (Jones *et al*., 1994). Research data showed that the VirB-specific transporter is not only used for transferring the T-complex, but also for exporting the cyclic T-pilin subunit to the bacterial cell surface, perhaps as a scaffold to facilitate efficient assembly of the T-pilus (Lai *et al*., 2000). Therefore, it was suggested that VirB3 specific localization, mediated by VirB4, might assist the mobilization of the cyclic T-pilin subunit VirB2 to the cell exterior (Zupan *et al*., 2000).

VirB5 is a minor component of T-pilus and is believed to function as auxiliary structural proteins in pili of T4SS (Schmidt-Eisenlohr *et al*., 1999). In contrast to VirB2, cellular levels of VirB5 were affected by other Vir proteins. When other Vir proteins are

absent, the cellular levels of VirB5 were strongly reduced. It was speculated that VirB5 decreased due to the degradation in the periplasm. So, other Vir proteins may protect VirB5 from degradation by protein-protein interaction (Schmidt-Eisenlohr *et al*., 1999).

VirB6~VirB10 proteins as well as one or more of the three ATPases (VirB4, VirB11 and VirD4) are thought to be the main channel components (Christie, 1997; Christie and Vogel, 2000). The protein-protein interactions of these VirB proteins were extensively studied by using dihybrid screens and complementary biochemical assays (Beaupre *et al*., 1997; Das *et al*., 1997; Das and Xie, 2000; Jakubowski *et al*., 2003; Krall *et al*., 2002; Shamaei-Tousi *et al*., 2004; Ward *et al*., 2002) (table 1.1). VirB6, a highly hydrophobic protein, contains multiple membrane-spanning domains and thus is believed to span the inner membrane several times (Beijersbergen *et al*., 1994; Christie, 1997). VirB6 is thought to be the best candidate for a channel-forming protein. It was suggested that VirB6 and two other VirB proteins, VirB8 and VirB10, which anchor to the inner membrane, constitute the inner membrane sub-complex. The oligomerization of VirB6 complex is believed to be essential for the formation of the functional pore (Das, 1998). VirB7 is translated to a 55-residue preprotein and then processed to a 41-residue mature lipoprotein. VirB7 is localized in the outer membrane and covalently attached to a lipid moiety by the N-terminal cysteine (Cys 15) (Fernandez *et al*., 1996a). VirB7 interacts with VirB9 via a disulfide bond between the Cys 24 of VirB7 and the Cys 262 of VirB9. Both VirB7 and VirB9 can form homodimers in the absence of each other. The VirB7-VirB9 heterodimer can further form heterotetramers (Anderson *et al*., 1996) and is essential for the stability of other VirB proteins during assembly of the T4SS (Christie and Vogel, 2000; Fernandez *et al*., 1996b). Yeast two-hybrid studies showed that VirB8,

VirB9 and VirB10 interact with one another (Das and Xie, 2000). Possibly, VirB8-VirB9 interaction is required for the formation of chemically crosslinked VirB10 oligomers (Christie and Vogel, 2000; Zupan *et al*., 2000). VirB10 contains a large C-terminal periplasmic domain and a short N-terminal cytoplasmic domain and thus is thought to link inner membrane and outer membrane VirB subcomplexes (Beaupre *et al*., 1997).

Like VirB4, VirB11 contains a conserved Walker A nucleotide-binding motif required for its function. Purified VirB11 also has weak ATPase activity (Christie, 1997). Both VirB4 and VirB11 ATPases are proposed to mediate T4SS apparatus assembly or function through dynamic, ATP-dependent conformation changes. VirB4 tightly associates within the inner membrane. It contains two periplasmic domains that confer this protein a transmembrane topology. This transmembrane topology was presumed to allow the ATP-dependent conformational change in the conjugation channel (Dang and Christie, 1997). VirB4 appears to function as a homomultimer *in vivo*. Homologues of both ATPases are widely found among the T4SS family members, but VirB11-like ATPase constitute a protein superfamily and members of VirB11-like ATPase family are present among all type II and IV secretion system (Planet *et al*., 2001). VirB11 proteins self-associate into homohexamers via two domains located in its N- and C-termini. The VirB11 homohexamer functions as a hexameric pore. The closure and opening of this hexameric pore is regulated by ATP binding/hydrolysis. Nucleotide binding 'locks' the hexamer into a symmetric and compact structure. It was proposed that VirB11 uses the mechanical leverage generated by such nucleotide-dependent conformational changes to facilitate the export of substrates or the assembly of the T4SS apparatus. So, VirB11 is thought to function as a gating molecule at the inner membrane (Savvides *et al*., 2003).

1.5.4. Coupling protein VirD4 and its roles in T-DNA transfer

Agrobacterium-mediated T-DNA transfer to plant shows striking similarities to the plasmid interbacterial conjugation (Stachel and Zambryski, 1986; Ream, 1989). Bacterial conjugation can be visualized as the merging of two ancient bacterial systems: the DNA rolling-circle replication system and type IV secretion system (T4SS) (Llosa *et al*., 2002). The DNA rolling-circle replication system in plasmid conjugation was also known as the DNA transfer and replication (Dtr) system. The Dtr system corresponds to the T-DNA relaxase nucleoprotein complex. The T4SS responding for the plasmid conjugation was initially called mating pair formation (Mpf) system. In order to recognize these two systems and link them, a protein is normally required for many conjugal plasmids to couple the Dtr to the Mpf. This protein was called coupling protein as its function (Gomis-Ruth *et al*., 2002).

VirD4 is a homologue of coupling protein family and is believed to be the coupling protein that links the T-complex and T4SS transporter. VirD4 is an inner membrane protein with potential DNA binding ability and ATPase activity. Membrane topology analysis of VirD4 revealed that VirD4 contains a N-terminal-proximal region, which includes two transmembrane helices and a small periplasmic domain, and a large C-terminal cytoplasmic domain (Cascales and Christie, 2003; Das and Xie, 1998). VirD4 localizes to the cell pole. The polar location of VirD4 was not dependent on T-DNA processing, the assembly of T4SS transporter and the expression of other Vir proteins (Kumar and Das, 2002). Both the small periplasmic domain and the cytoplasmic nucleotide-binding domain are required for the polar localization of VirD4 and essential for T-DNA transfer. VirD4 forms a large oligomeric complex (Kumar and Das, 2002).

VirD4 can recruit VirE2 to the cell poles (Atmakuri *et al*., 2003) and weakly interact with VirD2-T-strand complex (Cascales and Christie, 2004). Although VirD4 is essential for coordinating the T4SS to drive T-DNA transfer, it has been unclear whether VirD4 physically/directly interacts with the T4SS transporter. Recently, two reports showed that two VirD4 homologues TrwB and TraG interact with VirB10 homologues respectively (Gilmour *et al*., 2003; Llosa *et al*., 2003). However, the interaction between VirD4 homologues and the protein components of Dtr system exhibits specificity (Llosa *et al*., 2003). It was supposed that VirD4 protein might recruit T-complex to the T4SS transporter through contacts with the T-complex protein and then through the contacts with VirB10 coordinate the passage of T-complex through the T4SS channel (Cascales and Christie, 2003; Llosa *et al*., 2003). However, it should be pointed out that the recruitment of T-complex might be much more difficult than the recruitment of single VirE2 molecule due to the difference of molecular size between T-complex and VirE2. To demonstrate the architecture of the VirB/D4 transporter, a recent model that depicts the subcellular locations and interactions of the VirB and VirD4 subunits of the *A. tumefaciens* VirB/D4 T4SS is shown in Fig. 1.4 (Cascales and Christie, 2004).

1.5.5. Possible roles of VirE2 in T-DNA transfer

One recent report showed that VirE2 could form channels in artificial membranes. These channels are voltage gated and anion selective and can specifically facilitate the efficient transport of ssDNA through membranes (Dumas *et al*., 2001). Based on this evidence, it was supposed that VirE2 might assemble as a receptor or transport channel at the plant plasma membrane to dock the T-DNA transfer system and translocate the incoming VirD2-T-strand complex, VirE2 and VirF substrates (Dumas *et al*., 2001).

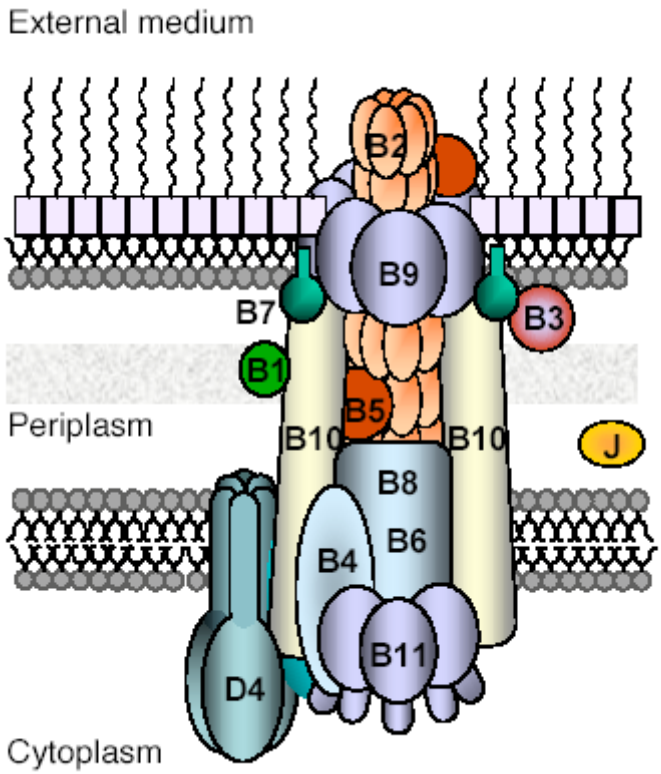

Fig. 1.4. A model of the VirB/D4 transporter of *A. tumefaciens*. The VirD4 coupling protein assembles as a homohexameric, F1-ATPase-like structure juxtaposed to the VirB channel complex. VirB11, a hexameric ATPase structurally similar to members of the AAA ATPase superfamily, is positioned at the cytoplasmic face of the channel entrance, possibly directing substrate transfer through a VirB6/VirB8 inner membrane (IM) channel. The VirB2 pilin and VirB9 comprise channel subunits to mediate substrate transfer to and across the outer membrane (OM). VirB10 regulates substrate transfer by linking IM and OM VirB subcomplexes (Cited from Cascales and Christie, 2004).

Interestingly, another report showed that *A. tumefaciens* could export low level of VirE2, VirD2 and VirF proteins to the extracellular milieu via a *virB*-independent export pathway (Chen *et al*., 2000). VirE2 exported by the *virB*-independent pathway might be used to assemble the VirE2 receptor or transport channel at the plant plasma membrane. This model can account for the extreme broad host range of the *A. tumefaciens*-mediated T-DNA transfer because *A. tumefaciens* can deliver its own receptor to target cells (Christie 2001; Dumas *et al*., 2001).

1.6. Nuclear Targeting of T-complex

1.6.1. Nuclear localization signal

Whether VirE2 coats to the ssT-strand within bacterium to assemble a VirD2-T-strand-VirE2 complex remains controversial. However, it is clear that VirE2 is necessary for T-DNA transfer inside plant cells (Citovsky *et al*., 1992), indicating that the ssT-strand must be coated by VirE2 inside plant cells and VirD2-T-strand-VirE2 complex exists inside plant cells. To deliver the T-DNA to target cell, the T-complex must target to the host cell nucleus and penetrate the nuclear membrane. The estimated size of the T-complex is 50,000 kDa, which far exceeds the 60 kDa size-exclusion limit of the nuclear pore, indicating that active transport processes are required for the nuclear import of T-complex. As a rule, active nuclear import of proteins requires a specific nuclear localization signal (NLS). Typical nuclear localization signals are short regions rich in basic amino acids (Silver, 1991). The most common type of NLS is the bipartite NLS that is originally found in nucleoplasmin from the amphibian *Xenopus laevis* (Robbins *et al*., 1991). Bipartite NLS contains two interdependent basic domains, both needed for full

activity. The first active basic domain consists of two adjacent basic residues and the second active domain contains at least three out of five basic amino acids. Between this two active domains is a variable-length linker (Dingwall and Laskey, 1991). NLS-binding proteins can recognize NLSs and guide the NLS-containing proteins to nuclear pores where active nuclear import occurs (Silver, 1991).

1.6.2. Nuclear localization signals in VirD2

Because T-strand is presumed to be completely coated with proteins inside plant cells it is impossible for T-strand itself to carry NLSs. Thus, the NLSs that guide T-complex nuclear import most likely reside in its associated proteins, VirD2 and VirE2. Sequence analysis reveals that both VirD2 and VirE2 contain NLSs. Two NLSs are found in VirD2. One is the typical bipartite NLS that resides in residues 396~413. The nuclear localizing function of this bipartite NLS was confirmed by the observation that VirD2-GUS fusion protein, when expressed in tobacco protoplasts, can target to plant cell nuclei (Howard *et al*., 1992; Tinland *et al*., 1992). However, mutations that destroy this bipartite NLS attenuate, and do not abolish tumorigenesis, indicating that although this NLS plays a role in T-DNA transfer, it is not essential (Rossi *et al*., 1993; Shurvinton *et al*., 1992). Another NLS in VirD2 is found in residues 32~35, adjacent to the active site in the endonuclease domain (Tinland *et al*., 1992). This NLS is a monopartite NLS. GUS proteins fused with this NLS accumulate in plant nuclei, but this NLS does not play a role in T-DNA nuclear localization (Shurvinton *et al*., 1992). The sequences of residues 419-423 at the C-terminus of VirD2, known as the ω domain, are important for tumorigenesis, but do not contribute to nuclear localization activity despite its proximity to the bipartite NLS. The ω domain was supposed to be involved in T-DNA integration (Mysore *et al*.,

1998).

1.6.3. Nuclear localization signals in VirE2

VirE2, the most abundant protein component of the T-complex, contains two bipartite NLSs in its central region (residues 205~221, and residues 273~287). When fused to GUS, each VirE2 NLS is capable of directing the fusion protein to the nucleus of a plant cell, but the maximum accumulation in the nucleus requires both VirE2 NLSs (Citovsky *et al*., 1992). Because these two NLSs overlap with the DNA binding domains, mutations of *virE2* that abolish the activity of one of these NLSs will also eliminate the DNA binding activity. So, no genetic evidence can be provided to verify the function of these two VirE2 NLSs in T-complex nuclear localization. When VirE2 binds to T-strand, the NLSs of VirE2 may be occluded and inactive. It has been observed that for the nuclear import of short ssDNA, VirD2 was sufficient, whereas import of long ssDNA additionally required VirE2 (Ziemienowicz *et al*., 2001). All the evidence argued against the function of VirE2 in T-complex nuclear localization. The experimental evidence that RecA, a NLS-lacking ssDNA binding protein, could substitute for VirE2 in the nuclear import of T-strand, further demonstrated that VirE2 functions not in the nuclear localization, possibly in mediating the passage of T-strand through the pore (Ziemienowicz *et al*., 2001). VirE2 was assumed to shape the T-complex such that it is accepted for translocation into the nucleus.

1.6.4. Plant proteins involved in T-complex nuclear targeting

Besides the agrobacterial proteins VirD2 and VirE2, some plant proteins were supposed to be involved in the T-complex nuclear translocation. Early yeast two-hybrid

screen identified an *A. thaliana* importin-α (AtKAP, now known as importin-α1) that interacts with VirD2 (Ballas and Citovsky, 1997). Importin-α proteins interact with NLS-containing proteins and guide the nuclear translocation of these proteins. Importin-α proteins constitute a protein family and *Arabidopsis* encodes at least nine of these proteins (Gelvin, 2003). Interaction between VirD2 and importin-α1 was verified to be VirD2 NLS dependent (Ballas and Citovsky, 1997). The importance of importin-α proteins in the T-complex transfer process was confirmed by the genetic evidence that a T-DNA insertion into the importin-α7 gene, or antisense inhibition of expression of the importin-α1 gene, highly reduces the transformation efficiency (Gelvin, 2003).

Two other plant proteins were identified to interact with VirD2. Deng *et al*. (1998) showed that an *Arabdopsis* cyclophilin interacted strongly with VirD2. They further characterized the interaction domain of VirD2 and found that a central domain of VirD2 (residues 274~337) was involved in the interaction with cyclophilin. No previous function of VirD2 had been ascribed this central region. Cyclosporin A, an inhibitor of VirD2-cyclophilin interaction, inhibits *Agrobacterium*-mediated transformation of *Arabidopsis* and tobacco (Deng *et al*., 1998). Cyclophilin were presumed to serve as a molecular chaperone to help in T-complex trafficking within the plant cell. In addition, a tomato type 2C protein phosphatase was identified to interact with VirD2 (Gelvin, 2003). This phosphatase was assumed to be involved in the phosphorylation and dephosphorylation of a serine residue near the C-terminal NLS in the VirD2. Overexpression of this phosphatase decreased the nuclear targeting of a GUS-VirD2-NLS fusion protein, suggesting that phosphorylation of the C-terminal NLS region may affect the nuclear targeting function of VirD2 (Gelvin, 2003).

Two VirE2-interacting proteins were designated VIP1 and VIP2. VIP1 was showed to facilitate the VirE2 nuclear import in yeast and mammalian cells. Tobacco VIP1 antisense plants were highly resistant to *A. tumefaciens* infection (Tzfira *et al*., 2001), whereas, transgenic plants that overexpress VIP1 are hypersusceptible to *A. tumefaciens* transformation (Tzfira *et al*., 2002). VIP1 is a basic leucine zipper (bZIP) motif protein and shows no significant homology to known animal or yeast proteins (Tzfira *et al*., 2001). So, how VIP1 facilitates the nuclear import of VirE2 remains unclear. Unlike VIP1, VIP2 was unable to mediate VirE2 into the yeast cell nucleus. However, VIP1 and VIP2 interacted with each other. Thus, VIP1, VIP2 and VirE2 were assumed to function in a multiprotein complex (Tzfira and Citovsky, 2000; 2002).

1.6.5. Possible roles of VirF in T-DNA transfer

Like VirD2 and VirE2, agrobacterial protein VirF can also be exported to plant cell (Vergunst *et al*., 2000). *VirF* gene is found only in the octopine-specific Ti plasmid. It is not essential for T-DNA transfer. Initially, VirF is thought to be a host-range factor of *Agrobacterium* (Regensburg-Tuink and Hooykaas, 1993). A recent report identified an *Arabidopsis* Skp1 protein as an interacting partner of VirF protein (Schrammeijer *et al*., 2002). Yeast Skp1 protein and its animal and plant homologs are subunits of the complexes involved in targeted proteolysis. This targeted proteolysis can regulate the plant cell cycle. So, it was suggested that VirF may function in setting the plant cell cycle to effect better transformation (Gelvin, 2003; Schrammeijer *et al*., 2002; Tzfira and Citovsky, 2002).

1.7. Integration of T-DNA into Plant Genome

1.7.1. Integration site

The integration of the incoming ssT-strand of the T-complex into plant genome is the final step of the T-DNA transfer. The DNA sequence analysis of several T-DNA-host DNA junctions revealed that these junctions, in general, appear more variable than the junctions created by insertions of transposons, retroviruses, or retrotransposons (Gheysen *et al*., 1987). Most recently, a statistical analysis of 88,000 T-DNA genome-wild insertions of *Arabidopsis* revealed the existence of a large integration site bias at both the chromosome and gene levels (Alonso *et al*., 2003). At the chromosomal level, fewer T-DNA insertions were found at the centromeric region. At the gene level, Insertions within promotor and coding exons make up nearly 50% of all insertion sites. However, these statistical results may be skewed by the antibiotic resistance selection of transformed plants (T1 plants) because only the T1 plants with transcriptionally active T-DNA insertions can be selected (Alonso *et al*., 2003; Valentine, 2003). Another statistical analysis of 9000 flanking sequence tags characterizing transferred DNA (T-DNA) transformants in *Arabidopsis* showed that there are microsimilarities involved in the integration of both the right and left borders of the T-DNA insertions (Brunaud *et al*., 2002). These microsimilarities occur only a stretch of 3 to 5 bp and can be between any T-DNA and genomic sequence. This mini-match of 3 to 5 bp basically allows T-DNA to integrate at any locus in the genome. It was also showed that T-DNA integration is favored in plant DNA regions with an A-T-rich content (Brunaud *et al*., 2002).

1.7.2. Integration mechanism

The observation of the random, as opposed to targeted, nature of T-DNA integration indicated that the integration occurs in illegitimate recombination, a mechanism that joins two double-stranded (ds) DNA elements that do not share extensive homology (Ziemienowicz, 2001). To date, it has not been possible to target T-DNA to any particular locus in the genome with any great efficiency. However, one of the major contributions of *A. tumefaciens* research has been the use of T-DNA as a mutagen to generate the desirable mutant (Valentine, 2003). So, the T-DNA integration has been one of the motives of intensive investigation of *A. tumefaciens*. But, the molecular mechanisms of the T-DNA integration remain largely unknown.

It is likely that after nuclear import, the ssT-strand is turned into double-stranded DNA (dsDNA) with the concomitant displacement of VirE2. Conversion of ssT-strand to a dsDNA form is supported by the observation that the level of transient expression of T-DNA genes is much greater than the expression from stably integrated T-DNA, because the conversion of the ssT-strand to a transcriptionally competent form requires the conversion of ssT-strand to a dsDNA form (Narasimhuhu, *et al*., 1996). In addition, the extrachromosomal homologous recombination of T-DNA prior to integration and the complex pattern of multiple T-DNA insertions at a single insertion site also supported that ssT-strand likely becomes double-stranded (De Buck *et al*., 1999). Although it is not sure whether these extrachromosomal dsT-DNAs are the substrates for integration, double-strand break repair via non-homologous end joining of the dsT-DNA is consistent with many of the products observed as a result of T-DNA integration (Britt, 1999; De Buck *et al*., 1999).

Unlike such mobile DNA elements as transposons and retroviruses, T-DNA itself does not encode enzymes that catalyze the integration. Thus, the integration of T-DNA into the plant genome must be mediated by proteins imported from *A. tumefaciens* or by host cell factors. Illegitimate recombination is an unfaithful DNA repair mechanism that often incorporates filler DNA, such as T-DNA, into the repair site. The sequence analysis of several T-DNA insertions and their respective pre-integration sites showed that the right junction is somewhat less variable than the left. In most cases the right junction of the T-DNA insertion includes all or almost all bases of the T-DNA. In contrast, the left junction of the T-DNA insertion lacks some of the sequences of the left end of the T-DNA. The number of missing bases ranges from a few up to 100 bp (Mayerhofer *et al*., 1991; Tinland *et al*., 1995). However, an *A. tumefaciens* mutant carrying an Arg to Gly substitution at position 129 in VirD2 resulted in the normally conserved 5′ end of the integrated DNA to be truncated or significantly rearranged, but did not affect the integration efficiency (Tinland *et al*., 1995). This VirD2 mutation affected the precision of the integration of 5′ end of T-DNA (the right junction of the T-DNA insertion) but not the efficiency, suggested that VirD2 is very important for the T-DNA integration process. Analysis of the T-DNA integration junctions also showed that VirE2 is required for integration fidelity at the 3′ but not the 5′ end of the T-DNA (Rossi *et al*., 1996).

1.7.3. Plant proteins involved in the T-DNA integration

The plant proteins that may be involved in the T-DNA integration process are only now beginning to be defined. A recent research showed that VirD2 interacts with CAK2Ms, a conserved plant ortholog of cyclindependent kinase-activating kinases, and the TATA box-binding protein (Bako *et al*., 2003). *In vivo*, VirD2 can be phosphorylated

by CAK2Ms. CAK2Ms also binds to and phosphorylates the C-terminal regulatory domain of RNA polymerase II largest subunit, which can recruit the TATA box-binding protein. TATA box-binding protein not only plays a defined role in the regulation of transcription, but also controls transcription-coupled repair, which ensures preferential and effective removal of DNA lesions from transcribed genes. These nuclear VirD2-binding factors provide a link between T-DNA integration and transcription-coupled repair, suggesting that transcription and transcription-coupled repair may play a role in T-DNA integration (Bako *et al*., 2003).

1.8. Aims and Significance of This Study

1.8.1. Significanc of this study

A. tumefaciens-mediated T-DNA transfer to plant has become the most popular method for the introduction of foreign genes into plant cells and the subsequent regeneration of transgenic plants because *A. tumefaciens*-mediated transformation has remarkable advantages over other direct transformation methods such as microinjection, electroporation and particle bombardment (De la Riva *et al*., 1998). The advantages of *A. tumefaciens*-mediated transformation include: (1) significantly high transformation efficiency; (2) easy to manipulate; (3) low copy number of the transgene, usually single copy insertion into the plant genome, potentially resulting in fewer problems with transgene cosuppresion and instability (Hansen *et al*., 1997); and (4) less frequent to form mosaic plants (Enriquez-Obregon *et al*., 1998). Now, many agronomically and horticulturally important species are routinely transformed using *A. tumefaciens*. Besides its natural host, dicotyledonous plants, the list of species that is susceptible to *A.*

tumefaciens-mediated transformation was enlarged to monocotyledonous plants (Chilton, 1993), yeast (Piers *et al*., 1996), fungi (Groot *et al*., 1998), and human cells (Kunik *et al*., 2001). Because *A. tumefaciens* represents a major tool for plant molecular breeding and for the delivery of DNA to other eukaryotic cells, the molecular mechanism by which it genetically transform the host cells has been the focus of research for a wide spectrum of biologists, from bacteriologists to molecular biologists to botanists, for a number of years.

In addition, *A. tumefaciens*-mediated T-DNA transfer to plant is the only known natural example of DNA transport between kingdoms. The T-DNA is transferred into eukaryotic cells in the form of nucleoprotein complex. Thus, the *A. tumefaciens*-mediated T-DNA transfer system can be used as a model system to study the molecular mechanism of a wide variety of biological processes such as nucleoprotein trafficking, nuclear targeting of nucleoprotein, and the export of virulence effector (Christie, 2001; Ziemienowicz *et al*., 2001). Many of these biological processes are relevant to human pathogen, human gene therapy, as well as HIV viral infection. Apparently, it is extremely important to understand how this nucleoprotein trafficking process occurs.

1.8.2. Aims of this study

Although the molecular mechanism of *A. tumefaciens*-mediated T-DNA transfer has been intensively studied in the past decades and our understanding of the molecular mechanisms of T-DNA transfer has grown immeasurably in recent years, many details of the T-DNA transfer still remain unclear. As discussed in the above, so few virulence proteins (only VirD1 and VirD2) are identified to be necessary for T-DNA production. Is there any bacterial housekeeping protein or enzyme of DNA repair and replication to be

implicated in this process? We do not know whether the VirD2-guiding T-complex movement to the bacterial export apparatus is an active movement or passive movement. We also do not know if the coupling protein VirD4 can recruit the T-complex to the bacterial export apparatus. Whether VirE2 can coat to the ssT-strand inside bacteria is still in controversy.

It is well known that during the T-DNA transfer process, VirD2 plays a crucial role. VirD2 participates the whole process of T-DNA transfer, including the T-DNA processing, the T-complex export, the nuclear localization of T-complex, and the integration of T-DNA into the plant genome. In order to identify any additional protein(s) that may be involved in the T-DNA transfer, VirD2 was used as a bait protein in a "pull-down" assay experiment to fish agrobacterial proteins that can bind with VirD2 protein. In this study, an agrobacterial protein, designated VBP1, was identified to bind VirD2 specifically. Two genes highly homologous to the *vbp1* gene are also found in *A. tumefaciens* genome and designated *vbp2* and *vbp3*. To understand the role of these *vbp* genes in *A. tumefaciens*, three *vbp* genes in the genome were mutated; a triple mutation of the three *vbp* genes exhibited attenuated bacterial ability to cause tumors on plants. These suggest that an additional virulence factor is important for the T-DNA transfer process. The redundancy of three homologs for the VirD2-binding ability indicates a conserved function that is important for the gene transfer. VBP proteins can also bind some components of VirD4/VirB T4SS and influnce the mobilization of a derivative of RSF1010, pML122, from *A. tumefaciens* to *E. coli*. VBP proteins were defined as a new class of proteins: recruiting proteins that can recruit cytoplasmic nucleoprotein complex to the membrane transport apparatus.

Chapter 2 Materials and Methods

2.1. Bacterial Strains, Plasmids, Primers and Bacterial Culture

Bacterial strains and plasmids used in this study are described in Table 2.1 and 2.2 respectively. Media used in this study for culturing bacteria were prepared as described in Table 2.3. For long-term storage, all bacterial strains were saved in LB with 50% glycerol at – 80 °C freezer. The sequences and purposes of primers used in this study are described in Table 2.4. *Escherichia coli* strains were grown at 37°C in Luria-Bertani (LB) liquid or agar medium (Sambrook and Russell, 2001). *Agrobacterium tumefaciens* strains were grown at 28°C in MG/L or IB medium (Cangelosi *et al*., 1991). LB and MG/L media were supplemented with appropriate antibiotics when necessary. The preparation and concentration of antibiotics and related stock solutions are described in Table 2.5.

2.2. DNA Manipulations

DNA manipulations followed standard molecular protocols with some modifications. Most of the DNA manipulation protocols are mainly cited from *Molecular Cloning* (Sambrook and Russell, 2001). *E. coli* DH5α strain was routinely used as the host for cloning experiments.

2.2.1. Preparation of plasmid DNA

Plasmid DNA was prepared according to the protocol described in *Molecular Cloning* (Sambrook and Russell, 2001) with minimum modifications. *E. coli* cells from 2 ml of overnight (12~14 hours) culture were collected by centrifugation at 6, 000 rpm (Eppendorf 5417C) for 1 min and subsequently washed once with sterile water. The cell pellet was resuspended in 100 μl of ice-cold alkaline lysis solution I (50mM glucose, 25

Table 2.1. Bacterial strains used in this study

Bacterial strain	Relevant characteristic(s)[a]	Source or reference
Escherichia coli		
DH5α	*EndA1 hsdR17 supE44 thi-1 recA1 gyrA96 relA1 (argF-lacZYA)* U169 ϕ80d*lacZ.* For DNA cloning.	Bethesda Research Laboratories
BL21(DE3)	*F*$^-$ *omp*T *hsdS*$_B$ *(r*$_B^-$*m*$_B^-$*) gal dcm (DE3).* For protein expression.	Invitrogen
MT607	*Pro-82 thi-1 hsdR17 supE44 end44 endA1 recA56*	Finan *et al*. 1986
MT616	MT607 (pRK600), mobilizer	Finan *et al*. 1986
Agrobacterium tumefaciens		
C58	Wild type, nopaline-type pTiC58 plasmid	Laboratory collection
A348	Wild type, A136 (pTiA6NC) (octopine-type)	Laboratory collection
LBA4404	A *vir* helper; harbors disarmed Ti plasmid pAL4404, a T-DNA deletion derivation of pTiAch5 (octopine type) Rf^R, Sm^R.	Ooms *et al*., 1982
WR1715	Harbors a Ti plasmid with 70% of *virD2* deleted (aa 94-388).	Shurvinton *et al*., 1992
A348ΔB4	Derivative of A348, VirB4:Tn5::VirB	Stachel and Nester, 1986
A348ΔB8	Derivative of A348 in which *virB8* was deleted.	Laboratory collection
A348ΔB11	Derivative of A348 in which *virB11* was deleted, Km^R.	Laboratory collection
GMI9017	C58 cured of pAtC58, Sm^R, Sp^R Rf^R	Rosenberg and Huguet, 1984
GMI9017Δvbp2	Derivative of GMI9017 in which *vbp2* was deleted.	This study

GMI9017Δvbp2Δvbp3	Derivative of GMI9017Δvbp2 in which *vbp3* was disrupted by plasmid pUC19, Cb^R.	This study
A348Δvbp2	Derivative of A348 in which *vbp2* was deleted.	This study
A348Δvbp2Δvbp3	Derivative of A348Δvbp2 in which *vbp3* was disrupted by plasmid pUC19, Cb^R.	This study

[a]Amp, ampicillin; Cb, carbenicillin; Gm, gentamycin; Km, kanamycin; Nal, nalidixic acid; Rf, rifampicin; Sm, streptomycin; Tc, tetracycline.

Table 2.2. Plasmids used in this study

Plasmids	Relevant characteristic(s)[a]	Source or reference
pUC19	Cloning vector, ColE1 *oriV bla*, Amp^R	US Biochemical
pEX18Tc	Counterselectable plasmid carrying *sacB* marker, *oriT*, Tc^R	Hoang *et al*., 1998
pIG121Hm	Binary vector plasmid, carrying β-glucuronidase gene (*gusA*) between T-border, Km^R.	Ohata *et al*., 1990
pQM118	Derivative of pEX18Tc in which Tc^R was replaced by npt III from pCB301, Km^R.	This study
pMAL-cRI	Expression vector carrying full-length maltose binding protein (MBP); Amp^R	New England Biolabs
pSQ166	pMAL-cRI containing a *malE::VirD2* fusion encoding MBP-VirD2 with MBP fused onto VirD2 at the *Pst*I site of *virD2*; Amp^R	This study
pSQ190	pMAL-cRI containing a *malE::VirJ* fusion encoding MBP-VirJ with MBP fused onto VirJ at the *Pst*I site of *virJ*; Amp^R	This study
pSQ203	pMAL-cRI containing a *malE::VirD2* fusion encoding MBP-C-VirD2 with MBP fused onto VirD2 C-terminal domain at the *BamH*I site of the *virD2* gene; Amp^R	This study
pXQ15	pRSET-A carrying a 2.17 kb *Xho*I – *Kpn*I fragment containing the full length *katA* ORF fused in-frame with $(His)_6$, Amp^R.	Xu *et al*., 2001
pEXKmVD	pQM118 carrying a 2.183 kb *Hind*III fragment from vbp_2 downstream, Km^R.	This study
pEXKmVUD	pEXKmVD carrying a 1.395 kb *BamH*I fragment from vbp_2 upstream, Km^R.	This study
pUCvbp3	PUC19 carrying a 596 bp *BamH*I fragment from vbp_3 N-terminus without start code, Amp^R.	This study
pRvbp1	pRSET-A carrying a 947 bp *Xho*I fragment containing the full length *vbp1* ORF fused in-frame with $(His)_6$, Amp^R.	This study

pRvbp2	pRSET-B carrying a 952 bp *BamH*I fragment containing the full length *vbp2* ORF fused in-frame with $(His)_6$, Amp^R.	This study
pRvbp3	pRSET-B carrying a 936 bp *BamH*I fragment containing the full length *vbp3* ORF fused in-frame with $(His)_6$, Amp^R.	This study
pCBvbp1C	pCB301 carrying a 2054 bp *Hind*III fragment containing the 941 bp full length *vbp1* ORF as well as its 597 bp upstream and 516 bp downstream sequence, Km^R.	This study
pCBvbp2C	pCB301 carrying a 2031 bp *Hind*III fragment containing the 935 bp full length *vbp2* ORF as well as its 602 bp upstream and 494 bp downstream sequence, Km^R.	This study
pCBvbp3C	pCB301 carrying a 2027 bp *Hind*III fragment containing the 926 bp full length *vbp3* ORF as well as its 597 bp upstream and 504 bp downstream sequence, Km^R.	This study
pML122	A derivative of IncQ plasmid pRSF1010, Gm^R.	Labes *et al*., 1990

[a]Amp, ampicillin; Cb, carbenicillin; Gm, gentamycin; Km, kanamycin; Nal, nalidixic acid; Rf, rifampicin; Sm, streptomycin; Tc, tetracycline.

Table 2.3. Media used in this study and their preparation

Media or solutions	Preparation[a, b]	Reference
For routinely culturing *E. coli*		
LB (Luria broth)	Tryptone, 10 g; yeast extract, 5 g; NaCl, 10 g; pH 7.5	Sambrook *et al*., 1989
LB rich medium	Tryptone, 10 g; yeast extract, 5 g; NaCl, 5 g; glucose, 2 g	New England Biolabs
For preparing *E. coli* competent cells		
SOB	Tryptone, 20 g; yeast extract, 5 g; NaCl, 0.5 g; 10 ml of 250 mM KCl; pH 7.0, sterilize by autoclaving and add 5ml of filter-sterilized 2 M $MgCl_2$.	Sambrook *et al*., 1989
TB	10 mM PIPS, 55 mM $MnCl_2$, 15 mM $CaCl_2$, 250mM KCl;	Sambrook *et al*., 1989
For culturing *A. tumefaciens*		
MG/L	LB, 500 ml; mannitol, 10 g; sodium glutamate, 2.32 g; KH_2PO_4, 0.5 g; NaCl, 0.2 g; $MgSO_4 \cdot 7H_2O$, 0.2 g; biotin, 2 μg; pH 7.0.	Cangelosi *et al*., 1991
20 × AB salts	NH_4Cl, 20 g; $MgSO_4 \cdot 7H_2O$, 6 g; KCl, 3 g; $CaCl_2$, 0.2 g; Fe $SO_4 \cdot 7H_2O$, 50 mg.	Cangelosi *et al*., 1991
20 × AB buffer	K_2HPO_4, 60 g; NaH_2PO_4, 23 g; pH 7.0.	Cangelosi *et al*., 1991
0.5 M MES	MES, 97.6 g; pH 5.5.	Cangelosi *et al*., 1991
IB (Induction Medium)	20 × AB salts, 50 ml; 20 × AB buffer, 1 ml; 0.5 M MES (pH 5.5), 8 ml; 30% glucose, 60 ml (autoclaved separately before mix together).	Cangelosi *et al*., 1991
AB (Minimal Medium)	20 × AB salts, 50 ml; 20 × AB buffer, 50 ml; glucose, 4.5 g. (autoclaved separately before mix together).	Cangelosi *et al*., 1991

[a] Preparation for 1 liter, and sterilized by autoclaving; [b] For solid media, 1.5% agar was added.

Table 2.4. Primers used in this study

Primers	Sequence and purpose	Origin
Pvbp1-1	5'---ccgctcgagcatgaaacatcgctcg---3' (Amplify *vbp1* gene)	plasmid AT – 124902
Pvbp1-2	5'---ccgctcgagcccgctattcttcag---3' (Amplify *vbp1* gene)	plasmid AT – 123961
Pvbp1-3	5'---cgctgacgaactacacgccggcg---3' (Sequence *vbp1* gene in the expression vector)	plasmid AT – 124266
Pt7	5'---aatacgactcactatagg---3' (Sequence the genes in pRSET vector)	pRSET – T7 promoter
Pt7r	5'---ctagttattgctcagcg---3' (Sequence the genes in pRSET vector)	pRSET – T7 reverse primer
Pdow3	5'---tccaagcttgatcatatcccgcacag---3' (Amplify downstream of *vbp2* gene)	linear chromosome – 2045222
Pdow4	5'---cccaagcttccagcgcgagtaccag---3' (Amplify downstream of *vbp2* gene)	linear chromosome – 2047409
Pup10	5'---acaggatcccttcctgccacgcc---3' (Amplify upstream of *vbp2* gene)	linear chromosome – 2043756
Pup11	5'---gtgggatccatgaactttatacgcttc---3' (Amplify upstream of *vbp2* gene)	linear chromosome – 2045151
Pscreen1	5'---ctcgagagaggagacgcatcg---3' (Screen the *vbp2*-deleting mutant)	linear chromosome – 2044997
Pscreen2	5'---cagcgcatcctcgaactcctc---3' (Screen the *vbp2*-deleting mutant)	linear chromosome – 2045303
Pvbp3-1	5'---atgggatccagccttgaacatttgcc---3' (Amplify a fragment of *vbp3* gene)	linear chromosome – 2040241
Pvbp3-3	5'---gcgggatccactgcctgatgg---3' (Amplify a fragment of *vbp3* gene)	linear chromosome – 2040840
Ppuc1	5'---cggagcctatggaaaaacgcc---3' (Screen *vbp3*-disrupting mutant)	plasmid pUC19 – 881
Pvbps1	5'---cctctggaatggcccgtacag---3' (Screen *vbp3*-disrupting mutant)	linear chromosome – 2040192

Pvbps3	5'---gaggttgtgcgacgcaggc---3' (Screen *vbp3*-disrupting mutant)	linear chromosome – 2040895
Pvbp2p1	5'---gatggatccctcccttgatcatatc---3' (Amplify *vbp2* gene)	linear chromosome – 2045217
Pvbp2p2	5'---attggatcctgctttgacacctcg---3' (Amplify *vbp2* gene)	linear chromosome – 2046170
Pvbp3p1	5'---cat-gga-tcc-cag-cct-tga-aca-ttt-g---3' (Amplify *vbp3* gene.)	linear chromosome – 2040238
Pvbp3p2	5'---tgcggatccgtgaagctcaatcg---3' (Amplify *vbp3* gene)	linear chromosome – 2041180
Oligo G-402	5'---catacggcgtgacatcg---3' (Amplify T-DNA from "pull-down" T-complex.)	plasmid pIG121Hm
Oligo-intron	5'---acatggatccctacagg---3' (Amplify T-DNA from "pull-down" T-complex.)	plasmid pIG121Hm
nptIIIF	5'---gaagatctctcgagttggcagcatcacc---3' (Amplify nptIII from plasmid pCB301)	pCB301
nptIIIR	5'---gaagatcttactaaaacaattcatccag---3' (Amplify nptIII from plasmid pCB301)	pCB301
Pex18F	5'---gaagatctgttgaatactcatactcttc---3' (Amplify backbone of pEX18Tc)	pEX18Tc
Pex18R	5'---gaagatcttgtcagaccaagtttactcat---3' (Amplify backbone of pEX18Tc)	pEX18Tc
Pvbp1C1	5'---gaggaagcttaaaggatcctcggc---3' (Amplify *vbp1* with its flanking sequence)	Plasmid AT–123445
Pvbp1C2	5'---gcggaagcttgatgcttggtacg---3' (Amplify *vbp1* with its flanking sequence)	Plasmid AT–125499
Pvbp2C1	5'---gatcaagcttccaataattgcggcc---3' (Amplify *vbp2* with its flanking sequence)	linear chromosome – 2044606
Pvbp2C2	5'---gtctcaagcttgcgccgatagtg---3' (Amplify *vbp2* with its flanking sequence)	linear chromosome – 2046637
Pvbp3C1	5'---ccaaaagcttaaacgcgctgcaag---3' (Amplify *vbp3* with its flanking sequence)	linear chromosome – 2039641
Pvbp3C2	5'---cgagaagcttgcaaccggttcatg---3' (Amplify *vbp3* with its flanking sequence)	linear chromosome – 2041668

PvbpCS1	5'---gggctgcaggaattcgatatc---3' (Verify that plasmids pCBvbp1C, pCBvbp2C and pCBvbp3C were introduced into GMI9017Δvbp2Δvbp3)	.pCB301 near *Hind* III site
PvbpCS2	5'---gaggtcgacggtatcgataag---3' (Verify that plasmids pCBvbp1C, pCBvbp2C and pCBvbp3C were introduced into GMI9017Δvbp2Δvbp3)	pCB301 near *Hind* III site
Ptdna1	5'---gcggcggcgataactctcag----3' (Verify that T-DNA was co-immunoprecipitated by anti-VBP1 antibody)	Corresponding to the "*ipt*" gene of T-region in the Ti plasmid
Ptdna2	5'---ggaattgactatgagcagcttg---3' (Verify that T-DNA was co-immunoprecipitated by anti-VBP1 antibody)	Corresponding to the "*ipt*" gene of T-region in the Ti plasmid
Ptibac1	5'---gtggctgtgttggttatgagc---3' (Verify whether the co-immunoprecipitated DNA is T-DNA or Ti plasmid)	Corresponding to the "*virB1*" gene of Ti plasmid
Ptibac2	5'---gtcttcggatttgcggttgtc---3' (Verify whether the co-immunoprecipitated DNA is T-DNA or Ti plasmid)	Corresponding to the "*virB1*" gene of Ti plasmid
Prsf1	5'---ctgcgctaggctacacaccg---3' (Verify that plasmid pML122 was co-immunoprecipitated by anti-VBP1 antibody)	Region of RSF1010 in plasmid pML122
Prsf2	5'---cgacgaactccggcatgtgc---3' (Verify that plasmid pML122 was co-immunoprecipitated by anti-VBP1 antibody)	Region of RSF1010 in plasmid pML122

Table 2.5. Antibiotics and other stock solutions used in this study

(Sambrook *et al*., 1989; Cangelosi *et al*. 1991)

Antibiotics or soulutions	**Preparations**	**Stock Concentration (mg/ml)**	**Working Con. in *E. coli* (μg/ml)**	**Working Con. in *A. tumefaciens* (μg/ml)**
Ampicillin (Amp)	Dissolved in dH_2O, filter sterilized	100	100	100
Carbenicillin (Cb)	Same as above	100	100	100
Chloramphenical (Chl)	Dissolved in absolute ethanol	34	17	---
Gentamycin (Gm)	Dissolved in dH_2O, filter sterilized	50	10	50
Kanamycin (Km)	Dissolved in dH_2O, filter sterilized	100	50	100
Tetracycline (Tc)	Dissolved in absolute ethanol	5	10	5
Acetosyringone	Dissolved in dimethyl sulfoxide.	19.62	----	19.62
IPTG	Dissolved in dH_2O, filter sterilized	24	24	----
RNase	Dissolved in 10 mM Tris-HCl (pH7.5) and 15 mM NaCl	10	20	20
Proteinase K	Dissolved in dH_2O, filter sterilized	20	50	50

mM Tris-HCl, 10 mM EDTA, pH 8.0) supplemented with 100 mg/l RNase. The cell pellet must be vortexed to completely suspend the cells so that no clumps were visible in the suspension. Then, 200 µl of freshly prepared alkaline lysis solution II (0.2 N NaOH, 1% SDS) was added to the suspension. The contents were gently mixed by inverting the tube 3~5 times until the suspension became viscous and slightly clear solution. Adding 150 µl of alkaline lysis solution III (3 M potassium, 5 M acetate) to the viscous bacterial lysate, the mixture was inverted for 4~6 times to disperse alkaline lysis solution III through the viscous bacterial lysate. The bacterial lysate was extracted with equal volume of chloroform once. The aqueous upper layer in the emulsion was collected by centrifugation at 14, 000 rpm (Eppendorf 5417C) for 5 min and then was transferred to a clean eppendorf tube. Two volumes of ethanol were added to the supernatant to precipitate the plasmid DNA. The solution was mixed by vortexing and was stood for 2 minutes at room temperature so that the plasmid DNA is able to completely precipitate. The precipitated plasmid DNA was collected by centrifugation at 14, 000 rpm (Eppendorf 5417C) for 5 min. The DNA pellet was washed once with 70% ethanol and dried in a vacuum concentrator (Eppendorf 5301). The isolated plasmid DNA was dissolved in 20 ml (for low copy plasmid) or 50 ml (for high copy plasmid) of sterile water and stored at -20 °C, ready for subsequent use.

2.2.2. Preparation of *A. tumefaciens* genomic DNA

Total DNA of *A. tumefaciens* was prepared according to Charles and Nester (1993). Cells from 100 ml of overnight culture were collected by centrifugation at 4, 000 rpm for 5 min. The cell pellet was washed once with 4 ml of TES (10 mM Tris-HCl, 25 mM EDTA, 150 mM NaCl, pH 8.0), and then resuspended in 4 ml of TE buffer (10 mM Tris-

HCl, 25 mM EDTA, pH 8.0) by vortexing. Adding 500 µl of 5 M NaCl, 500 µl of proteinase K (5 mg/ml), and 500 µl of 10% SDS to the suspension, the mixture was incubated at 68 °C for 30 min to lyse the cells. The cell lysate was extracted once with 1:1 phenol-chloroform and pure chloroform respectively. The aqueous upper supernatant was transferred to a clean tube. Ammonium acetate solution (7.5 M) was added to the supernatant to a final concentration of 2 M and then 2 volumes of ethanol were added to the mixture to precipitate genomic DNA. The precipitated DNA was collected by centrifugation and washed once with 70% ethanol. The isolated genomic DNA was dried in a vacuum concentrator and then stored at -20 °C. When used, the genomic DNA can be dissolved in 500 µl of sterile water or TE buffer (10 mM Tris-HCl, 1 mM EDTA, pH 8.0).

2.2.3. Preparation of *E. coli* competent cells

Highly efficient competent cells of *E. coli* DH5α and BL21 (DE3) strains were prepared according to the Inoue protocol (Sambrook and Russell, 2001). Freshly growing *E. coli* colonies from LB agar plates were inoculated into 100 ml of SOB medium in a 1-liter conical flask and then allowed to grow at room temperature (about 19°C) with vigorous shaking (250 rpm). After the cells grow to an OD_{600} of 0.5~0.7, the culture was chilled on ice for 10 min and the cells were collected by centrifugation at 3, 600 rpm (Eppendorf 5810R) for 5 min at 4 °C. The cell pellet was resuspended in 30 ml of ice-cold TB buffer (10 mM PIPS, 55 mM $MnCl_2$, 15 mM $CaCl_2$, 250mM KCl, pH 6.7; all components except $MnCl_2$ were dissolved and autoclaved; 1M $MnCl_2$ solution was filter-sterilized and added to make TB buffer; store at 4 °C) and incubated on ice for 10 min. The cells were washed once by TB buffer and resuspended in 5 ml of ice-cold TB buffer. Thereafter DMSO was added to the cell suspension to a final concentration of 7%. The

competent cell suspension was aliquoted to pre-cooled sterile eppendorf tubes at 100 μl each and then frozen in liquid nitrogen immediately. The competent cells were stored at –80 °C freezer ready for using.

2.2.4. Amplification of DNA by polymerase chain reaction (PCR)

DNA fragments and related genes were amplified by the basic polymerase chain reaction (PCR). The composition of the PCR reaction mixture was shown as following.

10 × PCR buffer (without $MgCl_2$)	5 μl
$MgCl_2$ (25 mM)	3 μl
Primer 1 (10 μM)	2 μl
Primer 2 (10 μM)	2 μl
dNTPs (10 mM each)	1 μl
Template DNA (20-100 ng/μl)	1 μl
Taq DNA polymerase (1 unit/μl)	1 μl
Add distilled water to a final volume of 50 μl	

The basic PCR was normally run using the following program.

1 cycle	95 °C for 0.5 ~ 1 min
28 cycles	95 °C for 30 seconds
	Annealing at (Tm-5) °C for 30 seconds
	Extension at 72 °C for 1 min per kb
1 cycle	72 °C for 10 min

2.2.5. DNA digestion and ligation

DNA digestion and ligation were conducted according to the instruction manual provided by the enzyme supplier. Usually, the DNA digestion mixture comprised of buffer, DNA, restriction endonuclease and sterile water. The mixture was incubated at 37 °C for 2 hours to overnight as required. For single-digestion vectors, dephosphorylation is required for the subsequent ligation. In this case, one unit of shrimp alkaline phophatase (SAP) was added to the digestion mixture to conduct the dephosphorylation. The digested vectors and DNA fragments used for ligation were further purified using agarose gel electrophoresis and QIAGEN gel extraction kit. Bacteriophage T4 DNA ligase was used to ligate the digested DNA fragments to the digested vectors. The ligation was performed at 16 °C (or room temperature) for 3~4 hours (or overnight).

2.2.6. Agarose gel electrophoresis and DNA purification

DNA fragments were separated by agarose gel electrophoresis in TAE buffer (0.04M Tris-acetate, 0.001 M EDTA, pH 8.0) along with a standard DNA ladder (Fermentas). Normally, the concentration of agarose gel is 1% and ethidium bromide (EB) was directly added to the agarose gel to a final concentration of 0.5 μg/ml. The separated DNA fragments were recovered from the agarose gel by using QIAquick Gel Extraction Kit (QIAGEN). The recovery procedure provided by the manufacturer was briefly described as following. The agarose gel containing the band of the interesting DNA was cut out and transferred to a pre-weighted eppendorf tube. Three gel volumes (300 μl buffer to 100 mg gel) of QG buffer were added to the gel. The gel was allowed to incubate with the QG buffer in a 55 °C waterbath for 5~10 min to dissolve completely. For DNA fragments larger than 4 kb or smaller than 500 bp, one gel volume of isopropanol was added to the

mixture to increase the recovery efficiency of DNA. To bind DNA, the mixture was transferred to a QIAquick spin column in a 2-ml collection tube and centrifuged for 1 min at 14, 000 rpm (Eppendorf 5417C). The DNA bound column was washed once with 750 µl of PE buffer by centrifugation. After the flow-through was discarded, the column required one additional centrifugation to remove any residual ethanol. To elute DNA, the column was placed into a clean 1.5-ml tube and 50 µl of sterile water was applied to the center of the column membrane. The eluted DNA was collected by centrifugation at 14, 000 rpm (Eppendorf 5417C) for 1 min.

2.2.7. Transformation of bacterial cells

In most operations, DNA was transferred into *E. coli* cells by heat-shock following the standard protocol (Sambrook and Russell, 2001). Frozen competent cells (100 µl) were thawed on ice. The transforming DNA (up to 25 ng per 50 µl of competent cells), including plasmid and ligation product, was added to the competent cell suspension in a volume not exceeding 5% of that of the competent cells. The competent cells were mixed with the transforming DNA by swirling gently and were then incubated on ice for 30 minutes. The mixture of cells and DNA were heat-shocked at 42 °C for 90 seconds and immediately chilled on ice for 2 min. 900 µl of fresh LB medium were added to the transformed cells. The transformed cells were incubated at 37 °C for 45 min with shaking to allow the bacteria to recover and to express the antibiotic resistance marker encoded by the transforming DNA. The cells were collected by centrifugation and spread onto LB agar plates containing the appropriate antibiotic(s). Colonies usually appeared after overnight incubation at 37 °C.

Plasmids were introduced into *A. tumefaciens* by electroporation (Cangelosi *et al*., 1991). Occasionally, electroporation was also used to introduce plasmid DNA into *E. coli* cells (Sambrook and Russell, 2001). Plasmid DNA used for electroporation was prepared using alkaline lysis with SDS (Sambrook and Russell, 2001) and further purified by GeneClean Kit (QIAGEN). Electrocompetent bacterial cells were prepared by growing cells on agar plates, washing the bacteria cells extensively at low temperature, and then resuspending the cells in ice-cold 10% glycerol solution. The detail operation procedure was as follows. Bacterial cells were inoculated onto agar plates (*A. tumefaciens* onto MG/L plates, *E.coli* onto LB plates) and grew overnight (*A. tumefaciens* at 28 °C, *E.coli* at 37 °C) or until the bacterial cells reached a specific amount. The bacterial cells were scraped from the agar plates with a sterile wooden stick and then transferred to an eppendorf tube. The cells were washed twice with ice-cold sterile water and then washed once with ice-cold 10% glycerol. The cell pellet was resuspended in 50μl of ice-cold 10% glycerol. The transforming plasmid DNA (0.5~1 μg in 10 μl or less of water) was added to the electrocompetent bacterial cell suspension. The mixture of cells and DNA was incubated on ice for 2 min and then transferred into a pre-chilled 0.2-cm BioRad electroporation cuvette. Gene Pulser II Electroporation System (BioRad) was set at 25 μF capacitance, voltage of 2.5 kV and the pulse controller to 400 Ω (for *E. coli* set to 200 Ω). The condensation and moisture on the outside of the cuvette should be wiped away with tissue paper before the cuvette was slide into the shocking chamber base. After delivering a pulse of electricity to the cells at the settings indicated above, 1 ml of liquid medium (MG/L to *A.tumefaciens*, LB to *E. coli*) was immediately added to the electroporated cells. Then, the mixture was transferred to a 15-ml culture tube and

cultured for 1 hour (*A. tumefaciens* at 28 °C, *E.coli* at 37 °C) with shaking to allow the electroporated bacterial cells to recover and to express the antibiotic resistance marker encoded by the transforming plasmid. The cells were collected by centrifugation and spread onto agar plates (*A. tumefaciens* onto MG/L plates, *E. coli* onto LB plates) containing selectable antibiotics. Colonies usually appeared on the third day for *A. tumefaciens* and on the second day for *E. coli*. In successful transformations, the time constant was typically about 9 milli-seconds for *A. tumefaciens* and 4.5 milli-seconds for *E. coli*.

2.2.8. DNA sequencing

Sequencing templates (plasmids or PCR products) were purified by using GeneClean Kit (QIAGEN). The sequencing PCR run mixture contains 2 μl of BigDye^{TM} Ready Mix (v 3.0), 0.5 μl of primer (10 μmol l^{-1}), 2 μl of template (purified plasmids or PCR products, 100~200 ng μl^{-1}) and 5.5 μl of deionized water. The total volume of the run mixture is 10 μl. The cycle sequencing was normally performed using the following program.

1 cycle	96 °C for 0.5 ~ 1 min
25 cycles	96 °C for 15 seconds
	Annealing at 50 °C for 15 seconds
	Extension at 60 °C for 4 min
	Hold at 4 °C until ready to purify

After the cycle sequencing is finished, the contents in the PCR tube were spun down and then were transferred into a clear 1.5-ml tube. 25 μl of absolute ethanol and 1 μl of 3

M sodium acetate were added to the tube. The contents in the tube were mixed by vortexing and the tube was allowed to stand at room temperature for 15 min to precipitate the extension products. The pellet was collected by centrifugation at 14,000 rpm (Eppendorf 5417C) for 20 min. The pellet was washed with 70% ethanol twice and then centrifuged at 14,000 rpm (Eppendorf 5417C) for 10 min. After the supernatants were carefully aspirated from the tube, the pellet was dried in a vacuum centrifuge for 10~15 minutes and stored at –20 °C. This pellet was ready to be submitted for running electrophoresis.

2.3. Protein Analytical Techniques

2.3.1. SDS-PAGE gel electrophoresis

Proteins were separated by SDS-PAGE gel electrophoresis according to their molecular weight. The buffers and solutions used in SDS-PAGE gel electrophoresis are listed in Table 2.6. The electrophoresis apparatus used in SDS-PAGE gel electrophoresis was the Mini-Protean III Electrophoresis Cell (BioRad). The apparatus was assembled according to the instruction manual provided by the manufacturer. Acrylamide/bis-acrylamide solution was prepared as described in Molecular Cloning (Sambrook *et al*, 1989) and stored in the dark at 4 °C. Ammonium persulfate (APS) solution was freshly prepared before each use. Separating gel buffer and stacking gel buffer were stored at room temperature. Electrophoresis buffer was prepared as 10 × stock solution and stored at room temperature. Sample-loading buffer was prepared without DTT and stored at room temperature; when used, DTT was added to the sample-loading buffer from 1 M DTT stock solution. DTT stock solution was stored at –20 °C. SDS stock solution was stored at room temperature.

Table 2.6. Buffers and solutions used in SDS-PAGE gel electrophoresis

Buffer or Solution	Concentration	Preparation
Acrylamide/bis-acrylamide solution	30% acrylamide, 0.8% bis-acrylamide.	150 g acrylamide, 4 g bis-acrylamide, dissolved in 500 ml H_2O and filtered with Whatman paper
Separating gel buffer	3 M Tris-HCl, pH 8.8	181.5 g Tris dissolved in 500 ml H_2O and adjusted pH to 8.8 with HCl
Stacking gel buffer	0.5 M Tris-HCl, pH 6.8	30 g Tris, 10 ml concentrated HCl dissolved in 500 ml H_2O and adjusted pH to 6.8
Ammonium persulfate (APS) solution	10% (W/V) ammonium persulfate	1 g ammonium persulfate dissolved in 10 ml H_2O
SDS stock solution	10% (W/V) SDS	50 g SDS dissolved in 500 ml H_2O
Sample-loading buffer	2 × buffer 100 mM Tris-HCl, 4% SDS, 20% glycerol, 0.002% bromophenol blue	16 ml Stacking gel buffer, 3.2 g SDS, 16 ml glycerol, 1.6 mg bromophenol blue bring to 80 ml.
DTT stock solution	1 M DTT	1.543 g DTT dissolved in 10 ml H_2O
Electrophoresis buffer	10 × buffer 0.25 M Tris, 2.5 M Glycine, 1% SDS, pH 8.3	30.2 g Tris, 188.0 g Glycine, 10 g SDS dissolved in 1000 ml H_2O and adjusted pH to 8.3
Staining solution	0.5 g Coomassie Brilliant Blue R250 in 180 ml methanol: H_2O (1:1, V/V) and 20 ml glacial acetic acid	Coomassie Brilliant Blue R250 should be dissolved in methanol, and then add H_2O.
Destaining solution	Methanol: H_2O: glacial acetic acid (V/V) = 9:9:1	

For the routine analysis of proteins, 10% PAGE gel was used. For proteins whose molecular weight is below 10 kDa, 15% or 17.5% PAGE gel was used. The polyacrylamide gels (PAGE) were prepared as follows.

Separating polyacrylamide gels

Gel concentration	7%	10%	12%	15%	17.5%
Separating gel buffer	1.9 ml	1.9 ml	1.9 ml	1.9ml	1.9ml
Acrylamide/bis-acrylamide solution	3.5 ml	5 ml	6ml	7.5 ml	8.75ml
10% (W/V) SDS	150 µl	150 µl	150 µl	150 µl	150 µl
10% (W/V) APS	150 µl	150 µl	150 µl	120 µl	100 µl
TEMED	9 µl	9 µl	9 µl	8 µl	6 µl
H_2O	9.21 ml	7.71 ml	6.71 ml	5.24 ml	4.01 ml
Total volume (ml)	15	15	15	15	15

Stacking gel was 2.5% and prepared by mixing 2 ml stacking gel buffer, 1.3 ml acrylamide/bis-acrylamide solution, 80 µl 10% SDS, 80 µl 10% APS, 8 µl TEMED and 4.5 ml H_2O. Before loading, 40 µl of protein sample was mixed with 50 µl sample-loading buffer and 10 µl of 1 M DTT solution. The sample mixture was heated at 95 °C for 5 minutes to reduce the disulfide bonds. Usually the gel was run at a constant voltage of 100 V until the bromophenol blue reached the bottom of the gel. After the gel was stained in staining solution for 2~4 hours, the gel was destained with destaining solution for 3~4 times and the protein bands would appear.

2.3.2. Western blot analysis

For Western blot analysis, proteins separated by SDS-PAGE gel electrophoresis were transferred electrophoretically to an Immun-Blot™ PVDF membrane (Bio-Rad)

with Hoefer TE 22 Mighty Small Transfer Tank Transfer Unit (Amersham Pharmacia Biotech). The transfer buffer used in this study was Towbin buffer [48 mM Tris, 38 mM Glycine, 0.37% (W/V) SDS, pH 8.3, 20% (V/V) Methanol]. Transfer was performed either at 100 mA for 2~3 hours or at 60 mA overnight. After transfer was completed, the PVDF membrane was removed from the sandwich and then incubated with 10% non-fat milk in TBST buffer [20 mM Tris, 150 mM NaCl, 0.1% (V/V) Tween-20, pH 7.5] to block the remaining protein-binding sites in the PVDF membrane. The blocking reaction required 2 hours at room temperature on an orbital shaker. After blocking reaction finished, the PVDF membrane was washed at least three times with TBST buffer for ten minutes each on a rocking platform. Then, the PVDF membrane was incubated with the TBST-diluted primary antibody (usually in a 1:5000 dilution) for 1 hour at room temperature while continuously rocking the sample. To remove the unbound primary antibody, the PVDF membrane were washed at least three times as the aforementioned. After washing finished, the PVDF membrane was incubated with the TBST-diluted second antibody (usually in a 1:10000 dilution). The unbound second antibodies were washed away by three extensive TBST washes. The fluorescence produced by the HRP-conjugated second antibody was detected with the ECL Western blotting analysis system (Amersham Life Science).

2.4. Pull-down Assay

2.4.1. Preparation of recombinant proteins

The plasmids encoding maltose-binding protein (MBP), MBP-VirD2 fusion protein, MBP-VirJ fusion protein, and MBP-VirD2 C-termini (MBP-C-VirD2) fusion protein were introduced into *E. Coli* respectively. The bacterial cells were grown to a

concentration of approximately OD_{600} = 0.5; isopropyl β–D-thiogalactoside (IPTG) was added to the cultures in a final concentration of 0.3 mM to induce the expression of fusion proteins. The bacterial cultures were allowed to grow for additional 2~3 hours. All the subsequent operations were performed at 4°C. The cells of 500 ml culture were harvested by centrifugation and resuspended in 25 ml lysis buffer [150 mM NaCl; 10 mM EDTA; 10 mM EGTA; 20 mM Tris; 2 mM DTT; 2 mM phenylmethylsulfonyl fluoride (PMSF); 0.25% Tween-20; 10 mg l^{-1} leupeptins; 5 mg l^{-1} antipain; pH = 7.4]. The cell suspension was sonicated to near clarity and centrifuged at 17,000 × g for 20 min. Aliquots of the supernatant were stored at -20°C. Fusion protein purification was conducted as described by Pan *et al*. (1995) with minor modifications. Briefly, 2 ml amylose resin (New England Biolabs) was washed five times with column buffer (30 mM NaCl; 2 mM EDTA; 2 mM EGTA, 20 mM Tris; 1 mM DTT; 2.5 mM $MgCl_2$; 1 mM PMSF; 2 mg l^{-1} leupeptins, 1 mg l^{-1} antipain, pH = 7.4). Then, 15 ml *E. coli* lysate, which was diluted five times from 3 ml supernatant with 12 ml column buffer, was added to the amylose resin and incubated for 45 min with rocking. The protein-bound amylose resin was loaded to a column. After the column was washed with 15 ml column buffer, the bound proteins were eluted with column buffer containing 10 mM maltose. The purity of the purified fusion proteins were examined by 10% SDS-PAGE. All the purified fusion proteins were concentrated by Centra-prep and freeze-dried.

2.4.2. Isolation of VirD2-binding proteins

To prepare *A. tumefaciens* protein extracts, *A. tumefaciens* strain A348 was grown at 28°C in MG/L medium for 16~18 h. The bacterial cells were collected by centrifugation, washed once with water, and then resuspended to OD_{600} of 0.4 in the IB

medium containing 200 μM acetosyringone (AS). The IB cell cultures were incubated at 28°C for another 16~18 h with shaking. The cells harvested from 5 L of IB cell culture were washed once with water, and resuspended in 15 ml of *Agrobacterium* lysis buffer A (30 mM NaCl; 10 mM $MgCl_2$; 5 mM EDTA; 5 mM EGTA; 20 mM Tris; 2 mM DTT; 2 mM PMSF; 0.5% Triton-100; 10 mg l^{-1} leupeptins; 5 mg l^{-1} antipain; pH = 7.4). The cells were disrupted by French Press (cell pressure: 35K psi). The protein extract was collected by centrifugation at 12,000 × g for 15 min at 4°C and diluted with equal volume of lysis buffer A (but without Triton-100). The aliquots of the extract were stored at –20°C until the pull-down assay.

To conduct the pull-down assay, *E. coli* protein extracts containing MBP, MBP-VirJ, MBP-C-VirD2, or MBP-VirD2 were prepared as described above and allowed to incubate with pre-equilibrated amylose resins (50% v/v) for 45 min at 4°C with rocking. Care was taken to ensure that an equal amount of each of the proteins remained bound to the resin. The protein-bound amylose resins were washed with column buffer. Then, an equal amount of *Agrobacterium* protein extract was added to each of the protein-bound amylose resins and incubated for 60 min at 4°C with rocking. The resulting amylose resins were loaded to columns and washed with 6~10 column volumes of column buffer. The bound protein complexes were eluted with column buffer containing 10 mM maltose and concentrated by Centra-prep. The concentrated pull-down protein samples were freeze-dried and stored at -20°C.

2.5. In-gel Digestion, MALDI-TOF Analysis and Tandem MS Sequencing

All the pulled down protein samples were adjusted to the same protein concentration and separated by 10% or 12% SDS-PAGE gel. Protein bands were carefully excised from Coomassie Blue-stained gels, cut into small pieces, and then destained with several washes of 50 mM ammonium bicarbonate in 50% aqueous acetonitrile. The gel pieces were dehydrated with 100% acetonitrile, dried in Savant Speed-vac, rehydrated with a solution containing 10 mM DTT and 100 mM ammonium bicarbonate, and incubated at 57°C for 60 min to reduce the disulfide bonds. The reduced sulfhydryl group was alkylated by 55 mM iodoacetamide in 100 mM ammonium bicarbonate at room temperature for 60 min. After alkylation, the gel pieces were washed with 100 mM ammonium bicarbonate solution, dehydrated with 100% acetonitrile at least 6 times, and then dried in Savant Speed-vac again. Sequencing grade modified trypsin (12.5 mg l^{-1} in 50 mM ammonium bicarbonate, pH 8.0) was added to the dried gel pieces and incubated overnight at 37°C. The resulting trypsinized peptides were extracted with 20 mM ammonium bicarbonate solution, 5% formic acid in 50% aqueous acetonitrile, and 100% acetonitrile, respectively. The extracted peptides were combined, lyophilized, and then resuspended in 0.1% trifluoroacetic acid (TFA). An aliquot of the resuspended peptides was spotted onto the stainless steel MALDI sample plate and overlaid with equal volume of matrix solution (20 g l^{-1} α-cyano-4-hydroxycinnamic acid in 0.1% TFA; 50% aqueous acetonitrile). The sample/matrix mixture was air dried. An Applied Biosystems Voyager-DE STR MALDI mass spectrometer was used to acquire the MALDI-time of flight (TOF) spectra. The instrument was operated in the positive reflector delayed extraction mode. Peptide mass spectra were searched against theoretically derived spectra

from proteins in the nonredundant databases of National Center for Biotechnology Information (NCBI) to match peptide mass fingerprints.

Partial amino acid sequence of a single peptide was obtained by quadrupole-time of flight (Q-TOF) hybrid tandem mass (MS/MS) spectrometer. For Q-TOF MS/MS analysis, the trypsinized peptide samples were concentrated and desalted by the Zip-Tip method. Based on the mass spectra acquired by MALDI-TOF, dominant peptides were selected for MS/MS analysis. After peptides were selected, the Q-TOF mass spectrometer was automatically switched from MS to MS/MS mode and the Q-TOF MS/MS spectra were collected. The amino acid sequences were determined by searching the Q-TOF MS/MS spectra against the NCBI non-redundant protein databases.

2.6. Expression of VBP Proteins and Generation of Anti-VBP Protein Antibodies

2.6.1. Expression and purification of VBP proteins

To over-express VBP1, VBP2 and VBP3 proteins, the full-length *vbp1, vbp2, vbp3* genes were amplified from *A. tumefaciens* C58 genomic DNA by PCR and were subcloned into vector pRSET-A or pRSET-B (Invitrogen™) to make in-frame fusions to the histidine (His) tag. The resulting plasmids pRvbp1, pRvbp2, and pRvbp3 were introduced to *E. coli* strain BL21 (DE3) to over-express the His-VBP1, His-VBP2, and His-VBP3 proteins, respectively. The IPTG-induced *E. coli* BL21 cells harboring these plasmids were collected and resuspended in lysis buffer 2 (300 mM NaCl; 2 mM PMSF; 50 mM sodium phosphate, pH 7.4). Bacterial cells were disrupted by French Press (cell pressure: 35K psi). The pellet was collected by centrifugation at 17,000 × g for 15 min at 4°C, resuspended in denaturing column buffer (8 M urea; 300 mM NaCl; 2 mM PMSF;

50 mM sodium phosphate; pH 7.4), and then incubated at room temperature for 1 hour with shaking. The supernatant was collected by centrifugation and incubated with the pre-equilibrated TALON metal affinity resin (Clontech) at room temperature for 1 hour. After His-VBP protein was bound to TALON metal affinity resin, the resin was loaded to a column and washed with 10~15 resin volumes of denaturing column buffer. His-VBP protein was eluted with denaturing column buffer plus 150 mM imidazol. In each purification operation, eight fractions of the eluate were collected with 1.5 ml per fraction. The purity and concentration of His-VBP in each collected fraction were assessed by SDS-PAGE with standard BSA as a reference protein. The collected fractions with the highest concentration of His-VBP were combined and further purified by preparative SDS-PAGE electrophoresis. After the His-VBP protein was separated by the preparative SDS-PAGE gels, the gels were shortly stained with 1 M KCl and the lightly white protein band was then cut out with a scalpel. The gel slices were placed in a dialysis tube (Gibco) containing 1× electrophoresis buffer (Table 2.6). The protein in the gel slices was eluted by electrodialysis in a transfer apparatus with the electrophoresis buffer. The electrodialysis was performed in a cold room (4~8 °C) at a constant current of 100 mA for overnight. The protein eluted from the gel slices was transferred to a clear dialysis tube and dialyzed against five liters of water in a cold room (4~8 °C) for overnight. After the dialysis is finished, a large amount of protein precipitate should appear in the dialysis tube. The protein precipitate was collected by centrifugation and dissolved in small amount of Tris-HCl buffer (50 mM Tris, pH 8.2). The concentration of the His-VBP protein was adjusted to 0.2 g l^{-1}. The purified His-VBP protein was ready to inject into rabbit to generate anti-His-VBP antibody.

2.6.2. Generation of anti-His-VBP antibodies

To obtain the polyclonal antibody against VBP proteins, the purified His-VBP1, His-VBP2 and His-VBP3 were intramuscularly injected into New Zealand wild type female rabbits respectively. A small amount (about 5 ml) of preimmune blood was drawn from each rabbit prior to any injections so that we can examine them for background activity. Zero point five ml of purified His-VBP protein (0.1 mg) was mixed and emulsified with an equal volume of Incomplete Freund's Adjuvant (IFA). The freshly prepared emulsion was immediately injected into one limb of the rabbit. The first boost was done four weeks later. The dosage for each booster is 50 μg, which was emulsified in 0.5 ml of IFA emulsion and injected into another limb. After the first booster, the rabbit would boost every week and the limbs were used in rotation during the subsequent boost injections. A small amount (about 5 ml) of blood was drawn before each boost injection. The serum was used to test the antibody titers by Western blotting. Usually, large bleed would be done after the sixth boost. The blood collected from rabbit was allowed to clot at room temperature for overnight. The antiserum was collected from the clot by centrifugation at 1,500 × g for 10 minutes at room temperature and was stored at –20 °C.

2.7. Pulling down of *A. tumefaciens* Proteins by VBP Proteins

2.7.1. Binding of VBP proteins to T-complex (or VirD2)

To detect the binding of VBP protein to T-complex (or VirD2), the denaturant urea and salt were removed from the protein-bound resin. His-VBP bound resin was washed with buffers having NaCl gradient from 300 to 0 mM and urea gradient from 8 to 0 mM. Eventually, the His-VBP bound resin was washed with incubating buffer (2.5 mM $MgCl_2$; 50 mM NaCl; 2 mM PMSF; 20 mg l^{-1} leupeptines; 30 mM Tris-HCl; pH 7.4). To

refold the denatured His-VBP protein, the His-VBP bound resin was incubated with incubating buffer at 4°C for 60 min with rocking, and then washed three times with incubating buffer. T-complex-containing *A. tumefaciens* extract was prepared as described for the pull-down assay, but *Agrobacterium* lysis buffer A was replaced by incubating buffer. His-KatA (Xu *et al*., 2001) was used as a negative control. The resin-bound T-complex was eluted with incubating buffer containing 150 mM imidazol. The eluted proteins (or T-complex) were concentrated and freeze-dried. VirD2 and VirE2 in the pulled-down T-complex were analyzed by Western blot and further identified by MALDI-TOF. To get the T-strand from the pulled-down T-complex, the T-complex-containing fraction collected from eluate was extracted with phenol:chloroform immediately. Detection of T-strand in the pulled-down T-complex was done by PCR. To test the strength of the VirD2-VBP1 interaction, $MgCl_2$ and NaCl in the incubating buffer were adjusted to different concentrations ($MgCl_2$: 0mmolL^{-1} or 2.5mmolL^{-1}; NaCl: 0mmolL^{-1}, 50mmolL^{-1}, 100mmolL^{-1}, 200mmolL^{-1} or 300mmolL^{-1}).

2.7.2. Binding of VBP proteins to T4SS components

The procedure for the binding of VBP proteins to T4SS components was similar to that for the binding of VBP protein to VirD2 (or T-complex). However, because most of the T4SS components are membrane proteins and the extraction of T4SS components may require detergent, T4SS components-containing *A. tumefaciens* extract was prepared using different buffers. Two different kinds of buffer were used to prepare the T4SS components-containing *A. tumefaciens* extract and to conduct the binding assay. One kind of the buffer was the same buffer as in the binding of VBP protein to T-complex (2.5 mM $MgCl_2$; 50 mM NaCl; 2 mM PMSF; 20 mg l^{-1} leupeptines; 30 mM Tris-HCl; pH

7.4). The other kind of buffer contained 0.5% Triton-100. The composition of the second buffer is 2.5 mM $MgCl_2$, 50 mM NaCl, 2 mM PMSF, 20 mg l^{-1} leupeptines, 30 mM Tris-HCl, pH 7.4, and 0.5% Triton-100. Other operations were the same as described in the binding of VBP protein to T-complex. The pulled-down T4SS components were analyzed by Western blot.

2.8. Co-immunoprecipitation

2.8.1. Co-immunoprecipitation of T4SS components by anti-VBP1 antiserum

A. tumefaciens A348 cells harvested from 1 liter of IB culture were resuspended in 4 ml lysis buffer B (2.5mmolL^{-1} $MgCl_2$, 50mmolL^{-1} NaCl, 2mmolL^{-1} PMSF, 20μg/ml leupeptines, 10μg/ml antipain, 50mmolL^{-1} Tris-HCl, pH 7.4). The cells were disrupted by French Press (cell pressure: 35K psi). To dissolve membrane VirB/D4 proteins, Triton X-100 was added to a 0.5% final concentration and the mixture was incubated for 1 h at 4°C with rocking. The supernatant fraction was collected by centrifugation at 12,000 × g for 20 min at 4°C and was diluted 1 time with lysis buffer B. To reduce the background of nonspecific proteins, the diluted protein extract was pre-cleared with protein A-Sepharose and preimmune serum (Sambrook and Russell, 2001). Preimmune serum was added to the *Agrobacterium* protein extract at a dilution of 1:150 and 50% (w/v) slurry of protein A-Sepharose (in lysis buffer B) was added at a ratio of 1:6 (protein A-Sepharose:extract). The mixture was incubated at 4°C for 1 h with rocking. Protein A-Sepharose and non-specifically-coprecipitated proteins were removed by centrifugation at 5,000 g. The supernatant was the pre-cleared protein extract and was used to perform the co-immunoprecipitation. To co-immunoprecipitate the VBP1 binding proteins, anti-VBP1

antiserum was added to the pre-cleared protein extract at a dilution of 1:200 and 50% (w/v) slurry of protein A-Sepharose (in lysis buffer B) was added at a ratio of 1:8 (protein A-Sepharose:extract). The mixture was incubated at 4°C for 4 h with rocking. Protein A-Sepharose and co-immunoprecipitates were collected by centrifugation. The protein A-Sepharose and co-immunoprecipitates were washed twice with lysis buffer B supplemented with 0.1% Triton X-100 and three times with lysis buffer B. Nonreducing SDS loading buffer was added to the protein A-Sepharose and co-immunoprecipitates directly. The co-immunoprecipitated proteins were separated by SDS-PAGE and analyzed by Western blot. To demonstrate that the non-specifically-coprecipitated proteins were removed from the pre-cleared protein extract, two controls (protein A-Sepharose incubated with pre-cleared protein extract as well as protein A-Sepharose incubated with both pre-cleared protein extract and preimmune serum) were conducted.

2.8.2. Co-immunoprecipitation of T-complex by anti-VBP1 antiserum

The procedure for the co-immunoprecipitation of T-complex is similar to the co-immunoprecipitation of T4SS components. For the preparation of AS-induced *Agrobacterium* cell extract, the disrupted cells were not treated by 0.5% Triton X-100. The protein extract did not contain any detergent. Sepharose beads and co-immunoprecipitates were washed five times with lysis buffer B. The co-immunoprecipitates were eluted by incubation for 20 min at 96 ºC with the buffer of 10mmolL^{-1} Tris-HCl, pH 6.8. The eluted co-immunoprecipitates were used as the template to amplify the T-DNA. Proteins in the eluted co-immunoprecipitates were separated by SDS-PAGE and detected by Western blot.

2.8.3. Co-immunoprecipitation of plasmid pML122 by anti-VBP1 antiserum

For the co-immunoprecipitation of plasmid pML122, *A. tumefaciens* strains harboring pML122 were grown in MG/L liquid medium and did not undergo AS-induction. Other procedures were the same as for the co-immunoprecipitation of T-complex.

2.9. Mutation at *vbp* Genes

2.9.1. Mutation at *vbp2*

To generate *vbp2* mutation, the *sacB*-based gene replacement strategy (Hoang *et al*., 1998) was employed. The *sacB* gene encodes levansucrase, which synthesizes lavens (high molecular-weight fructose polymers) in the presence of sucrose. The accumulation of lavens in the periplasm of $Gram^-$ bacteria is toxic and thus causes the bacterial cells to die. To obtain a *sacB*-based suicide vector suitable for *A. tumefaciens* gene replacement, we replaced the Tc^R gene in plasmid pEX18Tc (Hoang *et al*., 1998) with Km^R gene. Primers Pex18F and Pex18R were used to amplify a 5-kb non-Tc^R-resistance fragment from plasmid pEX18Tc. A 1.04-kb Km^R-encoding cassette fragment was amplified by primers nptIIIF and nptIIIR from plasmid pCB301 (Xiang *et al*., 1999). These two fragments were ligated to generate the Km^R-plasmid pQM118. The *vbp2* gene replacement vector was constructed as follows. First, a 2.183-kb *vbp2* downstream fragment was amplified by primers Pdow3 and Pdow4 and inserted to the *Hind* III site of pQM118 to generate plasmid pEXKmVD. Then, primers Pup10 and Pup11 were used to amplify a 1.395-kb v*bp2* upstream fragment. Finally, the upstream fragment was inserted to the *BamH* I site of pEXKmVD to produce plasmid pEXKmVUD. The purified plasmid pEXKmVUD was introduced to *A. tumefaciens* cells by electroporation. The electroporated *A. tumefaciens* cells were plated on kanamycin-containing MG/L agar

plate to select for single cross-over transformants. The Km^R-colonies were purified once by streaking on fresh kanamycin-containing MG/L plate, and then were plated on MG/L agar plate containing 5% sucrose to select the double cross-over colonies. The *vbp2* mutant was identified from the Km-sensitive and sucrose-resistant colonies by PCR.

2.9.2. Mutation at *vbp3*

To generate *vbp3* mutation, single cross-over strategy was adopted to disrupt *vbp3* gene (Miller and Mekalanos, 1988). When the plasmid pUCvbp3 carrying a *vbp3* internal fragment was introduced to *A. tumefaciens*, the whole plasmid could insert into the *vbp3* gene of *A. tumefaciens* by homologous recombination and thus disrupt the *vbp3* gene. The plasmid pUCvbp3 was constructed by amplifying a 591-bp *vbp3* fragment, which is from the 4~595 nuleotides of the *vbp3* ORF (The full length of the *vbp3* ORF is 936 bp), with primers Pvbp3-1 and Pvbp3-3 and ligating it to the *BamH* I site of pUC19 to form the Ap^R-resistant plasmid pUCvbp3. The plasmid pUCvbp3 was electroporated to *A. tumefaciens* cells. After electroporation, the *vbp3* insertion mutant was selected by plating the electroporated cells on MG/L agar plate containing ampicillin and further confirmed by PCR.

2.10. Virulence Assays

A. tumefaciens strains were grown in MG/L liquid medium overnight at 28°C supplemented with appropriate antibiotics. The bacterial cells were collected by centrifugation and resuspended in fresh MG/L medium. Cell concentrations were adjusted to OD_{600} = 0.05, 0.1 and 1. The leaves of *Kalanchoe* plants were wounded with a hypodermic needle. Two μl of bacterial cell suspension was inoculated onto each

wound area. Each strain was inoculated in three different cell concentrations. Each inoculation was repeated at least two times on different leaves. The tumors were photographed 30~40 days after inoculation.

2.11. Conjugation Assay

Donor *Agrobacterium* strains were cultured in MG/L overnight at 28 ºC with appropriate antibiotics. Recipient *E. coli* MT607 (or helper MT616) were cultured in LB overnight at 37 ºC. Cells were washed with water twice and resuspended in cell concentration of OD_{600nm} = 1.0. Equal volume of donor and recipient cell suspension (or with helper) were mixed. Small amount of the cell mixture was diluted and plated on AB agar plate with appropriate antibiotics to count the number of input donor. For conjugation assay, cell mixture was spotted on LB agar plate and incubated overnight at 28 ºC. The agar plug was excised, suspended in water, and vigorously shaken to dislodge mating cells. Cells were collected by centrifugation and resuspended in water. Serial dilutions were then plated onto LB agar plate with gentamycin antibiotic and grown at 37 ºC to select and count transconjugant *E. coli.* cells.

Chapter 3 Identification and Characterization of a VirD2-binding Protein

3.1. Identification of a Novel VirD2-binding Protein

As we discussed before, VirD2 is a major player of the T-DNA transfer. Any protein that is involved in the T-DNA transfer may directly or indirectly interact with VirD2. Traditionally, two hybrid system was used to screen protein-interacting partners. However, this genetic approache often gave false results and the derived results required further verification by *in vitro* binding assay. In this study, we adopted a biochemical approach, which is a pull-down assay, to screen for protein-interacting partners. This biochemical approach would enable us to identify protein-interacting partners expeditiously and unequivocally.

To identify additional bacterial proteins that may be involved in T-DNA processing and T-complex movement, we fused VirD2 protein to maltose binding protein (MBP). MBP is a periplasmic protein encoded by *malE* gene of *E. coli*. It can specifically bind maltose, which allows a one-step purification for the MBP fusion proteins. So, the recombinant MBP-VirD2 protein should be able to bind to amylose resin specifically and can be used as an affinity ligand to pull down VirD2-binding proteins from AS-induced *A. tumefaciens* protein extracts. When we initially conducted the pull-down assay, we found that MBP-VirD2 fusion protein was easy to be degraded to smaller protein molecules (lane 3 in Fig. 3.1). The degradation of MBP-VirD2 made it difficult to identify any possible VirD2-binding proteins because the degraded MBP-VirD2 fusion proteins may overlay the potential VirD2-binding proteins during the SDS-PAGE

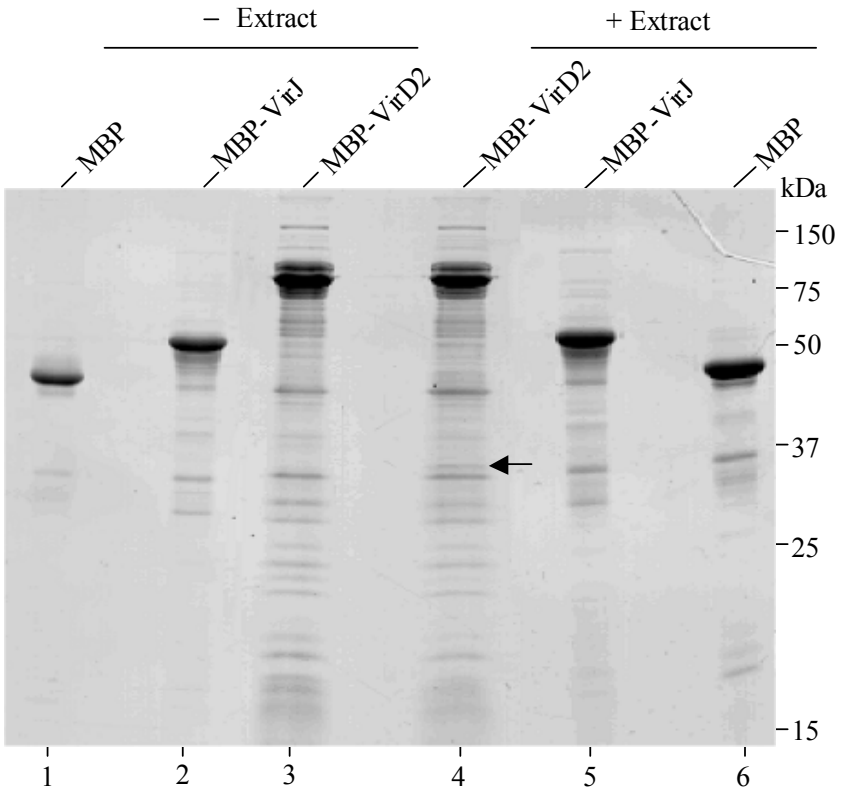

Fig. 3.1. Coomassie blue-stained SDS-PAGE analysis of proteins pulled down by MBP-VirD2 fusion protein. *E. coli* cells expressing MBP, MBP-VirJ and MBP-VirD2 were sonicated. The supernatants were loaded onto amylose resin columns; the unbound proteins were washed away. As negative controls, MBP (lane 1), MBP-VirJ (lane 2) and MBP-VirD2 (lane 3) were eluted with maltose directly. For the pull down assay, amylose resins bound with MBP-VirD2 (lane 4), MBP-VirJ (lane 5) and MBP (lane 6) were further incubated with AS-induced *A. tumefaciens* protein extract respectively. After washing, the bound proteins were eluted with maltose. Proteins were resolved by 12% SDS-PAGE gel. The unique band is indicated by an arrow (lane 4).

separation and may also disturb the subsequent MALDI-TOF MS identification of the potential VirD2-binding proteins. Consequently, we included proteinase inhibitors and two controls: MBP and MBP-VirJ fusion protein. Another problem we encountered is the cellular concentration of the potential VirD2-binding proteins. If the concentration of the potential VirD2-binding protein is very low in *A. tumefaciens* cells, we have to culture a large number of bacterial cells so that the amount of the potential VirD2-binding proteins pulled down by MBP-VirD2 is enough to support the SDS-PAGE analysis and MALDI-TOF MS identification. In this study, we cultured five liters of agrobacterial culture for each pull-down assay. The eluted fusion proteins and their pulled-down proteins were analyzed on SDS-PAGE gel (Fig. 3.1). We found one unique band in the MBP-VirD2 pulled-down proteins (indicated by an arrow in lane 4, Fig. 3.1). We excised all the protein bands in the MBP-VirD2 pulled-down proteins and other corresponding protein bands (around the same molecular weight as the prominent MBP-VirD2 binding protein) in the controls and identified all these proteins using MALDI-TOF MS. However, only the unique protein band in lane 4 gave an apparent match with an *A. tumefaciens* protein, whereas all other identified protein bands were matched with MBP, VirD2 or VirJ.

The peptide mass map of the prominent MBP-VirD2-binding protein is shown in Fig. 3.2. The top six protein candidates offered by MS-Fit search results of this peptide mass map are listed in Table 3.1, indicating that the top two protein candidates had significantly higher molecular weight search (MOWSE) scores than other candidates. The MOWSE score of the first protein candidate is 9.79e+007, whereas, the MOWSE score of the third protein candidate is 5.02e+004. Both of the top two protein candidates

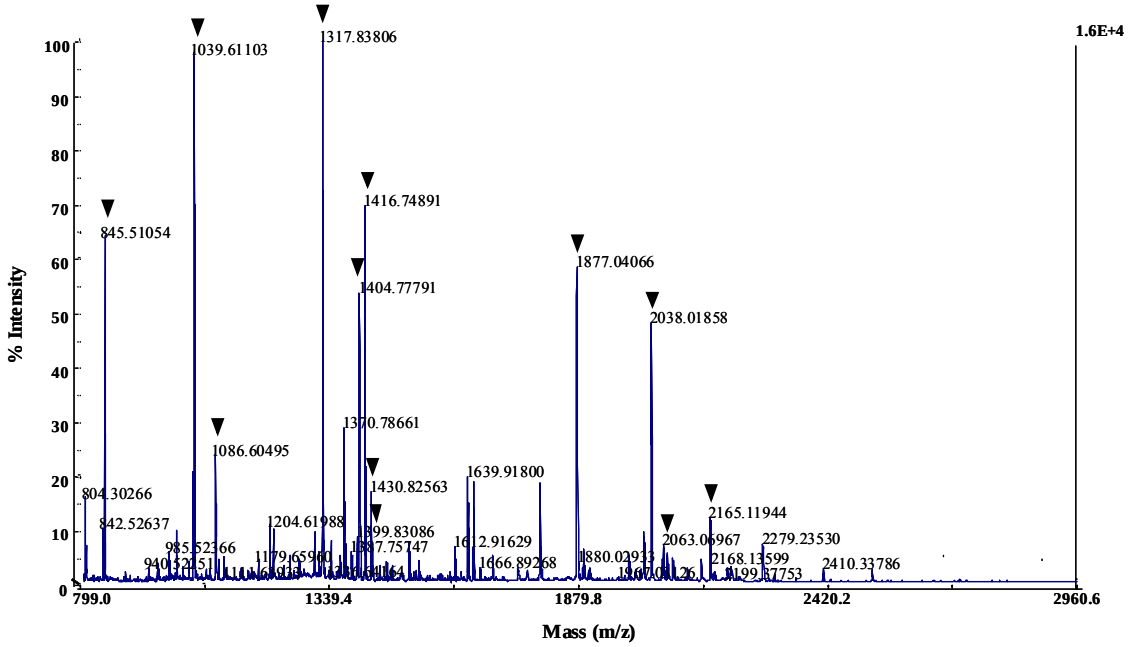

Fig. 3.2. MALDI-TOF peptide mass map of the prominent VirD2-binding protein. The unique protein band from lane 4 in Fig. 1 was excised and in-gel digested by trypsin. The resulting peptides were analyzed using a MALDI-TOF mass spectrometer to obtain the mass map. Peptide peaks that correspond to the calculated tryptic peptide masses of an *A. tumrfaciens* protein are indicated by triangles.

Table 3.1. MS-Fit search results of MALDI-TOF peptide mass map of the prominent VirD2 binding protein

MOWSE Score	Masses Matched (%)	Protein MW (Da) / pI	Species	NCBInr.020801 Accession	Protein Name
9.79e + 007	12/40 (30%)	35990.0/6.25	*Agrobacterium tumefaciens* Str. C58 (U. Washington)	17938703	(AE008936) hypothetical protein
2.23e + 007	11/40 (27%)	36319.4/6.25	*Agrobacterium tumefaciens* Str. C58 (Cereon)	16119344	(AE007884) AGR_pAT_170p
5.02e + 004	6/40 (15%)	68363.9/9.28	*Leptospira Interrogans*	5814317	(AF144879) unknown
5.02e + 004	6/40 (15%)	68426.0/9.28	*Leptospira Interrogans*	17940023	(AF316500) unknown
5.01e + 004	6/40 (15%)	68571.1/9.25	*Leptospira Interrogans*	13346897	(U61226) unknown
3.62e + 004	9/40 (22%)	79689.9/6.83	*Methanosarcina Mazeigoel*	21227282	(AE013348) oxidoreductase

had molecular weight and species consistent with the unique protein band. The amino acid sequences of these two protein candidates are shown in Fig. 3.3. Both protein candidates are encoded by an identical *A. tumefaciens* gene; one (Atu5117; accession: NC_003306.1) was predicted by the University of Washington genome project (Wood *et al*., 2001), another (AGR_pAT_170p; accession: NC_003064.1) by the Cereon genome project (Goodner *et al*., 2001). Twelve main peptide masses in the peptide mass spectrium (Fig. 3.2) matched with the calculated tryptic peptide masses from the first candidate. The matched peptide fragments are shown in shaded letters in Fig. 3.3 and cover 53% amino acids of the first protein candidate. Although the MS-Fit results have given us an unambiguous identification of an *A. tumefaciens* protein that may bind with VirD2 protein, we think that further confirmation is still required for this identification because only twelve (30%) of the forty submitted peptide masses were matched to the first protein candidate (Table 3.1). So many submitted peptides (70%) were not matched to the same protein candidate, demonstrating that this protein band may be a mixture of several proteins. Consequently, we sequenced the five dominant peptides of tryptic digestion production by using Q-TOF MS/MS analysis to further confirm the identification. The sequencing results were shown in Table 3.2. The sequences of these five peptides matched 100% with the *Agrobacterium* protein. The positions of these five sequenced peptides in the top two protein candidates were shown in Fig. 3.4. A peptide fragment matched exactly with the N-terminus of the first candidate (Fig. 3.3), indicating that the open reading frame predicted by the University of Washington genome project is correct. We designated this protein as VBP1.

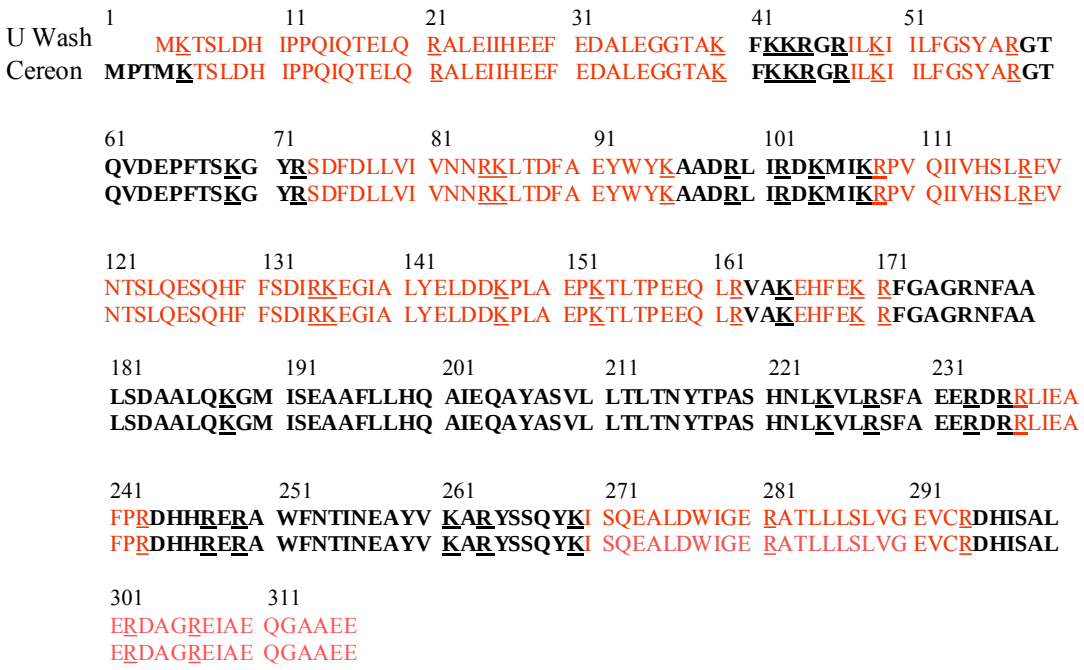

Fig. 3.3. Coverage map of the matched peptides from the top two candidates of VirD2-binding proteins. The matched peptide fragments are shown in shaded letters and cover 53% (166/313) or 52% (164/316) amino acids of the protein. The trypsin cleavage sites were underlined. Numeric indicates the position of amino acid in the proteins. U Wash represents the ORF predicted by University of Washington genome project. Cereon represents the ORF predicted by Cereon genome project. One mass peak matched exactly with the N-terminal peptide fragment of this protein, confirming that the ORF predicted by U Wash is correct.

Table 3.2. Details of the five peptides sequenced by Q-TOF-MS/MS analysis

Peptide	Observed M/Z	Mr (expt)	Mr (calc)	Delta	Miss	Score	Sequenced by Q-TOF-MS/MS
1	543.8	1085.73	1085.57	0.16	0	22	TLTPEEQLR
2	708.97	1415.93	1415.70	0.22	0	70	ISQEALDWIGER
3	732.48	1462.94	1462.71	0.23	1	56	KLTDFAEYWYK
4	634.43	1900.27	1899.98	0.29	0	34	EGIALYELDDKPLAEPK
5	679.72	2036.15	2035.96	0.19	0	33	EVNTSLQESQHFFSDIR

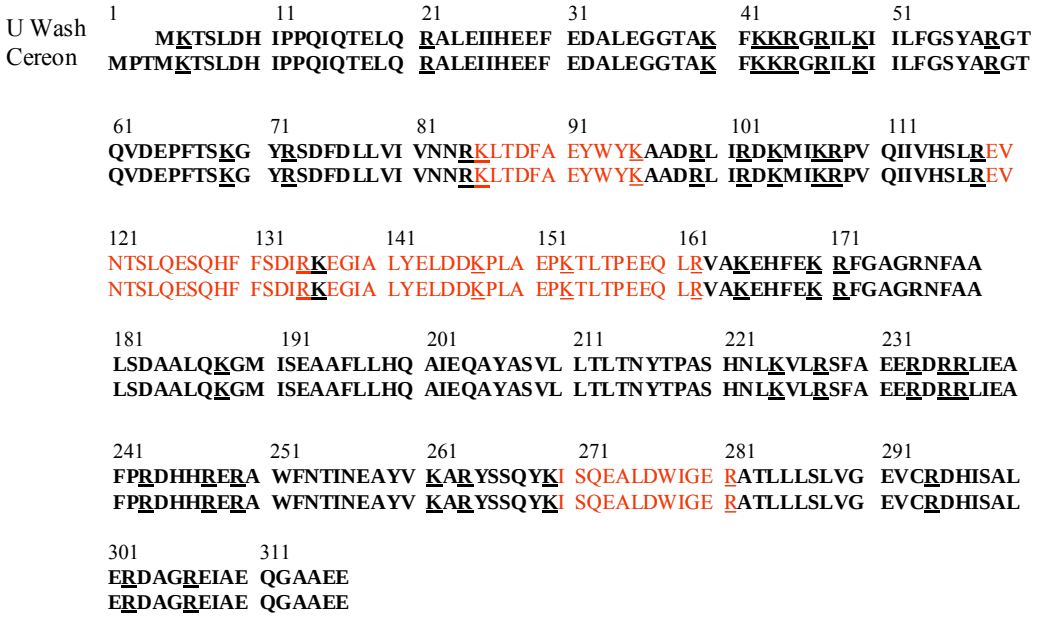

Fig. 3.4. Positions of five peptide fragments sequenced by Q-TOF. The sequenced peptide fragments are shown in shaded letters. The trypsin cleavage sites were underlined. Numbers indicate the positions of amino acid in the proteins. U Wash represents the ORF predicted by University of Washington genome project. Cereon represents the ORF predicted by Cereon genome project.

We determined the genomic locus of VBP1-encoding gene based on the genome data; *vbp1* gene is located on the AT plasmid. But, it was reported that AT plasmid is a cryptic plasmid and not essential for tumor induction (Rosenberg and Huguet, 1984). However, when we conducted the BLAST search, we surprisingly found that *A. tumefaciens* also has two other genes highly homologous to *vbp1*. These two homologous genes are Atu4860 (accession: NC_003305.1) and nucleotidyltranferase (accession: NC_003305.1) in the U. Wash. version of *A. tumefaciens* genome; AGR_L_53p (accession: NC_003063.1) and AGR_L_62p (accession: NC_003063.1) in the Cereon version of *A. tumefaciens* genome. Atu4860 gene and AGR_L_53p gene is the same gene; we designated them as *vbp2*. Nucleotidyltransferase gene and AGR_L_62p gene is the same gene; we designated them as *vbp3*. The sequence alignment of VBP1 and VBP2 was shown in Fig. 3.5. The amino acid sequence of VBP2 exhibits 72% identity and 80% similarity to VBP1. VBP3 also shows high homologous to VBP1 (Fig. 3.6). VBP3 shares 56% identity and 71% similarity with VBP1. Both of *vbp2* and *vbp3* are located on the linear chromosome and very close to each other. The distance between *vbp2* and *vbp3* genes is only 3.884 kb. Only three putative open read frames (ORF) lie between *vbp2* and *vbp3* genes. Each of these three VBP proteins contains a putative nucleotidyltransferase motif in their N-termini and a putative higher eukaryotes and prokaryotes nucleotide-binding (HEPN) domain in their C-termini based on a motif finding computer program (www.ncbi.nlm.nih.gov/BLAST) (Fig. 3.7). In the U. Wash. version of *A. tumefaciens* genome, the predicted VBP1, VBP2 and VBP3 proteins contain 313, 311 and 308 amino acids respectively.

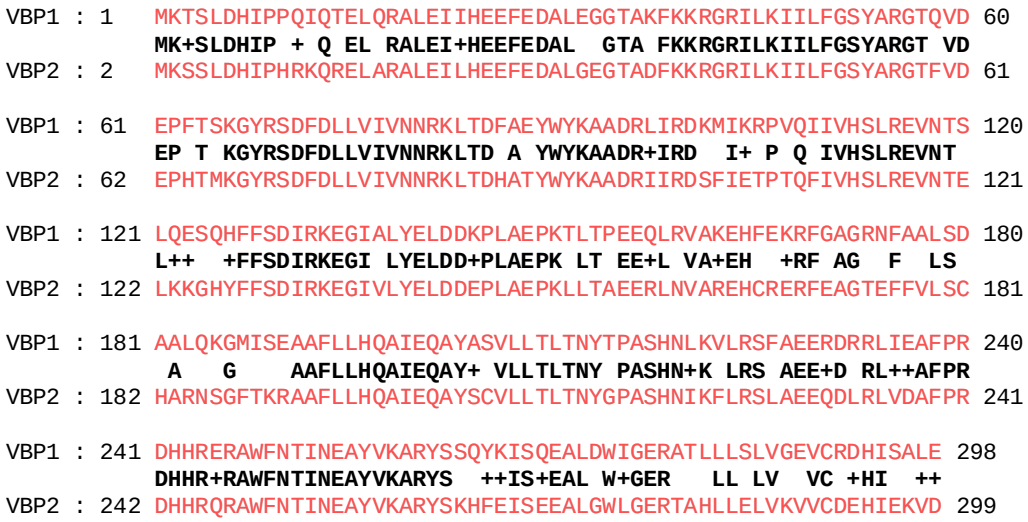

Fig. 3.5. Sequence comparison of VBP1 and VBP2 from *Agrobacterium tumefaciens*. The amino acid sequence of VBP2 shows 72% identity and 80% similarity to VBP1. The bolded letters show the identical amino acids. The "+" symbol represents similar amino acid. Numeric indicates the position of amino acid in the proteins.

```
VBP1: 1   MKTSLDHIPPQIQTELQRALEIIHEEFEDALEGGTAKFKKRGRILKIILFGSYARGTQVD 60
          MKTSL+H+P + Q EL R + II EEF D +E   +  KK GRI KIILFGSYARGT VD
VBP3: 1   MKTSLEHLPERKQRELARVVGIIQEEFADLVERSKSDAKKDGRIFKIILFGSYARGTWVD 60

VBP1: 61  EPFTSKGYRSDFDLLVIVNNRKLTDFAEYWYKAADRLIRDKMIKRPVQIIVHSLREVNTS 120
          EP TSKGYRSDFD+LVIV+N++L D  +YW K  DRL+ DK I+ PV +IVH  RE++
VBP3: 61  EPHTSKGYRSDFDILVIVSNKELAD-PKYWDKTTDRLMWDKEIETPVGLIVHGAREISNF 119

VBP1: 121 LQESQHFFSDIRKEGIALYELDDKPLAEPKTLTPEEQLRVAKEHFEKRFGAGRNFAALSD 180
          L + Q FF D+ +EGI LYE DD+PLAEPK L+P + LRVA++HF +     R+FA ++
VBP3: 120 LNDGQPFFVDLAREGIVLYEFDDRPLAEPKPLSPADALRVAEDHFLRHLPDARDFADVAK 179

VBP1: 181 AALQKGMISEAAFLLHQAIEQAYASVLLTLTNYTPASHNLKVLRSFAEERDRRLIEAFPR 240
            + KG +  AAF LHQA+E AY   LLTLTNY+PASHNLK LR  +E RDRRLI+ +PR
VBP3: 180 YLVAKGNLHLAAFNLHQAVETAYNCYLLTLTNYSPASHNLKFLRGLSEGRDRRLIDIWPR 239

VBP1: 241 DHHRERAWFNTINEAYVKARYSSQYKISQEALDWIGERATLLLSLVGEVCRDHISALERD 300
          D  R   W+N +NEAYVKARYS ++++S+EAL W+ ER   L  LV  +CR+HI  LE
VBP3: 240 DRQRFTTWYNILNEAYVKARYSKRFEVSEEALTWLQERTAELHKLVETLCREHIEKLEHA 299

VBP1: 301 AGR 303
          AG+
VBP3: 300 AGQ 302
```

Fig. 3.6. Sequence comparison of VBP1 and VBP3 from *Agrobacterium tumefaciens*. The amino acid sequence of VBP3 shows 56% identity and 71% similarity to VBP1. The bolded letters show the identical amino acids. The "+" symbol represents similar amino acid. Numeric indicates the position of amino acid in the proteins.

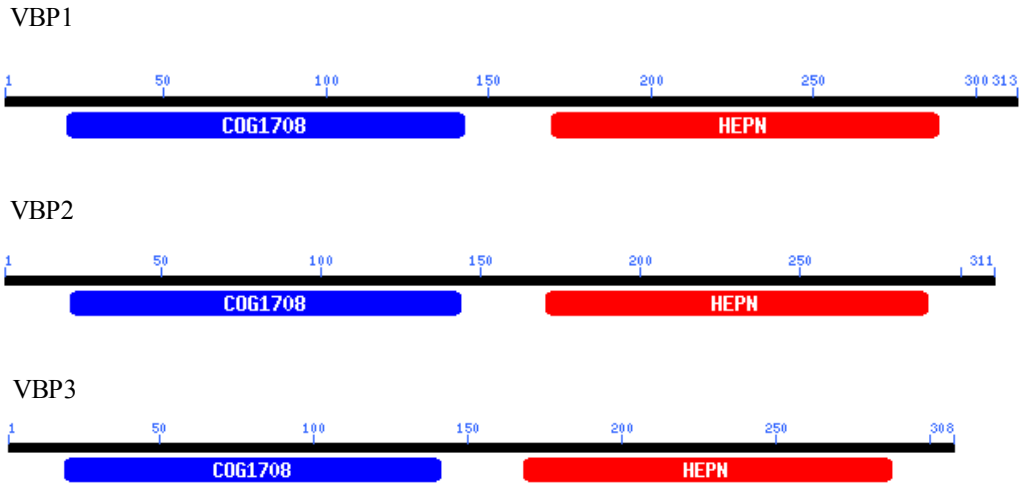

Fig. 3.7. Motif search results of three VBP proteins. All three VBP proteins contain a putative nucleotidyltransferase motif in their N-termini and a putative higher eukaryotes and prokaryotes nucleotide-binding (HEPN) domain in their C-termini. COG1708: Predicted nucleotidyltransferases (General function prediction only); HEPN: Higher Eukaryotes and Prokaryotes Nucleotide-binding domain. Numeric indicates the position of amino acid in the proteins.

3.2. Expression and Purification of Three VBP Proteins

After these three *vbp* genes, *vbp1*, *vbp2* and *vbp3*, were identified, we subsequently cloned and expressed these three *vbp* genes. In order to obtain enough VBP proteins for the generation of VBP antibodies, we used pRSET plasmids (Invitrogem^{TM}), pRSET-A and pRSET-B, as vectors to clone and express these three *vbp* genes. The pRSET plasmid has a multiple cloning site located in the downstream of a six-histidine encoding sequence, which allows us to insert the *vbp* gene and make the VBP protein in-frame fusion onto the C-terminus of the six-histidine (His) tag conveniently. The histidine tag functions as a metal binding domain and allows simple one-step purification of the recombinant proteins by immobilized metal affinity chromatography. In compared with other fusion proteins that allow simple one-step purification, such as MBP and GST fusion proteins (Nilsson *et al*., 1997), His-tagged fusion proteins possess several advantages in term of the expression and purification of protein: 1) His-tag has less adverse effects on protein function than other fusion proteins because His-tag has a smaller size. 2) His-tagged fusion proteins can be purified under extreme conditions, such as denaturing condition that is often required for dissolving the fusion proteins expressed as inclusion body. 3) This method is simple and the generation of fusion genes can be done through PCR (reviewed by Porath, 1992). In addition, an enterokinase cleavage site was designed between the His-tag and the N-terminus of fused protein. After the recombinant protein is purified, the His-tag can be cleaved to obtain the protein with the desired sequence.

3.2.1. Construction of plasmids for expressing VBP proteins

To construct the plasmid pRvbp1, which was used to express VBP1, a 947 bp DNA fragment containing the full length of *vbp1* gene was amplified from *A. tumefaciens* C58 genomic DNA by primers Pvbp1-1 and Pvbp1-2 and was inserted into the *Xho*I site of pRSET-A. The full-length sequence of *vbp2* is 952 bp. This DNA fragment was amplified by primers Pvbp2p1 and Pvbp2p2. The *vbp2* gene was inserted into the *BamH*I site of pRSET-B to generate the plasmid pRvbp2, which was used to express VBP2. The primers Pvbp3p1 and Pvbp3p2 were used to amplify the *vbp3* gene fragment. This 936 bp *vbp3* gene fragment was also inserted into the *BamH*I site of pRSET-B. The resulting plasmid pRvbp3 was used to express VBP3. All the inserted *vbp* genes in these three plasmids (pRvbp1, pRvbp2 and pRvbp3) were sequenced to confirm that the ligation is correct and the corresponding *vbp* gene was fused into the open read frame of His-tag (sequence data not shown). The construction procedure for these three plasmids was shown in Fig. 3.8.

3.2.2. Purification of three His-VBP fusion proteins

The pRSET vectors are T7 promoter-driven vectors. In order to over-express three His-VBP proteins, these three pRSET-derived plasmids (pRvbp1, pRvbp2 and pRvbp3) were introduced into *E. coli* strain BL21 (DE3) respectively. BL21 (DE3) strain carries lambda-DE3, which contains the T7 bacteriophage gene 1, encoding T7 RNA polymerase under the control of the *lac*UV5 promoter. The *lac*UV5 promoter can be induced by isopropyl-β-D-thiogalactopyranoside (IPTG). The time course of His-VBP1 expression was shown in the panel A of Fig. 3.9 (lanes 1~4). His-VBP1 protein could be induced by IPTG and the expression level of His-VBP1 protein was very high. His-VBP2 and His-VBP3 also showed high expression levels (data not shown). For the maximum expression

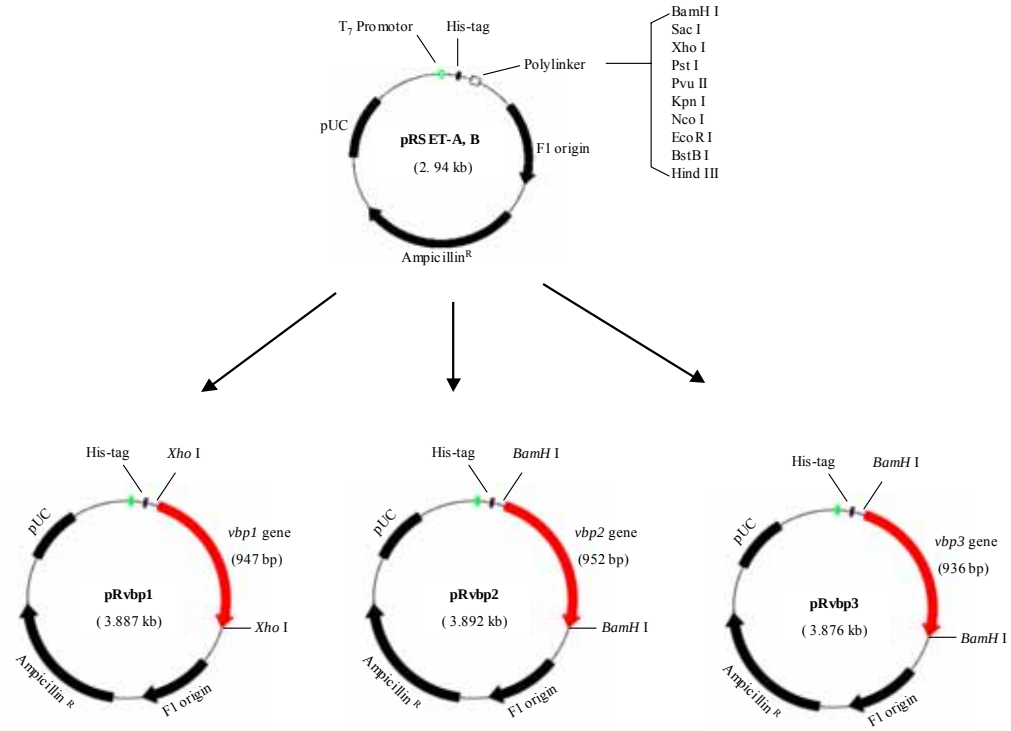

Fig. 3.8. Construction of three plasmids used for expressing three VBP proteins. The 947 bp *vbp1* gene was inserted into the *Xho*I site of pRSET-A. The 952 bp *vbp2* gene was inserted into the *BamH*I site of pRSET-B. The 936 bp *vbp3* gene was also inserted into the *BamH*I site of pRSET-B. pUC represents pUC origin. All three *vbp* genes were made in-frame fusions to the histidine (His) tag.

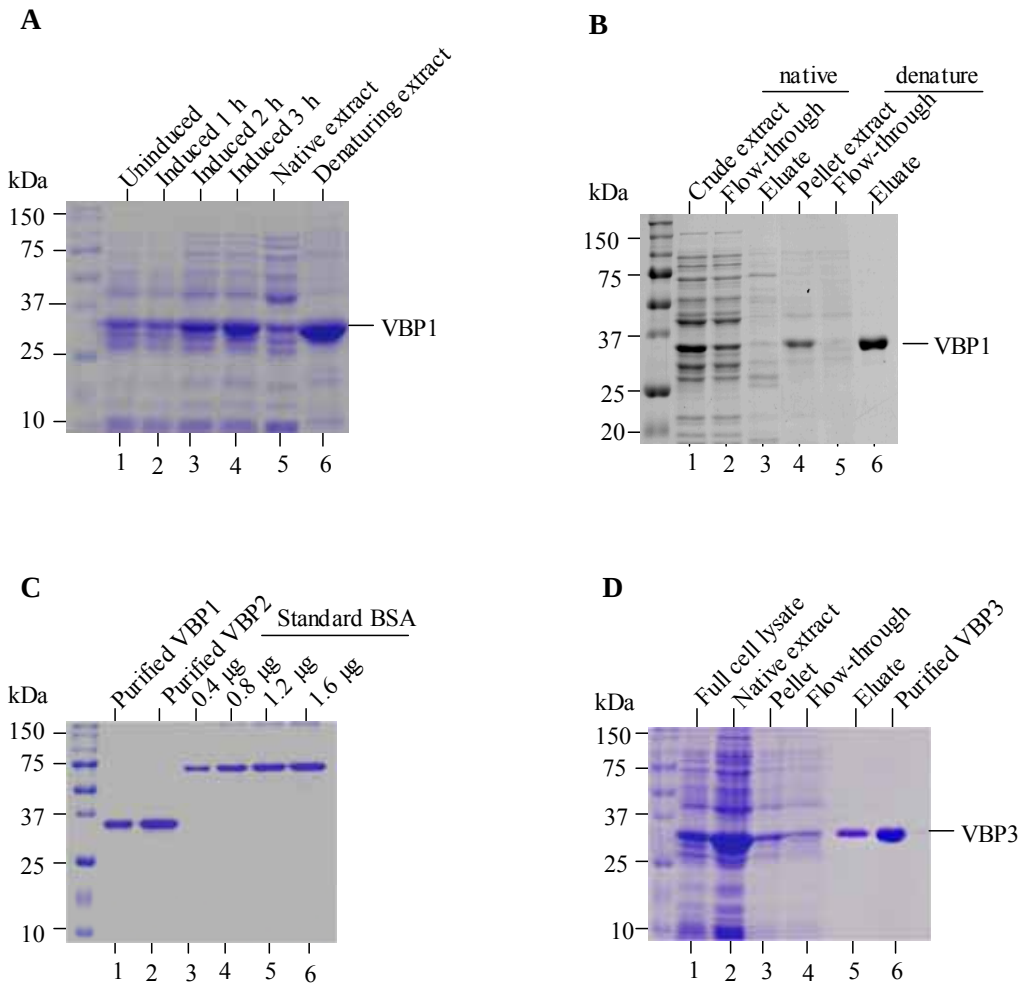

Fig. 3.9. Expression and purification of three His-VBP fusion proteins. (**A**). Inducing time course of His-VBP1 expression. (**B**). Purification of His-VBP1 under denaturing and non-denaturing conditions. (**C**). Estimation of the purity and concentration of purified His-VBP1 and His-VBP2 by compared with standard bovine serum albumin (BSA). (**D**). Purification of His-VBP3.

of these three proteins, bacterial cells were usually cultured for 3~4 hours after IPTG was added to the culture.

Since proteins over-expressed in bacteria are typically insoluble, we used different buffers to extract these three His-VBP fusion proteins. His-VBP1 showed a low solubility in native buffer and only small amount of His-VBP1 proteins was extracted by non-denaturing buffer (lane 5, panel A, Fig. 3.9). Most of His-VBP1 proteins required denaturing buffer to extract (lane 6, panel A, Fig. 3.9). Even if only small amount of His-VBP1 proteins could be extracted in non-denaturing buffer we still try to conduct the purification under native conditions. However, the soluble His-VBP1 cannot bind to the TALON metal affinity resin (lanes 1~3, panel B, Fig. 3.9), demonstrating that the His-tag in His-VBP1 may fold into the inside of the fusion protein under native conditions. When His-VBP1 was denatured, it can specifically bind to the TALON metal affinity resin (lanes 4~6, panel B, Fig. 3.9). So, we purified His-VBP1 under denaturing conditions. Similar results were obtained in His-VBP2 (data not shown). In contrast to His-VBP1 and His-VBP2, most of His-VBP3 proteins were soluble in native buffer (lanes 1~3, panel D, Fig. 3.9) and the native His-VBP3 protein could bind to the TALON metal affinity resin. However, many nonspecific bindings were observed under native conditions (data not shown). Considering the purification efficiency of His-VBP3 and the comparability of His-VBP3 to other two His-VBP proteins, His-VBP3 was also purified under denaturing conditions. The purity of the purified His-VBP1, His-VBP2 and His-VBP3 was checked by SDS-PAGE (lane 6 of panel B, panel C, and lanes 5, 6 of panel D in Fig. 3.9).

3.2.3. Antibody production

Each of the purified His-VBP proteins was injected to two rabbits for raising the antibody. The antiserum was subjected to Western blot analysis using the AS-induced *A. tumefaciens* A348 extract, the cell lysate of *E. coli* strain BL21 (DE3) harboring the corresponding plasmid and the purified His-VBP proteins. After third boost, the antibody titer has reached a plateau. Large bleeding was done after fourth boost. Because three VBP proteins possess high homology to each other, the ant-His-VBP antibodies also showed cross-reaction to each other (data not shown). Besides their high homology, their immigrating distances in SDS-PAGE were almost the same because their molecular weights showed little difference. Therefore, it is difficult to differentiate these three VBP proteins by using Western blotting analysis.

3.3. Verification of the Interactions between VirD2 and VBP Proteins

3.3.1. Specificity of binding between VirD2 and VBP1

During the initial experiments, the pulled-down proteins were analyzed by using Coomassie Blue-stained SDS-PAGE gel and then identified by MALDI-TOF MS. It is possible that trace VBP1 pulled down by the negative controls, such as MBP and MBP-VirJ fusion protein (Fig. 3.1), may not be detected by Coomassie blue staining because of the relative low sensitivity of Coomassie blue staining. To confirm that the binding between VirD2 and VBP1 is specific, we conducted the pull-down assay with MBP, MBP-VirJ fusion protein, MBP-VirD2 fusion protein and MBP-VirD2-C-terminus (MBP-C-VirD2) fusion protein. The pulled-down proteins were then analyzed by Western blot using anti-His-VBP1 antibody, as it is well known that the sensitivity of Western blot is much higher than that of Coomassie blue staining. Western blot analysis (Fig. 3.10) confirmed that VBP1 could specifically bind to MBP-VirD2 fusion protein

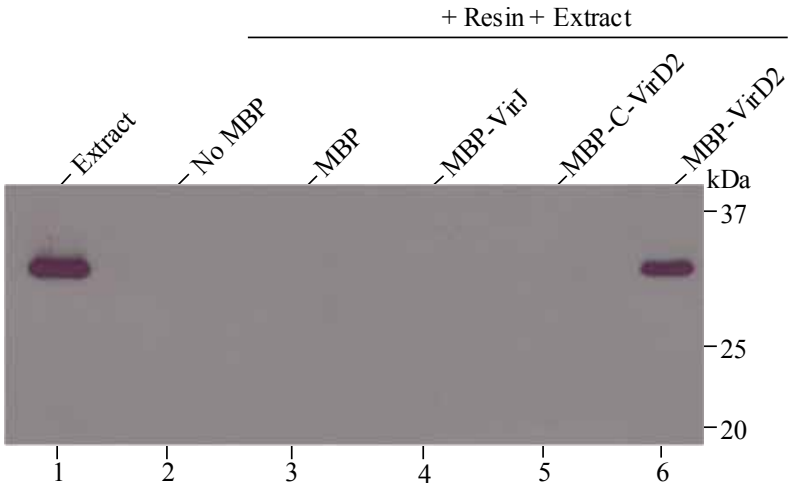

Fig. 3.10. Western blot analysis of proteins pulled down by MBP fusion proteins. An equal amount of AS-induced *A. tumefaciens* protein extract was incubated with amylose resin alone (lane 2), MBP bound amylose resin (lane 3), MBP-VirJ bound amylose (lane 4), MBP-C-VirD2 bound amylose resin (lane 5) or MBP-VirD2 bound amylose resin (lane 6) for 60 min at 4°C. The resins were washed and the bound proteins were eluted with maltose. The pulled down proteins were separated by SDS-PAGE. VBP1 protein was detected by Western blot with rabbit anti-His-VBP1 antibody. As a positive control of Western blot, *A. tumefaciens* protein extract was loaded onto lane 1.

(lane 6 in Fig. 3.10), but not to amylose resin alone (lane 2 in Fig. 3.10), MBP (lane 3 in Fig. 3.10), MBP-VirJ fusion protein (lane 4 in Fig. 3.10), or MBP-C-VirD2 fusion protein (lane 5 in Fig. 3.10). This result also demonstrated that the hypothetical protein (VBP1) indeed is present in *Agrobacterium* cell because the AS-induced *A. tumefaciens* A348 extract showed a single strong band (lane 1 in Fig. 3.10).

Because the bait protein that was used to "fish out" the native VBP1 protein is a recombinant MBP-VirD2 fusion protein, it is unknown whether the recombinant VirD2 protein can maintain its native conformation and function. It is necessary to verify that native VirD2 can bind to VBP1 protein. To confirm the specific binding between native VirD2 and VBP1, we used His-VBP1 fusion protein as an affinity ligand to pull down the native VirD2 protein from AS-induced *A. tumefaciens* cell extract. His-KatA fusion protein was used as a negative control as KatA is a catalase (Xu *et al*., 2001) and thus was not expected to bind VirD2. Because most of the His-VBP1 fusion protein over-expressed in *E. coli* was insoluble (panel A of Fig. 3.9), we used a denaturing buffer to dissolve both His-VBP1 and His-KatA. After the denatured His-VBP1 and His-KatA were bound to TALON metal affinity resin, the denaturant urea and salt were removed from the protein-bound resin by washing the columns with non-denaturing and low salt buffer. Before the His-tagged fusion protein-bound resins were used to bind VirD2, the fusion protein-bound resins were incubated at 4°C for 60 min to allow the denatured His-VBP1 and His-KatA to refold. The bound proteins were eluted with imidazole and resolved by SDS-PAGE. VirD2 protein was detected by Western blot using anti-His-VirD2 antibody (Fig. 3.11). Both AS-induced *A. tumefaciens* cell extract and His-VBP1 pulled-down protein sample showed VirD2 band (lanes 2 and 5 in Fig. 3.11). No VirD2

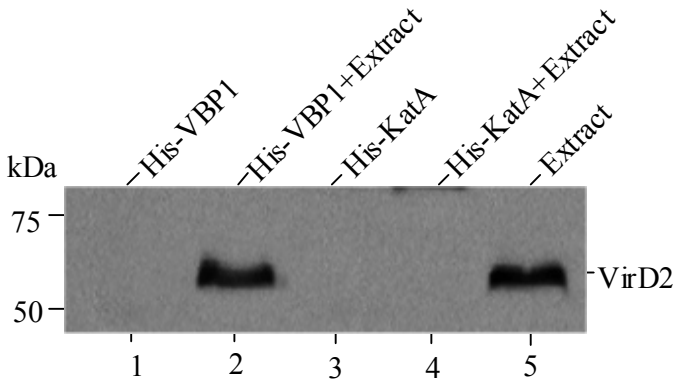

Fig. 3.11. Specific binding of VirD2 to His-VBP1. Equal amount of His-VBP1 bound resin (lane 2) or His-KatA bound resin (lane 4) was incubated with an equal volume of AS-induced *A. tumefaciens* protein extract. After incubation for 60 min at 4°C, the resins were washed and then eluted with imidazol. The eluted proteins were separated by SDS-PAGE. VirD2 was detected by Western blot with rabbit anti-His-VirD2 antibody. Purified His-VBP1 (lane 1) and His-KatA (lane 3) were used as negative controls. *A. tumefaciens* protein extract (lane 5) was used as a positive control.

band appeared on the lane of His-KatA pulled-down protein sample (lane 4 in Fig. 3.11). The result demonstrated that only His-VBP1 could pull down VirD2. Therefore, the binding between VBP1 and VirD2 is specific.

As we used the crude *A. tumefaciens* cell extract to perform the pull-down assay, the possibility may exist that a mutual partner protein(s) mediates this interaction. To further demonstrate if the interaction between VirD2 and VBP1 is direct or indirect, we used purified MBP-VirD2 fusion protein to bind purified His-VBP1 protein. Cell lysates from *E. coli* expressing MBP or MBP-VirD2 fusion proteins were used to bind the amylose resin. The unbound proteins were washed out. The MBP-bound amylose resin or MBP-VirD2 fusion protein-bound amylose resin were incubated with purified His-VBP1 or purified His-KatA respectively. The amylose resins were washed and the bound proteins were eluted with maltose. Coomassie blue staining result of the bound proteins showed that purified MBP-VirD2 fusion protein could specifically bind with purified His-VBP1 (lane 1 in Fig. 3.12), indicating that VirD2 interacts directly with VBP1.

3.3.2. Pulling down of VirD2 by VBP2 and VBP3

Since the amino acid sequences of VBP2 and VBP3 are highly homologous to VBP1 and all three VBP proteins contain a putative nucleotidyltransferase motif and a putative HEPN domain, we wanted to determine if VBP2 and VBP3 have the same function as VBP1. We tested whether VBP2 and VBP3 could also pull down VirD2. His-VBP2 and His-VBP3 were used to conduct the pull-down assay with the same operating procedure as His-VBP1. As shown in Fig. 3.13, both VBP2 (lane 4 in Fig. 3.13) and VBP3 (lane 5 in Fig. 3.13) could pull down VirD2 from AS-induced *A. tumefaciens* A348 protein extract. This indicates that both VBP2 and VBP3 can also bind VirD2.

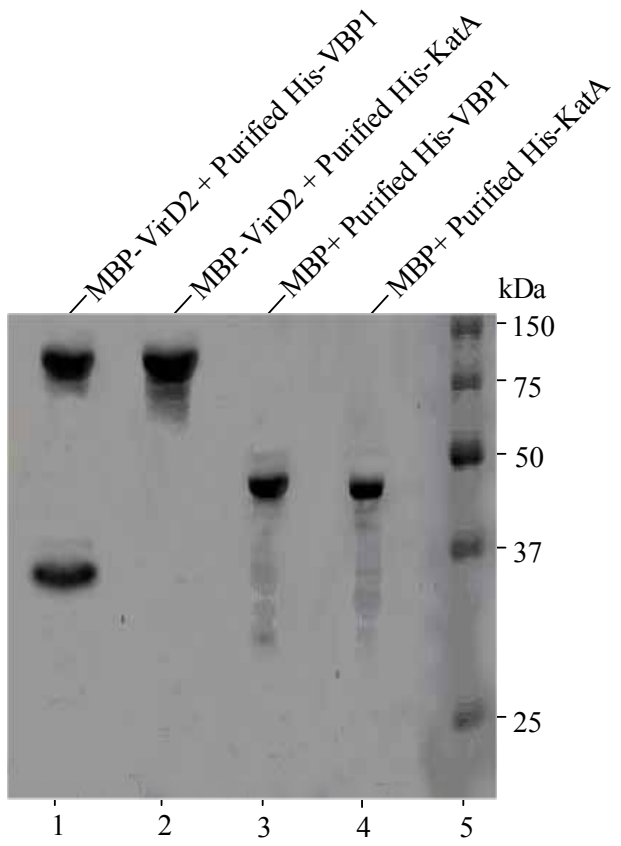

Fig. 3.12. Specific binding of purified His-VBP1 to purified MBP-VirD2. Equal amount of MBP-bound amylose resin (lanes 3, 4) or MBP-VirD2-bound amylose resin (lanes 1, 2) was incubated with equal amounts of purified His-VBP1 (lanes 1, 3) or purified His-KatA (lanes 2, 4) respectively. After incubation for 60 min at 4°C, the resins were washed and then eluted with maltose. The eluted proteins were separated by SDS-PAGE and analyzed by Coomassie blue stain.

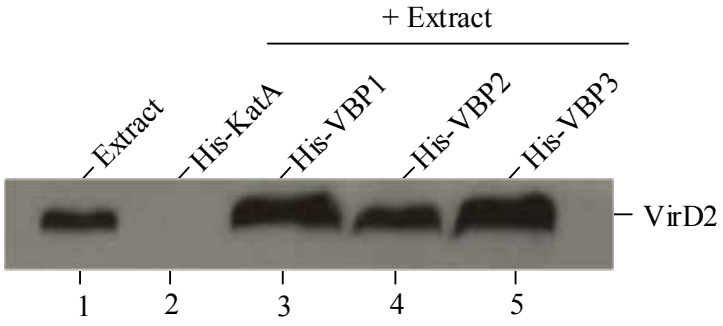

Fig. 3.13. Pulling down of VirD2 by VBP2 and VBP3. Equal amount of His-KatA bound resin (lane 2), His-VBP1 bound resin (lane 3), His-VBP2 bound resin (lane 4) or His-VBP3 bound resin (lane 5) was incubated with an equal volume of AS-induced *A. tumefaciens* protein extract. After incubation for 60 min at 4°C, the resins were washed and then eluted with imidazol. The eluted proteins were separated by SDS-PAGE. VirD2 was detected by Western blot with rabbit anti-His-VirD2 antibody. *A. tumefaciens* protein extract (lane 1) was used as a positive control.

3.3.3. Strength of VBP1-VirD2 interaction

After we confirmed the specific interaction between VBP1 and VirD2 as well as testified that both VBP2 and VBP3 could also bind VirD2, we next attempted to analyze the strength of VBP1-VirD2 interaction. To test the strength of the interaction between VBP1 and VirD2, we examined the effect of increasing salt concentration on the recovery of the VirD2 by His-VBP1. The effect of salt concentration on the protein-protein interaction was usually used as a criterion to judge the strength of the protein-protein interaction (Bachand *et al*., 1999; Luban *et al*., 1993). The His-VBP1 bound TALON metal affinity resin was incubated with AS-induced *A. tumefaciens* A348 protein extract containing different concentrations of salt and Mg^{2+}. Then, the resin was washed with the incubation buffer containing the same concentrations of salt and Mg^{2+} as in the A348 protein extract. At the same time, His-VBP1 bound resin was also incubated with the incubating buffer containing the tested concentrations of salt and Mg^{2+} to ensure that the tested concentrations of salt and Mg^{2+} would not affect the binding of His-VBP1 to the resin (data not shown). In another word, the bound His-VBP1 would not be washed away by the buffers containing different concentrations of salt and Mg^{2+}. The effect of increasing salt concentration on the recovery of the VirD2 was aroused by the VBP1-VirD2 interaction not by the binding between His-VBP1 and resin. The bound proteins were eluted with imidazol. The pulled down proteins were separated by SDS-PAGE and analyzed by both Coomassie blue staining and Western blotting. Coomassie blue staining results further confirmed that equal amounts of His-VBP1 were still present after incubating and washing with these different salt concentrations (data not shown). Western blotting analysis was shown in Fig. 3.14. Mg^{2+} is required for the binding

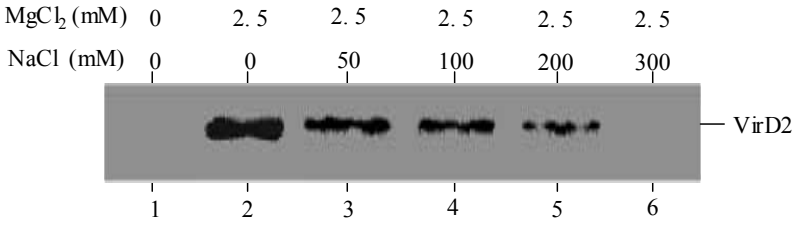

Fig. 3.14. Effect of the concentration of NaCl and Mg^{2+} on the VBP1-VirD2 interaction. His-VBP1 bound resin was incubated with AS-induced *A. tumefaciens* A348 extract under different concentrations of NaCl and Mg^{2+} at 4°C for 60 min, and subsequently washed with the incubating buffer containing specific concentration of NaCl and Mg^{2+} (indicated at the top of the lanes). The proteins were eluted with imidazol and analyzed by Western blotting.

between VBP1 and VirD2. The VBP1-VirD2 interaction could sustain 200 mM NaCl, indicating that The VBP1-VirD2 interaction was strong.

Chapter 4 The Role of VirD2-binding Protein in T-DNA Transfer

4.1. Generation of *vbp* Mutants in *A. tumefaciens*

VBP proteins could specifically bind with VirD2 and the VBP1-VirD2 interaction was strong. However, it is still unknown whether the VBP1-VirD2 interaction plays important roles in T-DNA transfer. Determining the biological function of the identified VirD2-binding protein(s) is one of the important goals of this study. To study the biological functions of these three VBP proteins, we adopted the mutagenesis strategy. If these three VBP proteins were important in the T-DNA complex trafficking, the mutation of the *vbp* genes would affect the T-DNA transfer. Because all three VBP proteins could bind with VirD2, they may functionally complement each other. Thus, we must "knock out" all three *vbp* genes to determine the biological functions. Since *vbp1* is harbored on the cryptic plasmid AT, the effect of *vbp1* may be removed by using *A. tumefaciens* strain GMI9017, which lacks the *vbp1*-containing AT plasmid (Rosenberg and Huguet, 1984). Therefore, we focused on generating mutations at *vbp2* and *vbp3*.

4.1.1. Generation of *vbp2* mutants in *A. tumefaciens*

To generate *vbp2* mutants, we electroporated *sacB*-based suicide plasmid pEXKmVUD, which carries both upstream and downstream sequences of *vbp2*, to A348 and GMI9017 (Fig. 4.1). Km^R-transformants could only result from the integration of the plasmid into the agrobacterial genome because this plasmid cannot replicate inside agrobacterial cells. Therefore, kanamycin-containing MG/L agar plates were used to select for single cross-over transformants due to the integration of the suicide vector into

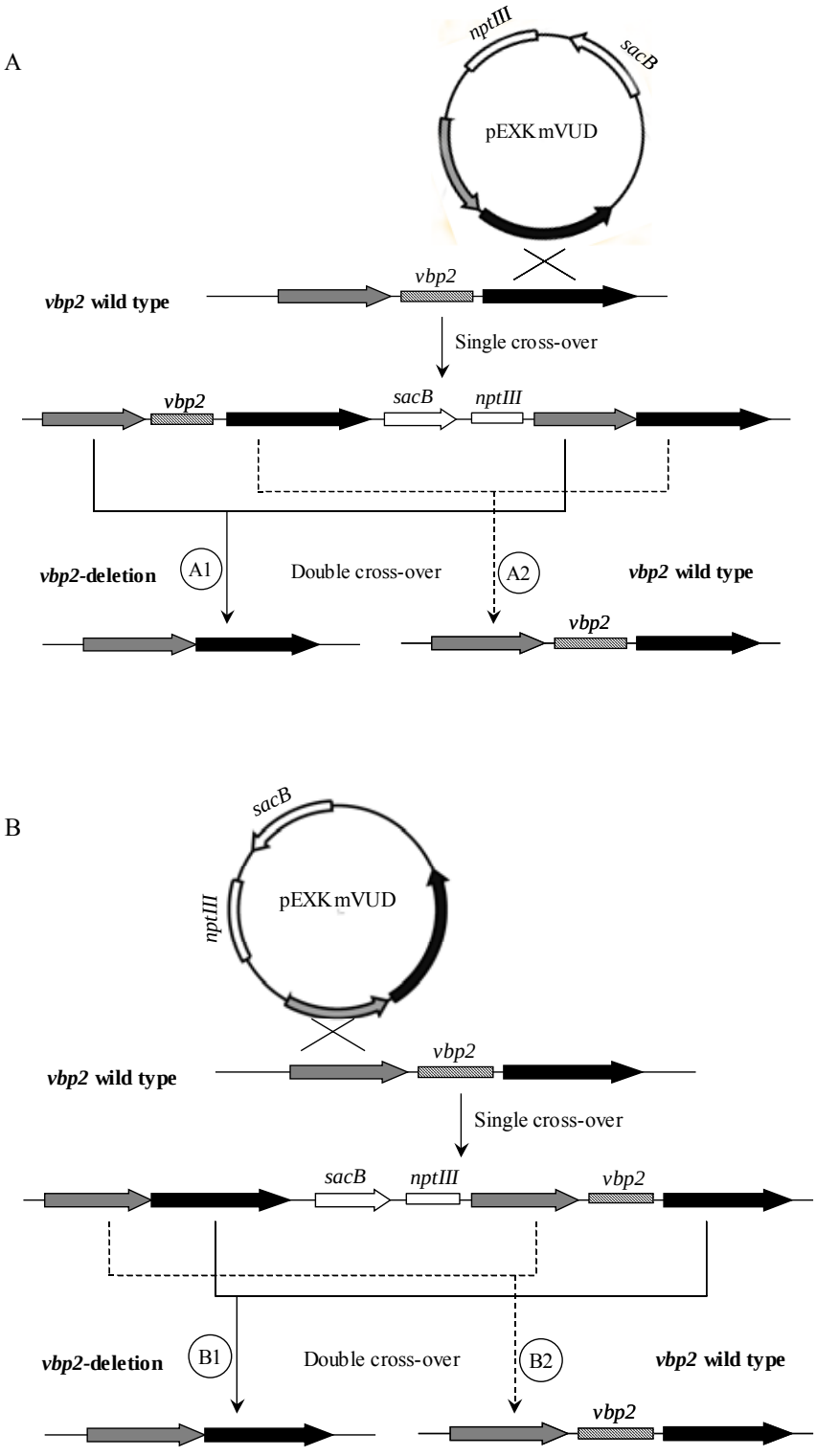
A
nptIII
sacB
pEXK mVUD
vbp2
vbp2 wild type
Single cross-over
vbp2
sacB
nptIII
vbp2-deletion
A1
Double cross-over
A2
vbp2 wild type
vbp2
B
sacB
nptIII
pEXK mVUD
vbp2
vbp2 wild type
Single cross-over
sacB
nptIII
vbp2
vbp2-deletion
B1
Double cross-over
B2
vbp2 wild type
vbp2

Fig. 4.1. Schematic diagram of *vbp2* mutation strategy. The plasmid pEXKmVUD carries two DNA fragments amplified from *A. tumeficiens* C58 genomic DNA that correspond to the upstream (shadowy arrows) and downstream (black arrows) sequences of *vbp2* gene. The *nptIII* (open rectangles) represents kanamycin-resistant gene. The *sacB* (open arrows) is a counterselectable marker gene that confers sucrose sensitivity. A fragment of *vbp2* gene was shown in stippled rectangles. Colonies having undergone single cross-over homologous recombination (×) were screened as kanamycin resistance and sucrose sensitivity. Double cross-over homologous recombination event was selected by plating the single cross-over colonies on media containing 5% sucrose. The *vbp2*-deletion mutants were screened from the kanamycin-sensitive and sucrose-resistant colonies. (**A**). The plasmid pEXKmVUD was integrated into the *A. tumefacien* genome by homologous recombination at the downstream of *vbp2*. (**B**). The plasmid pEXKmVUD was integrated into the *A. tumefacien* genome by homologous recombination at the upstream of *vbp2*. Double cross-over homologous recombination may occur in the two fragments homologous to the upstream of *vbp2* (A1 and B2, two shadowy arrows) or in the two fragments homologous to the downstream of *vbp2* (A2 and B1, two black arrows).

the agrobacterial genome. The suicide plasmid pEXKmVUD could be integrated into the agrobacterial genome on either the upstream (Fig. 4.1B) or the downstream (Fig. 4.1A) of the *vbp2* gene in the single cross-over event. Previous observations showed that the frequency of the first recombination event, *i.e.* the frequency of the plasmid into the host's genome DNA, appears to be dependent upon the length of homologous DNA (Edwards *et al*., 1998; Watt *et al*., 1985). The plasmid pEXKmVUD carries a 2.183-kb *vbp2* downstream fragment and a 1.395-kb v*bp2* upstream fragment. The length of the downstream homologous DNA is significantly longer than that of the upstream. To demonstrate the effect of the length of homologous DNA on the frequency of the single cross-over event, the Km^R-transformants from the integration of plasmid pEXKmVUD into the downstream of *vbp2* gene (Fig. 4.1A) were differentiated from those from the integration of plasmid pEXKmVUD into the upstream of *vbp2* gene (Fig. 4.1B) by using PCR. Our results showed that most of the single cross-over mutants, the Km^R-transformants, resulted from the single cross-over event occurring on the downstream of the *vbp2* gene (data not shown).

The purified and PCR-confirmed Km^R-transformants were used to screen for the double cross-over mutants. To select the double cross-over mutants, the Km^R-transformants were plated on sucrose-containing MG/L plate to select for the $sucrose^R$-transformants. The $sucrose^R$-transformants were generated due to the double cross-over homologous recombination, which resulted in the loss of the integrated suicide plasmid. The double cross-over homologous recombination could also occur in two ways, either on the upstream homologous region (A1 and B2 in Fig. 4.1) or on the downstream homologous region (A2 and B1 in Fig. 4.1). So, two classes of $sucrose^R$-transformants

were identified: the *vbp2* wild type colonies (A2 and B2 in Fig. 4.1) and the *vbp2*-deletion mutants (A1 and B1 in Fig. 4.1). The *vbp2*-deletion mutants were screened from the sucrose^{R}-transformants by PCR using Pscreen1 and Pscreen2 as the primers. As shown in Fig. 4.2, *vbp2*-deletion mutant was obtained based on PCR analysis, which was followed by restriction digestion.

In contrast to the first homologous recombination event, the frequency of the second homologous recombination event appears to be independent of the length of homologous DNA. Previous studies on homologous recombination in *E. coli* (Bi and Liu, 1995) have showed that for plasmid- or chromosomal-located regions of homology greater than 100 bp the length of the intervening sequence has a greater influence over the deletion frequency than the length of the homologous regions on either side. When we used two different kinds of single cross-over mutants to screen the double cross-over mutants, we found that the percentage of *vbp2*-deletion mutant colonies appeared in the first kind of single cross-over mutant (Fig. 4.1A) was different from that appeared in the second kind of single cross-over mutant (Fig. 4.1B). The frequency of *vbp2*-deletion mutant colonies appeared in Fig. 4.1B was significantly higher than that in Fig. 4.1A (data not shown). This result was consistent with the previous studies in *E. coli* (Bi and Liu, 1995), indicating that the double cross-over homologous recombination mechanism in *A. tumefaciens* may be similar to that *in E.coli*.

To confirm that the *vbp2* fragment was indeed deleted as expected, the PCR fragments amplified by the primers Pscreen1 and Pscreen2 from both the wild type and the *vbp2*-deletion mutant were sequenced. Sequencing results showed that *vbp2* gene fragment was deleted as expected in the *vbp2*-deletion mutant (Fig. 4.3). The *vbp2*-

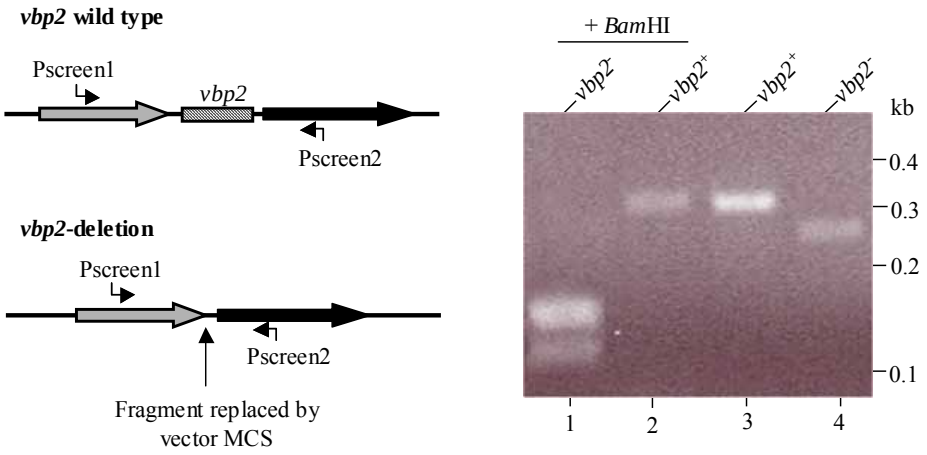

Fig. 4.2. Screening of *vbp2*-deletion mutants. The *vbp2*-deletion mutants were screened by PCR. Two oligonucleotides Pscreen1 (annealed to upstream of *vbp2*) and Pscreen2 (annealed to downstream of *vbp2*) were used as the primers. The PCR products from a *vbp2*-deletion mutant (lanes 1 and 4) and from a wild type (lanes 2 and 3) were treated by *Bam*HI (lanes 1and 2) or without restriction digestion (lanes 3 and 4). The PCR product from *vbp2*-deletion mutant was digested to two fragments (lane 1) because a small fragment from vector's multiple-cloning sites (MCS) was inserted. The PCR product from the wild type could not be digested to two fragments (lane 2) because the DNA fragment does not have the *Bam*HI site. These two PCR fragments were sequenced to confirm that the *vbp2* fragment was deleted as expected (sequence data was show in Fig. 4.3). $vbp2^-$ represents *vbp2*-deletion mutant. $vbp2^+$ represents *vbp2* wild type.

VBP2 wild type: -----agcacttt-tggcatttga-tcaacgtgtc-gaagcgtata-aagttcatgg-
VBP2 mutant: -----agcacttt-tggcatttga-tcaacgtgtc-gaagcgtata-aagttcat-gg

at-**accaccag-cgcgattgcg-tgggtgtcgc-aatcgcaagc-tagtcagata-**
a-----tcc-tct-aga-gtc-gac-ctg-cag-gca-tgc-aag----------

cctcgttccc-atg-atg-aaa-tcc-tcc- ctt-gat-cat-atc-ccg-cac-aga-
---------- ctt-gat-cat-atc-ccg-cac-aga-

aag-cag-cga-gag-ctc-gcc-cgt-gcg----
aag-cag-cga-gag-ctc-gcc-cgt-gcg----

Fig. 4.3. Sequence of the deleted *vbp2* fragment. The bold letters indicate the deleted *vbp2* fragment. The shadowy letters represent the small fragment replaced by vector's multiple-cloning sites (MCS). The underlined letters highlight the start code.

deletion mutants derived from A348 and GMI9017 were designated A348Δvbp2 and GMI9017Δvbp2, respectively.

4.1.2. Generation of *vbp3* mutants in *A. tumefaciens*

For the mutation of *vbp3*, we initially also wanted to construct a *sacB*-based suicide plasmid that carried both upstream and downstream sequences of *vbp3* and to use the same methodology as in the *vbp2* mutation, because the counterselectable marker *sacB* gene allows these rare double cross-over events to be identified in the general bacterial population. In addition, this *sacB*-based method allows the creation of deletions in specific genes on the chromosome eventually devoid of any unwanted selection marker and thus the gene inactivation created by this in-frame deletion often has a reduced polar effect on downstream genes in the same operon. However, when we tried to construct the *sacB*-based suicide plasmid that carried both upstream and downstream sequences of *vbp3*, we found that the *vbp3* upstream fragments could not be inserted into this suicide vector. We could not get the *sacB*-based suicide plasmid carrying both upstream and downstream sequences of *vbp3*. Therefore, a different strategy was used to generate the *vbp3* mutants.

Mutation at *vbp3* was generated by insertion of a plasmid containing part of the *vbp3* gene into the chromosomal copy of *vbp3* by homologous recombination (Fig. 4.4). We inserted a short fragment of *vbp3* into plasmid pUC19 to generate pUCvbp3. Plasmid pUCvbp3 was electroporated to A348Δvbp2 and GMI9017Δvbp2 strains. The transformants were selected by carbenicillin-containing MG/L plate. The *vbp3*-insertion mutants were screened from the Cb^R-transformants by PCR. Screening results were shown in Fig. 4.5. The upper panel showed that the PCR products amplified by primers

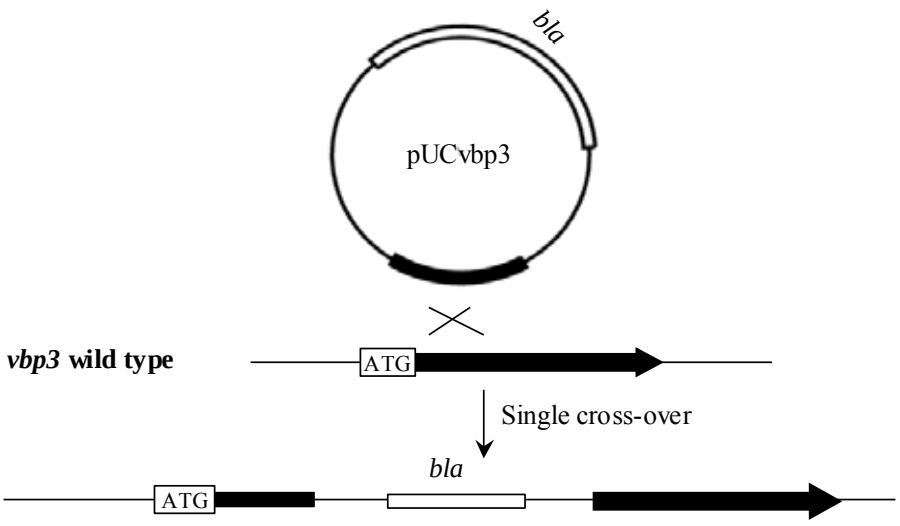

***vbp3*-insertion mutant** (*vbp3* gene was disrupted by a plasmid)

Fig. 4.4. Schematic diagram of *vbp3* mutation strategy. The plasmid pUCvbp3, which carried a short fragment of *vbp3* gene, was integrated into the *A. tumefacien* genome by homologous recombination at the locus of *vbp3*. The *vbp3* gene was disrupted by the plasmid pUCvbp3. *bla* (open rectangles) represents the carbenicillin resistant gene. The filled rectangles stand for the *vbp3* gene fragment near to the start code. The filled arrows indicate the remaining *vbp3* fragment close to the stop code.

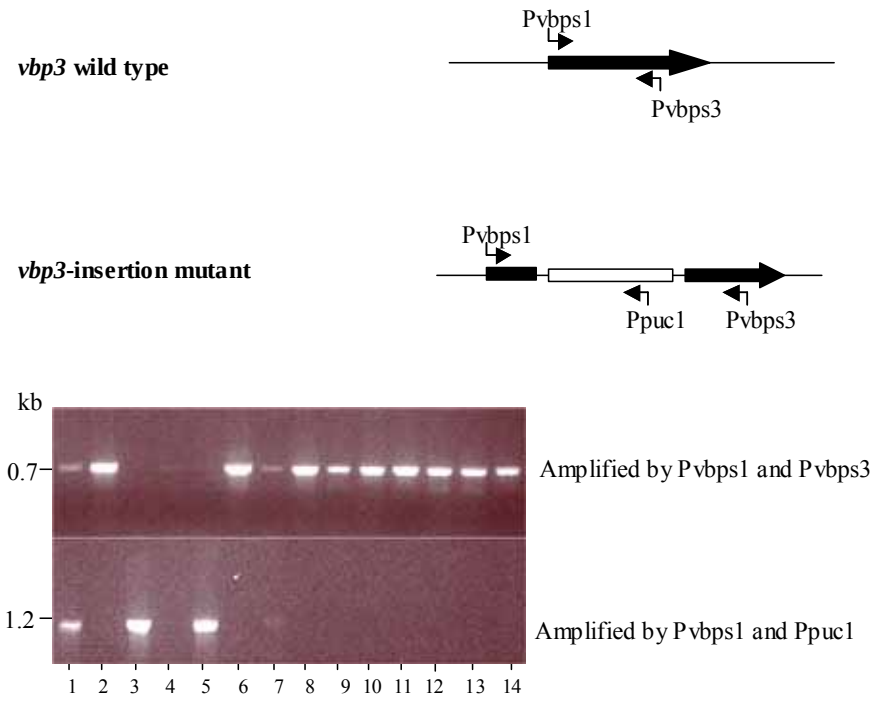

Fig. 4.5. **Screening of *vbp3*-insertion mutants.** The *vbp3*-insertion mutants were screened from Cb^R-transformants by PCR. Three primers, Pvbps1 (annealed to the 5′ region of *vbp3*), Pvbps3 (annealed to the 3′ region of *vbp3*), and Ppuc1 (annealed to the sequence of plasmid) were used to amplify the PCR product. If a Cb^R-transformant was generated because of the integration of plasmid pUCvbp3 into the *vbp3* locus, a PCR fragment can be generated by primers Pvbps1 and Ppuc1 and not by primers Pvbps1 and Pvbps3. Otherwise, the Cb^R-transformant was generated by illegal integration. The colonies in lanes 3 and 5 are the desirable *vbp3*-insertion mutants.

Pvbps1 and Pvbps3 from different Cb^R-colonies. The lower panel showed that the PCR products from the same Cb^R-colonies as the upper panel except amplified by primers Pvbps1 and Ppuc1. As shown in Fig. 4.5, if *vbp3* gene was disrupted by the plasmid pUC19, a PCR fragment can be generated by primers Pvbps1 and Ppuc1 and not by primers Pvbps1 and Pvbps3. The colonies in lanes 3 and 5 (Fig. 4.5) were shown to be the *vbp3*-insertion mutants. The PCR fragment amplified by primers Pvbps1 and Ppuc1 from *vbp3*-insertion mutants was sequenced to confirm that *vbp3* was disrupted by the insertion of plasmid pUC19 into the 595^{th} nucleotide of *vbp3* gene, whereas, the full length of the *vbp3* gene is 936 nucleotides (data not shown). The confirmed *vbp3*-insertion mutants derived from A348Δvbp2 and GMI9017Δvbp2 were designated A348Δvbp2Δvbp3 and GMI9017Δvbp2Δvbp3, respectively.

4.2. Effect of *vbp* Mutation on Tumorigenesis

To test the effect of *vbp* mutation on *A. tumefaciens* ability to cause tumors, we inoculated different *vbp* mutation strains, A348Δvbp2, GMI9017Δvbp2, A348Δvbp2Δvbp3, GMI9017Δvbp2Δvbp3, as well as their parent strains A348 and GMI9017, onto the leaves of *Kalanchoe* plants. As shown in Fig. 4.6A, GMI9017Δvbp2Δvbp3 strain, in which no fully functional *vbp* gene remained, was highly attenuated in the ability to cause tumors on plants, whereas other three *vbp* mutation strains, A348Δvbp2, GMI9017Δvbp2 and A348Δvbp2Δvbp3, did not show apparent difference in tumor formation when compared with their parent strains. This demonstrated that all three *vbp* genes, *vbp1*, *vbp2* and *vbp3*, could functionally complement each other. This result also demonstrated that the mutations of both *vbp2* and *vbp3* did not exert polar effects on their upstream or downstream transcription or

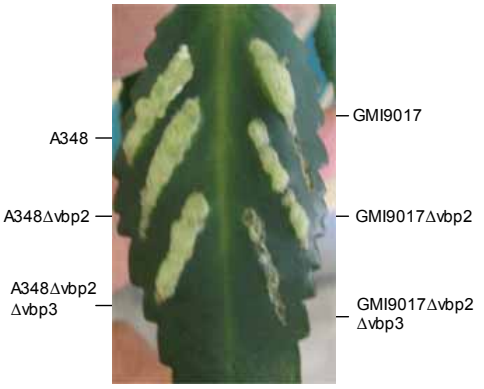
A348
A348Δvbp2
A348Δvbp2
Δvbp3
GMI9017
GMI9017Δvbp2
GMI9017Δvbp2
Δvbp3

A

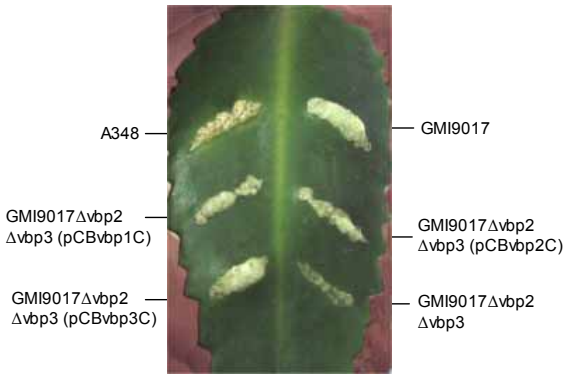
A348
GMI9017Δvbp2
Δvbp3 (pCBvbp1C)
GMI9017Δvbp2
Δvbp3 (pCBvbp3C)
GMI9017
GMI9017Δvbp2
Δvbp3 (pCBvbp2C)
GMI9017Δvbp2
Δvbp3

B


GMI9017
GMI9017Δvb2
Δvbp3

C


GMI9017
GMI9017Δvbp2
Δvbp3

D


GMI9017
GMI9017Δvbp2
Δvbp3

E

Fig. 4.6. Effect of *vbp* mutation on tumorigenesis. (A) Tumorigenesis comparison of different *Agrobacterium tumefaciens* strains. *A. tumefaciens* strains A348, GMI9017, A348Δvbp2, GMI9017Δvbp2, A348Δvbp2Δvbp3, and GMI9017Δvbp2Δvbp3 were grown in MG/L medium at 28°C for 1 day. The cell concentration was adjusted to 1×10^8 cells/ml. Then 2 μl of cell suspension was inoculated onto each wounded line on the leaves of *Kalanchoe* plants. **(B)** The tumorigenicity of the stain GMI9017Δvbp2Δvbp3 lacking all three VBP activities was restored by the reintroduction of any *vbp* gene on the pCB301 replicon. DNA fragments containing full length of three *vbp* genes and their flanking sequences were inserted to the *Hind* III site of plasmid pCB301 respectively to generate three plasmids pCBvbp1C, pCBvbp2C and pCBvbp3C. These three plasmids were introduced into GMI9017Δvbp2Δvbp3 respectively. Cell concentrations of all strains were adjusted to 1×10^8 cells/ml. Then 2 μl of cell suspension was inoculated onto each wounded line. **(C, D, E)** Effect of inoculation concentrations on the tumorigenesis of GMI9017Δvbp2Δvbp3. The cell concentrations of GMI9017Δvbp2Δvbp3 were adjusted to 1×10^9 cells/ml (C), 1×10^8 cells/ml (D) and 5×10^7 cells/ml (E). Then 2 μl of cell suspension was inoculated onto each wounded line. The tumors were photographed 35-42 ds after inoculation.

translation because the *vbp2* and *vbp3* double mutation strain A348Δvbp2Δvbp3 did not show apparent difference in tumor formation. If the mutations of *vbp2* and *vbp3* exert polar effects on the upstream or downstream genes, the polar effects would be manifested in the A348Δvbp2Δvbp3 strain. Even so, we still used pCB301 replicon to construct three plasmids pCBvbp1C, pCBvbp2C and pCBvbp3C, which carry full length of *vbp1* gene, *vbp2* gene and *vbp3* gene as well as their flanking sequences. We introduced these three plasmids to GMI9017Δvbp2Δvbp3 strain one by one to test whether the reintroduction of any one single *vbp* gene could restore the tumorigenicity of GMI9017Δvbp2Δvbp3 strain. Fig. 4.6B showed that the reintroduction of any one single *vbp* gene could fully restore the ability of the no fully functional *vbp* gene mutant to cause tumors. To further compare the virulence of GMI9017Δvbp2Δvbp3 and its parent strain GMI9017, we infected *Kalanchoe* plants with different cell concentrations. At a high concentration of 1×10^9 cells/ml (Fig. 4.6C), GMI9017Δvbp2Δvbp3 strain could induce much less and smaller tumors on plants than GMI9017. At all other tested concentrations less than 1×10^8 cells/ml (Fig. 4.6D, E), GMI9017Δvbp2Δvbp3 strain could not induce tumors on plants. Similar results were obtained when we inoculated these strains onto the stems of tobacco plants (data not shown). We wondered whether the *vbp* mutation would affect the growth rate of *A. tumefaciens* cells. Therefore, we compared the growth curves of GMI9017Δvbp2Δvbp3 and its parent strain GMI9017. No significant difference in growth rate between GMI9017Δvbp2Δvbp3 and its parent strain GMI9017 was observed (Fig. 4.7). These suggested that *vbp* is important for the bacterial virulence to cause tumors on plants.

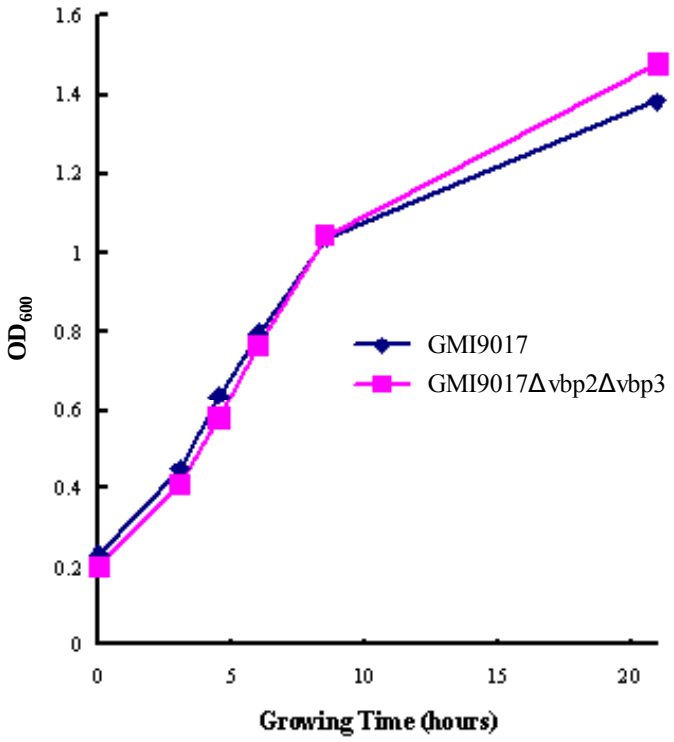

Fig. 4.7. The growth curves of *Agrobacterium tumefaciens* strains GMI9017 and GMI9017Δvbp2Δvbp3. The *A. tumefaciens* cells were grown in MG/L liquid media. The OD_{600} of culture was measured at different time intervals.

4.3. Evidence for the Existence of VirD2-T-strand-VirE2 Complex in the Induced *Agrobacterium* Crude Extract

4.3.1. Pulling down of VirD2-T-strand-VirE2 complex by VBP1

As discussed in chapter 1, VirD2 covalently associated with the 5′-end of the T-strand. VirE2, as a single-stranded (ss) DNA-binding protein, possibly coated the ssT-strand along its length to form a VirD2-T-strand-VirE2 complex structure. However, some recent studies argued against the existence of such a T-complex structure inside *A. tumefaciens* cells. VBP1 can specifically and strongly bind to VirD2. Consequently, we attempted to pull down the VirD2-T-strand-VirE2 complex from AS-induced *A. tumefaciens* cell extract by using VBP1 as the affinity ligand. If the VirD2-T-strand-VirE2 complex exists inside *A. tumefaciens* cells, it should be pulled down by VBP1.

When we used anti-VirE2 antibody to analyze the VBP pulling-down proteins by Western blotting, we found that VirE2 can also be pulled down. As shown in Fig. 4.8, all three VBP proteins can specifically pull down VirE2 protein. Based on the Western blotting results, we estimated a large amount of VirE2 protein was pulled down as compared with VirD2. So, we want to determine if VirE2 was pulled down in the form of VirD2-T-strand-VirE2 complex. To ensure that VirE2 and T-strand can be pulled down in the form of T-complex, we chose four *A. tumefaciens* strains, A348 (wild type), WR1715 (VirD2 deletion), LBA4404 (T-DNA deletion), and LBA4404 harboring pIG121Hm (known T-DNA), to perform the binding between VBP1 and VirD2-T-strand-VirE2 complex. His-tagged VBP1-bound resin was incubated with the AS-induced cell extracts of these four strains respectively. The complexes pulled down from these four strains were analyzed by Western blot (Fig. 4.9). From the total bacterial lysate of

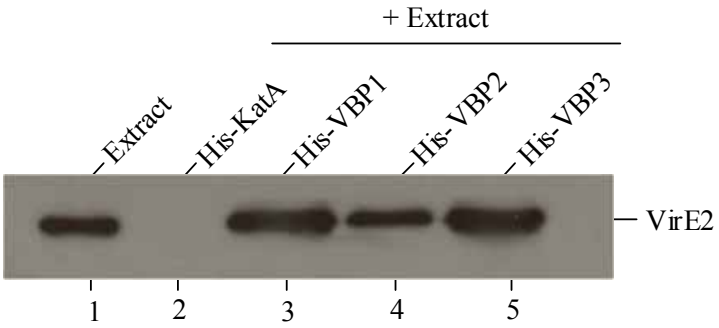

Fig. 4.8. Detection of VirE2 in the VBP-pulling down protein samples. Equal amount of His-KatA bound resin (lane 2), His-VBP1 bound resin (lane 3), His-VBP2 bound resin (lane 4) or His-VBP3 bound resin (lane 5) was incubated with an equal volume of AS-induced *A. tumefaciens* crude extract. After incubation for 60 min at 4°C, the resins were washed and then eluted with imidazol. The eluted proteins were separated by SDS-PAGE. VirE2 was detected by Western blot with rabbit anti-His-VirE2 antibody. *A. tumefaciens* crude extract (lane 1) was used as a positive control.

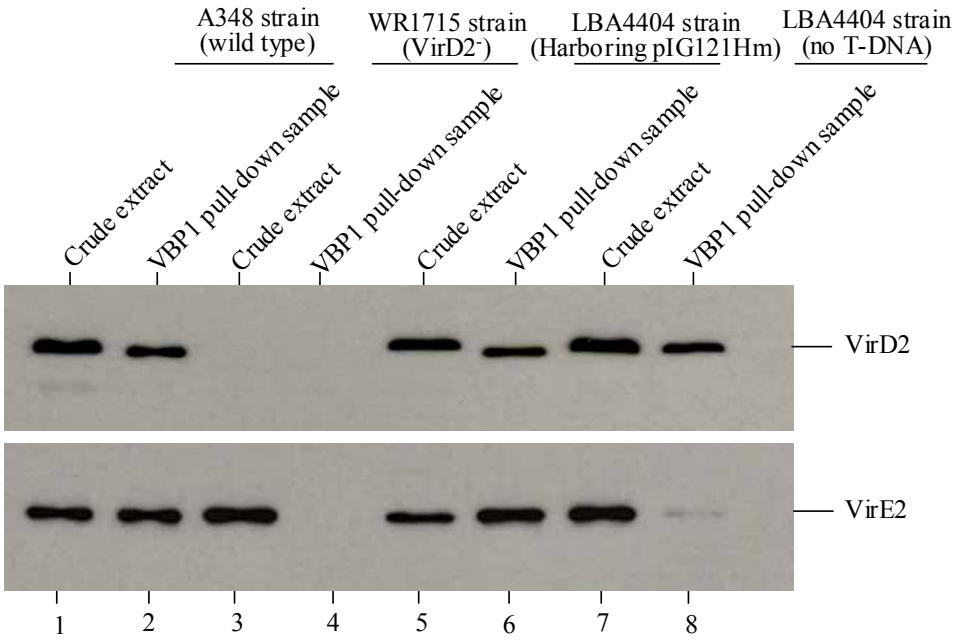

Fig. 4.9. VirE2 was pulled down by VBP1 in the form of VirD2-T-strand-VirE2 complex. Equal quantities of His-tagged VBP1 bound resin were incubated with equal volume of AS-induced A348 extract (lane 2), WR1715 extract (lane 4), extract of LBA4404 harboring pIG121Hm (lane 6), and LBA4404 extract (lane 8) respectively. Following a 60min-incubation at 4°C, the resins were washed and then eluted with imidazol. The eluted complexes were separated by SDS-PAGE. VirD2 (upper panel) and VirE2 (lower panel) were detected by Western blot with rabbit anti-His-tagged VirD2 antibody and anti-His-tagged VirE2 antibody respectively. As positive controls of Western blot, small amounts of A348 extract (lane 1), WR1715 extract (lane 3), extract of LBA4404 harboring pIG121Hm (lane 5), or LBA4404 extract (lane 7) were loaded onto the same SDS-PAGE gel.

induced wild type strain A348 cells, both VirD2 and VirE2 can be pulled down by VBP1 (lane 2 in Fig. 4.9). WR1715 is a VirD2 mutant. In this strain, 70% of *virD2* sequence was deleted (Shurvinton *et al*., 1992). No VirD2 protein was detected in the WR1715 extract, but VirE2 can still be detected in the cell extract (lane 3 in Fig. 4.9). When we used the AS-induced WR1715 cell extract to conduct the pull down assay, VirE2 cannot be pulled down (lane 4 in Fig. 4.9), indicating that the pulling down of VirE2 by VBP1 is dependent on VirD2. LBA4404 is a *vir* helper strain. This strain harbors the disarmed Ti plasmid pAL4404. In this strain, T-DNA was deleted, but all other virulence proteins work (Ooms *et al*., 1982). When His-tagged VBP1-bound resin was incubated with the AS-induced LBA4404 cell extract, VirE2 cannot be pulled down either (lane 8 in Fig. 4.9), although both VirD2 and VirE2 can be detected in the cell extract (lane 7 in Fig. 4.9). This demonstrated that the pulling down of VirE2 by VBP1 is also dependent on T-strand. When plasmid pIG121Hm was introduced to LBA4404, the pIG121Hm-harboring LBA4404 strain can generate the VirD2-T-strand-VirE2 complex because the pIG121Hm plasmid carries a known T-region (Ohata *et al*., 1990). So, VirE2 can be pulled down (lane 6 in Fig. 4.9). All these results demonstrated that VirE2 was pulled down due to the existence of VirD2-T-strand-VirE2 complex.

To determine whether the T-strand can be pulled down by VBP1. Plasmid pIG121Hm was introduced into WR1715 strain. The pIG121Hm-harboring WR1715 strain was used as a negative control because this strain cannot generate the VirD2-T-strand-VirE2 complex due to the *virD2* deletion. As shown in Fig. 4.10, T-DNA fragment can be amplified in the pulled-down complexes from the pIG121Hm-harboring LBA4404 (known T-DNA) by PCR (lane 2 in Fig. 4.10), but cannot be amplified in the pulled-

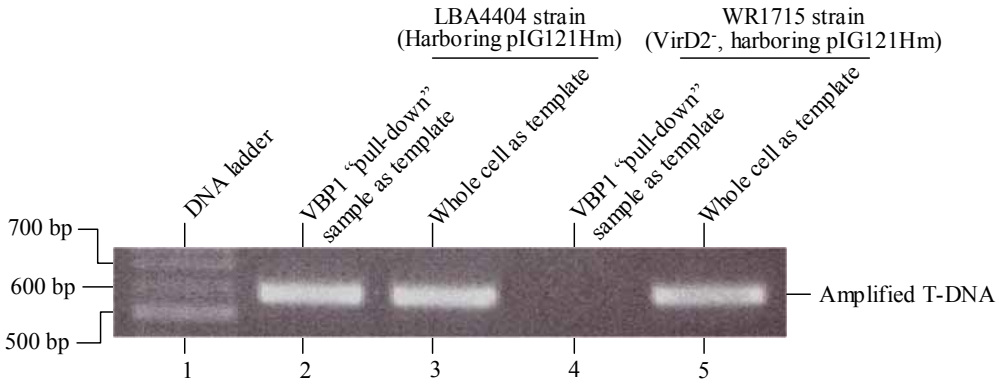

Fig. 4.10. Amplification of T-DNA from the VBP1-pulling down protein samples. To obtain the T-strand from the VBP1-pulling down protein samples, The protein samples pulled down from the extract of LBA4404 harboring pIG121Hm (lane 2) and the extract of WR1715 harboring pIG121Hm (lane 4) were extracted by phenol:chloroform immediately and then centrifuged. The T-strand was precipitated by 70% ethanol from the aqueous supernatant. The precipitate was used as the template to amplify the T-DNA fragment by PCR. As positive controls of PCR, the extract of LBA4404 harboring pIG121Hm (lane 2) and the extract of WR1715 harboring pIG121Hm (lane 5) were also used as templates to amplify the T-DNA. DNA ladder was loaded onto lane 1.

down complexes from the pIG121Hm-harboring WR1715 (known T-DNA, but VirD2 deletion) (lane 4 in Fig. 4.10) by PCR. This demonstrated that the template in the pulled-down complexes from the pIG121Hm-harboring LBA4404 is the T-strand, not plasmid pIG121Hm itself, *i.e*. the T-strand was pulled down.

In order to show how much proteins of VirD2 and VirE2 were pulled down by VBP1, the pulled down complexes from different strains were also analyzed by Coomassie blue staining (Fig. 4.11). The corresponding protein bands (around the same molecular weight as VirD2 and VirE2) in SDS-PAGE gel were excised and then identified by MALDI-TOF. In Fig. 4.11, VirE2 was identified in the position of band 1 and VirD2 was identified in the position of band 2. Both VirD2 and VirE2 protein bands were identified in samples from A348 (lane 1 in Fig. 4.11) and the pIG121Hm-harboring LBA4404 (lane 2 in Fig. 4.11). Only VirD2 protein band was identified in the sample from LBA4404 (lane 4 in Fig. 4.11). Neither VirD2 nor VirE2 was identified in the sample from WR1715 (lane 3 in Fig. 4.11). The VirE2 protein bands (lane 1 and 2 in Fig. 4.11) were very dark. Their concentrations were estimated to be the same as VBP1 protein band. Whereas the VirD2 protein band, whose position was beneath the VirE2, was very faint in all identified lanes. The peptide mass spectrum of band 1 from lane 1 of Fig. 4.11 was shown in Fig. 4.12. Fourteen main peptide masses matched with the calculated tryptic peptide masses from VirE2 (the peaks indicated by black triangle in Fig. 4.12). The matched peptides cover 46**%** (249/533) amino acids of the VirE2 protein. The MS-Fit search results of peptide masses of band 1 were summarized in Table 4.1. VirE2 got significant higher MOWSE score than other candidates. Fig. 4.13 is the peptide mass spectrum of band 2 from lane 1 of Fig. 4.11. In this peptide mass spectrum, sixteen

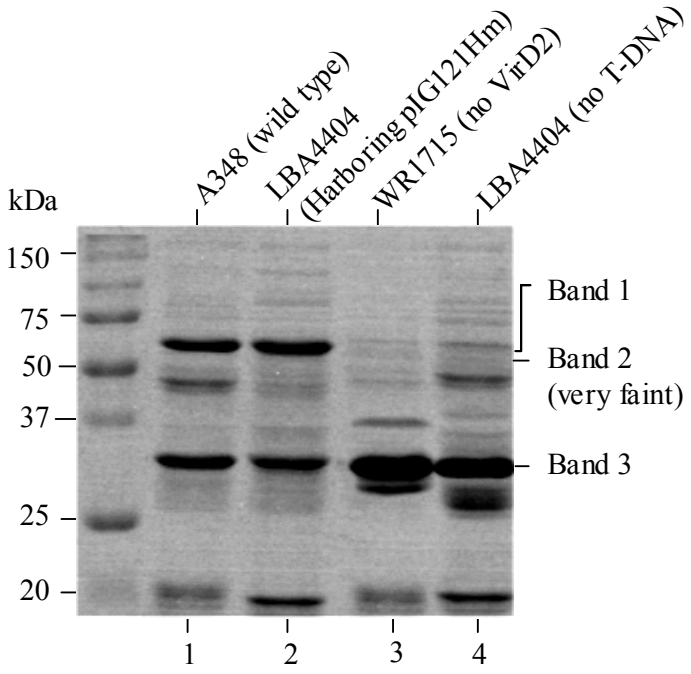

Fig. 4.11. Coomassie blue-staining analysis of VBP1-pulling down protein samples. For Coomassie blue-staining detection of VirD2 and VirE2, larger amounts of His-tagged VBP1 bound resin and *A. tumefaciens* extracts were used to carry out the pull down assay. The eluted protein samples were further concentrated and then freeze-dried. The protein samples from A348 (lane 1), LBA4404 harboring pIG121Hm (lane 2), WR1715 (lane 3), and LBA4404 (lane 4) were separated by 10% SDS-PAGE gel. Proteins were detected by Coomassie blue stain. The related protein bands were excised, in-gel digested by trypsin, and eventually identified by MALDI-TOF. The top dark bands (positions in band 1) in lane 1 and 2 were identified as VirE2. The faint bands beneath the top dark band (positions in band 2) were identified as VirD2. Three lanes (1, 2, 4) have VirD2 band, but only two lanes (1, 2) have VirE2 band. Neither VirD2 nor VirE2 was identified in lane 3. The bottom dark bands (positions in band 3) were identified as VBP1.

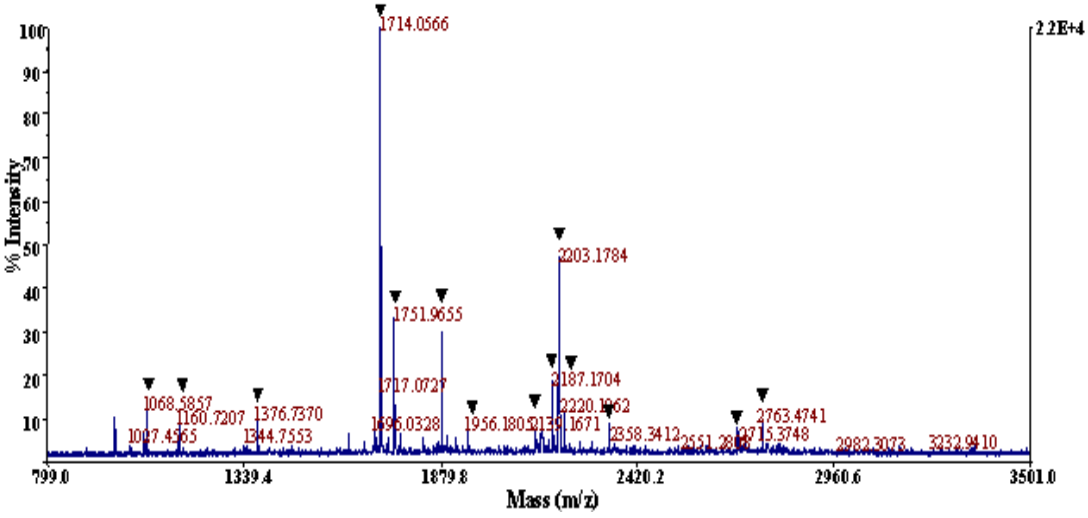

Fig. 4.12. MALDI-TOF peptide mass map of the band 1 from lane 1 of Fig. 4.11. The band 1 from lane 1 of Fig. 4.11 was excised and in-gel digested by trypsin. The resulting peptides were analyzed using a MALDI-TOF mass spectrometer to obtain the mass map. Peptide mass peaks that correspond to the calculated tryptic peptide masses of *A. tumefaciens* VirE2 protein are indicated by triangles.

Table 4.1. MS-Fit search results of MALDI-TOF peptide mass map of the band 1

MOWSE Score	Masses Matched (%)	Protein MW (Da) / pI	Species	NCBInr.030602 Accession	Protein Name
7.29e+010	14/17 (82%)	60587.7 / 6.56	*Agrobacterium tumefaciens*	10955163	VirE2 protein
8.77e+009	13/17 (76%)	60603.8 / 6.57	*Agrobacterium tumefaciens* plasmid pTiA6	77949	gi|77949|pir||B26446 virE2 protein
6.94e+004	4/17 (23%)	5759.8 / 8.87	HUMAN IMMUNODEFICIENCY VIRUS 1	2582742	env
6.05e+004	4/17 (23%)	6605.7 / 4.48	METHANOSARCINA BARKERI	23051505	hypothetical protein
4.76e+004	5/17 (29%)	31151.1 / 4.39	PARACENTROTUS LIVIDUS	21950765	An1 protein
1.6e+004	5/17 (29%)	12269.2 / 8.67	ENTEROCOCCUS FAECALIS V583	29376549	hypothetical protein

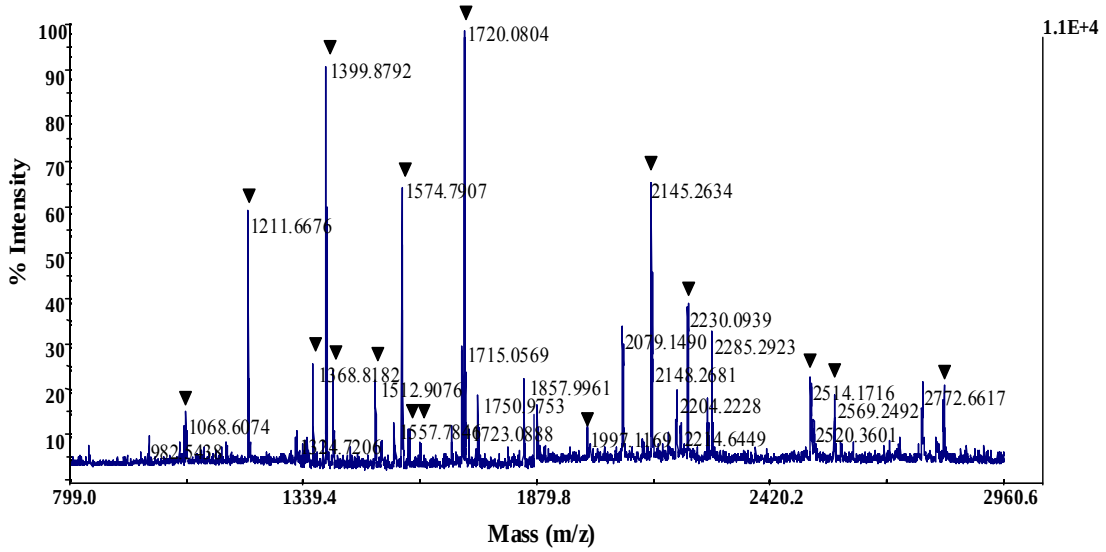

Fig. 4.13. MALDI-TOF peptide mass map of the band 2 from lane 1 of Fig. 4.11. The band 2 from lane 1 of Fig. 4.11 was excised and in-gel digested by trypsin. The resulting peptides were analyzed using a MALDI-TOF mass spectrometer to obtain the mass map. Peptide mass peaks that correspond to the calculated tryptic peptide masses of *A. tumefaciens* VirD2 protein are indicated by triangles.

main peptide masses matched with the calculated tryptic peptide masses from VirD2. The matched peptides covered 49**%** (209/424) amino acids of the VirD2 protein. The MS-Fit search results of peptide masse map of band 2 showed that this protein band got an unambiguous match with VirD2 (Table 4.2). The corresponding protein bands in other lanes of Fig. 4.11 obtained similar peptide mass spectra and MS-Fit search results (data not shown). All these data support the contention that VBP1 can pull down the T-complex and the VirD2-T-strand-VirE2 complex exists in *A. tumefaciens* crude extract.

Our result that the VirD2-T-strand-VirE2 complex can be pulled down by VBP1 strongly supported the existence of the VirD2-T-strand-VirE2 complex in *A. tumefacins* crude extract, which is coincident with an early study (Christie *et al*., 1988). This early study showed that T-strand-VirE2 complex can be immunoprecipitated by VirE2-specific antiserum from crude cell extract and VirE2 protein was detected primarily in the cytoplasm. *In vitro*, VirE2-single stranded DNA complex can be formed favorably (Citovsky *et al*., 1997). Other research facts showed that VirE2 accumulates in *A. tumefaciens* at the same time as the T-strand and in stoichiometric amounts sufficient to bind the T-strand completely (Citovsky *et al*., 1988; Zambryski, 1992). We cannot imagine why the VirD2-T-strand-VirE2 complex cannot be formed in *A. tumefaciens* cytoplasm if both of free VirD2-T-strand complex and VirE2 molecules co-exist in the cytoplasm. Although recent studies (Simone *et al*., 2001; Schrammeijer *et al*., 2003; Cascales and Christie, 2004; Vergunst *et al*., 2000; Chen *et al*., 2000) strongly support that VirD2-T-strand complex and VirE2 are transported separately, separate transport of VirD2-T-strand complex and VirE2 cannot exclude the existence of the VirD2-T-strand-VirE2 complex.

Table 4.2. MS-Fit search results of MALDI-TOF peptide mass map of the band 2

MOWSE Score	Masses Matched (%)	Protein MW (Da) / pI	Species	NCBInr.030602 Accession	Protein Name
1.92e+010	16/31 (51%)	47546.7 / 7.97	*Agrobacterium tumefaciens*	10955158	VirD2 protein
2.43e+004	7/31 (22%)	130905.2 / 4.77	STREPTOMYCES COELICOLOR A3(2)	21220338	cobalamin biosynthesis protein
1.66e+004	8/31 (25%)	102185.6 / 5.11	PSEUDOMONAS SYRINGAE PV. TOMATO STR. DC3000	28867782	organic solvent tolerance protein, putative
1.37e+004	9/31 (29%)	95914.4 / 6.42	FUSOBACTERIUM NUCLEATUM SUBSP. VINCENTII ATCC 49256	27886085	Pyruvate,phosphate dikinase
1.12e+004	5/31 (16%)	8006.6 / 7.73	HUMAN IMMUNODEFICIENCY VIRUS TYPE 1	13604548	pol protein
8.58e+003	7/31 (22%)	34629.5 / 5.55	SPHINGOMONAS PAUCIMOBILIS	8777587	4-carboxy-2-hydroxymuconate-6-semialdehyde dehydrogenase

4.3.2. Co-immunoprecipitation of the VirD2-T-strand-VirE2 complex by anti-VBP1 antiserum

We have demonstrated that recombinant His-VBP1 protein could pull down the VirD2-T-strand-VirE2 complex. To further confirm that native VBP1 protein can bind the VirD2-T-strand-VirE2 complex and provide more solid evidence for the existence of VirD2-T-strand-VirE2 complex, we used anti-VBP1 antiserum to co-immunoprecipitate the VBP1-VirD2-T-strand-VirE2 complex from the AS-induced *Agrobacterium* crude extract. We used three *Agrobacterium* strains, C58, GMI9017Δvbp2Δvbp3, and GMI9017Δvbp2Δvbp3 harboring plasmid pCBvbp1C, to perform the co-immunoprecipitation. C58 is a wild type strain whose genome was completely sequenced. GMI9017Δvbp2Δvbp3 strain is derivative of C58. In this strain plasmid AT was cured and both *vbp2* and *vbp3* were deleted. Plasmid pCBvbp1C can express VBP1 protein and restore the tumorigenicity of GMI9017Δvbp2Δvbp3 strain (Fig. 4.6B). Two pairs of primers were designed to amplify the DNA from co-immunoprecipitates. One pair of primers that correspond to the "*ipt*" gene can amplify the T-strand from the VBP1-VirD2-T-strand-VirE2 complex and the T-region from Ti-plasmid. The other pair of primers that correspond to the "*virB1*" gene can amplify the backbone of Ti-plasmid. If the DNA template from co-immunoprecipitate is T-strand, only the T-strand gene "*ipt*" can be amplified. If the DNA template from co-immunoprecipitate is Ti-plasmid, both the T-region gene "*ipt*" and Ti-plasmid backbone gene "*virB1*" can be amplified. As we expected, the VBP1-VirD2-T-strand-VirE2 complex can be co-immunoprecipitated by anti-VBP1 antiserum because all three proteins, VBP1, VirD2 and VirE2 can be detected in the co-immunoprecipitate and only the T-DNA fragment corresponding to the "*ipt*"

gene can be amplified from the co-immunoprecipitate (lane 2 of Fig. 4.14), whereas both T-DNA fragment and Ti-plasmid backbone fragment can be amplified from supernatant (lane 1 in Fig. 4.14). When the cell extract from GMI9017Δvbp2Δvbp3 strain was used to perform the co-immunoprecipitation, no component of VBP1-VirD2-T-strand-VirE2 complex was detected in the co-immunoprecipitate (lane 4 in Fig. 4.14). However, when the plasmid pCBvbp1C, which can express VBP1 protein, was introduced into GMI9017Δvbp2Δvbp3 strain, all components of VBP1-VirD2-T-strand-VirE2 complex can be co-immunoprecipitated (lane 6 in Fig. 4.14). This result confirmed that native VBP1 could bind VirD2 and the existence of VirD2-T-strand-VirE2 complex in *Agrobacterium* crude extract.

4.4. Interactions between VBP Protein and T4SS Components

4.4.1. Pulling down of T4SS components by VBP1

VBP1 can strongly bind VirD2. We asked whether VBP1 accompanies VirD2 to the membrane transport site. Next, we wanted to know if T4SS components could be pulled down by VBP1. As we know, most of the T4SS components are membrane proteins. The extraction of T4SS components may require detergent. However, detergent may affect the binding between VBP1 and T4SS components. So, we used 0.5% Triton-buffer and non-Triton-buffer to extract T4SS components. To ensure the reliability of the pull down assay, we conducted two negative controls, one is the blank resin, and the other is the His-tagged KatA bound resin. As mentioned before, KatA is a catalase (Xu *et al*., 2001) and thus was not expected to bind T4SS components. We used equal amounts of blank resin, His-tagged KatA bound resin, and His-tagged VBP1 bound resin to incubate with

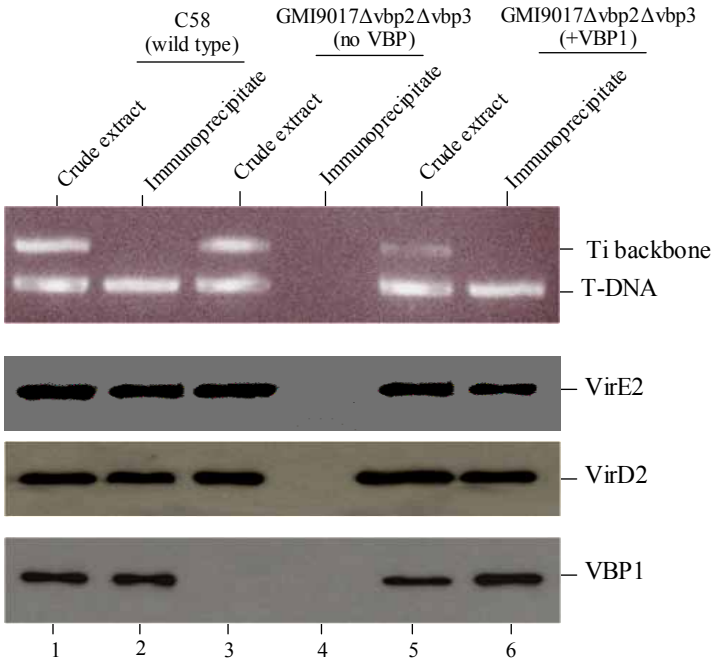

Fig. 4.14. Co-immunoprecipitation of T-complex by anti-VBP1 antiserum. AS-induced cell crude extracts from three *A. tumefaciens* strains were pre-cleared by protein A-Sepharose and preimmune serum to reduce the background of nonspecific proteins. The pre-cleared crude extracts were incubated with protein A-Sepharose and anti-VBP1 antiserum at 4°C for 4 h with rocking. The co-immunoprecipitates bound to Sepharose beads were washed five times and then eluted from the beads by incubation at 96°C for 20 min with small amount of buffer. Proteins in the co-immunoprecipitates were separated by SDS-PAGE and analyzed by Western blot. DNA in the co-immunoprecipitates was detected by PCR amplification and gel electrophoresis (top panel). Strains: C58 is a wild type strain; GMI9017Δvbp2Δvbp3 is a *vbp* mutant in which all three *vbp* genes were mutated; GMI9017Δvbp2Δvbp3 (+VBP1) is the GMI9017Δvbp2Δvbp3 mutant producing VBP1 from plasmid pCBvbp1C. T-complex was co-immunoprecipitated from C58 (lane 2) and GMI9017Δvbp2Δvbp3 (+VBP1) (lane 6).

equal volumes of AS-induced *Agrobacterium* extract. The pulled down proteins were separated by SDS-PAGE and analyzed by Western blot with the related antibodies. In all detected 6 VirB proteins (Fig. 4.15), VirB4, VrB8, and VirB11 can be specifically pulled-down by VBP1 (lanes 4 and 5 in Fig. 4.15) because these three proteins cannot be detected in two negative controls (lanes 2 and 3 in Fig. 4.15). VirB9 and VirB10 showed non-specifically binding to resin as we can see that both of them can be pulled down by blank resin and His-tagged KatA bound resin (lanes 2 and 3 in Fig. 4.15). This result also showed that VirB9 and VirB10 couldn't be detected in the pulled down proteins from the non-Triton extract, demonstrating that VirB9 and VirB10 may not be extracted by non-Triton buffer (lane 5 in Fig. 4.15). VirB7 cannot be detected in all the pulled down protein samples.

As we know T4SS components interact with each other (Ward *et al*., 2002) and VBP1 can bind VirD2, it is possible that some T4SS components may be pulled down via interacting with other components not directly by VBP1. Based on the specific interactions between the T4SS components and VirD2-T-strand substrate, the T4SS components can be divided into three classes (Cascales and Christie, 2004). Class I includes VirB11, VirB9, VirB8, VirB6, and VirB2. These proteins show close contacts with the T-strand during translocation and were proposed to correspond to channel subunits of the secretory apparatus. Class II comprises VirB10, VirB7, VirB5, and VirB4. These proteins show indirect contacts with the T-strand. They possibly interact with the transfer intermediate in some way. VirB1, VirB3, and another presumptive secretory component, VirJ are defined as class III. This protein class does not show contacts with the transfer intermediate.

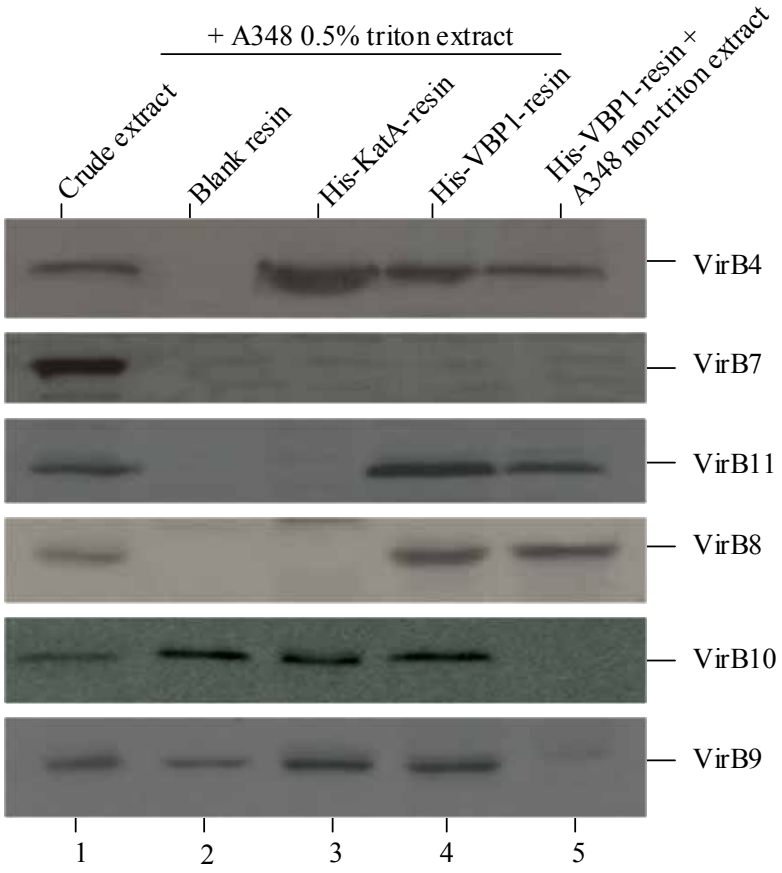

Fig. 4.15. Detection of T4SS components in the VBP1-pulling down proteins. Pre-equilibrated blank TALON metal affinity resin, His-tagged KatA bound TALON metal affinity resin, or His-tagged VBP1 bound TALON metal affinity resin were incubated with AS-induced *A. tumefaciens* A348 0.5% Triton extract or non-Triton extract at 4°C for 1 hour. The resins were washed 5 times with incubating buffer. The pulled down proteins were dissolved in the SDS-PAGE loading buffer directly. A348 0.5% Triton extract was loaded onto lane 1 as a positive control. Protein pulled down by blank resin was loaded onto lane 2. Protein pulled down by His-tagged KatA was loaded onto lane 3. Lane 4 and 5 were loaded proteins pulled down by His-tagged VBP1, but proteins in lane 5 were pulled down from A348 non-Triton extract. The separated proteins were analyzed by using Western blot.

VirB8 and VirB11 that were shown to bind to VBP1 specifically in this study belong to the proteins of the class I that show close contacts with the VirD2-T-strand substrate during translocation. To determine if these proteins were pulled down by VBP1 directly or indirectly, we used three mutated *A. tumefaciens* strains, WR1715 (*virD2* deletion), A348ΔB8 (*virB8* deletion), and A348ΔB11 (*virB11* deletion) to carry out the pull down assay. Results were shown in Fig. 4.16. In the protein sample pulled down from the AS-induced WR1715 cell extract, both VirB8 and VirB11 could be detected (lane 4 in Fig. 4.16), indicating that VirD2 did not affect the pulling down of VirB8 and VirB11. In the AS-induced A348ΔB11 crude extract, VirB8 could be detected (lane 5 in Fig. 4.16). When the AS-induced A348ΔB11 crude extract was used to conduct the pull down assay, VirB8 could not be pulled down by VBP1 (lane 6 in Fig. 4.16), demonstrating that the pulling down of VirB8 by VBP1 was dependent on VirB11. However, when we used the AS-induced A348ΔB8 crude extract to conduct the pull down assay, VirB11 could be pulled down by VBP1 (lane 8 in Fig. 4.16), suggesting that the pulling down of VirB11 by VBP1 did not require VirB8. Results in Fig. 4.16 gave us such a conclusion that VirB11 was pulled down by VBP1 directly and VirB8 was pulled down by VBP1 via VirB11.

4.4.2. Pulling down of VirB11 by VBP2 and VBP3

We have confirmed that all three VBP proteins could specifically interact with VirD2 (Fig. 3.13). We also have shown that VBP1 could specifically pull down VirB11. To further determine if VBP2 and VBP3 have the same function as VBP1. We tested whether VBP2 and VBP3 could also pull down VirB11. His-VBP2 and His-VBP3 were used to conduct the pull down assay with the same operating procedure as His-VBP1. As

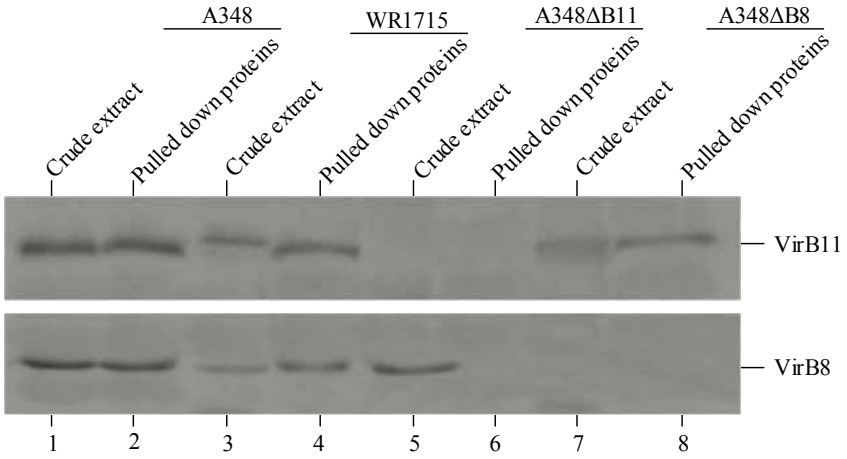

Fig. 4.16. VirB11 interacts with VBP1 directly and VirB8 is pulled down via VirB11. His-tagged VBP1-bound TALON metal affinity resin was incubated with related *A. tumefaciens* mutant strain 0.5% Triton extract. The pulled down proteins were separated by SDS-PAGE and analyzed by Western blot. Lane 1: A348 crude extract; Lane 2: proteins pulled down from A348; Lane 3: WR1715 (VirD2 deletion) crude extract; Lane 4: proteins pulled down from WR1715; Lane 5: A348ΔB11 (*virB11* deletion) extract; Lane 6: proteins pulled down from A348ΔB11; Lane 7: A348ΔB8 (*virB8* deletion) extract; Lane 8: proteins pulled down from A348ΔB8

shown in Fig. 4.17, both VBP2 (lane 4 in Fig. 4.17) and VBP3 (lane 5 in Fig. 4.17) could pull down VirB11 from AS-induced *A. tumefaciens* A348 protein extract. This indicates that both VBP2 and VBP3 can also bind VirB11 and further confirms that all three VBP proteins could functionally complement each other.

4.4.3. Co-immunoprecipitation of T4SS components by anti-VBP1 antiserum

The pull-down results showed that VirD4 (data not shown), VirB4 and VirB11 can be pulled down by His-VBP1, but VirD4 showed non-specifically binding to the blank TALON metal affinity resin (data not shown) and VirB4 showed non-specifically binding to the His-KatA (lane 3 in Fig. 4.15). To clear the ambiguous pull-down results, we further used co-immunoprecipitation approach to verify the interaction between VBP1 and T4SS components. Co-immunoprecipitation results showed that VirD2, VirD4, VirB4 and VirB11 were co-immunoprecipitated by anti-VBP1 antiserum (lane 4 in Fig. 4.18), but not by preimmune serum (lane 3 in Fig. 4.18). Other T4SS components cannot be co-immunoprecipitated by anti-VBP1 antiserum. Results also showed that protein A-Sepharose beads do not bind T4SS components. As we know VBP1 can bind VirD2, we want to know whether the co-immunoprecipitation of T4SS components by ant-VBP1 antiserum is dependent on VirD2 and we also need to know whether the co-immunoprecipitation is VBP1-specific. We used four *A. tumefaciens* strains to perform the co-immunoprecipitation. As shown in Fig. 4.19, in a *vbp* mutant GMI9017Δvbp2Δvbp3, in which all three *vbp* genes were mutated, VirD2, VirD4, VirB4 and VirB11 cannot be co-immunoprecipitated by anti-VBP1 antiserum (lane 4 in Fig. 4.19). When plasmid pCBvbp1C was introduced into this *vbp* mutant to produce VBP1 protein, all these four proteins (VirD2, VirD4, VirB4 and VirB11) can be co-

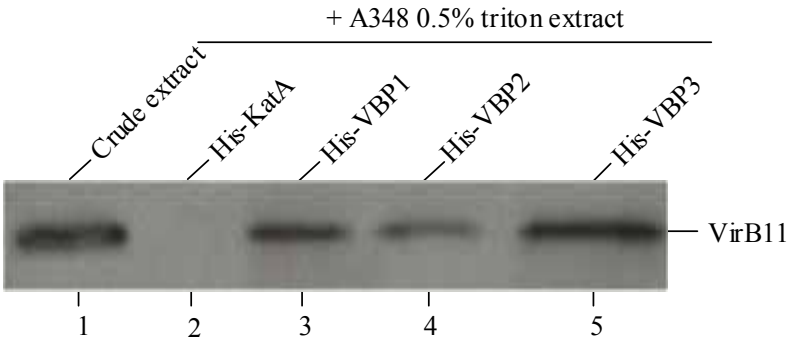

Fig. 4.17. Pulling down of VirB11 by VBP2 and VBP3. Equal amount of His-KatA bound resin (lane 2), His-VBP1 bound resin (lane 3), His-VBP2 bound resin (lane 4) or His-VBP3 bound resin (lane 5) was incubated with an equal volume of AS-induced *A. tumefaciens* A348 protein extract. After incubation for 60 min at 4°C, the resins were washed 5 times with incubating buffer. The pulled down proteins were dissolved in the SDS-PAGE loading buffer directly and separated by SDS-PAGE. VirB11 was detected by Western blot with rabbit anti-VirB11 antibody. *A. tumefaciens* A348 protein extract (lane 1) was used as a positive control.

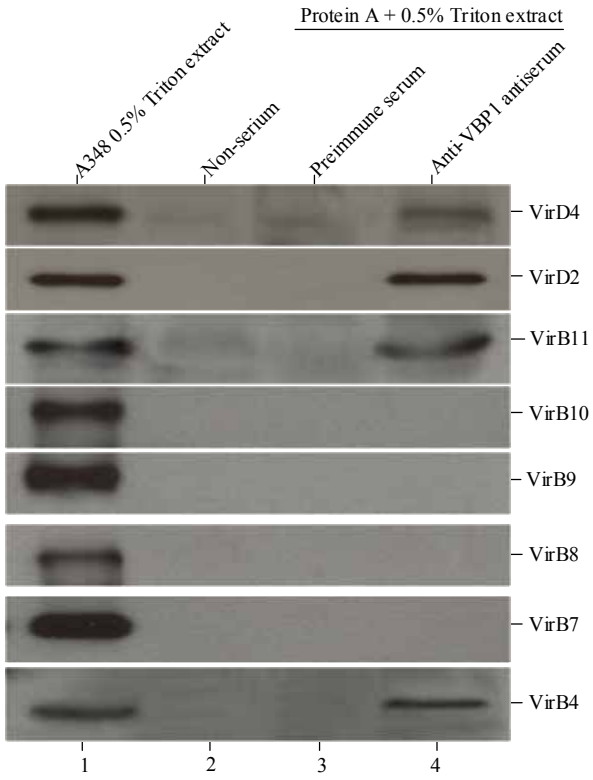

Fig. 4.18. Co-immunoprecipitation of T4SS components by anti-VBP1 antiserum. *Agrobacterium* A348 0.25% Triton extract was pre-cleared by protein A-Sepharose and preimmune serum to reduce the background of nonspecific proteins. Equal amounts of pre-cleared A348 0.25% Triton extract were co-immunoprecipitated with equal volume of preimmune serum (lane 3) or anti-VBP1 antiserum (lane 4) at 4°C for 4 h with rocking. As a negative co-immunopreciptation control, blank protein A-Sepharose bead (lane 2) was also used to incubate with pre-cleared A348 0.25% Triton extract. After incubation, the protein A-Sepharose beads were washed twice with lysis buffer B supplemented with 0.1% Triton X-100 and three times with lysis buffer B. The co-immunoprecipitated complexes were dissolved in the SDS-PAGE loading buffer directly and analyzed by Western blot. As a positive blotting control, crude A348 0.25% Triton extract was loaded onto lane 1.

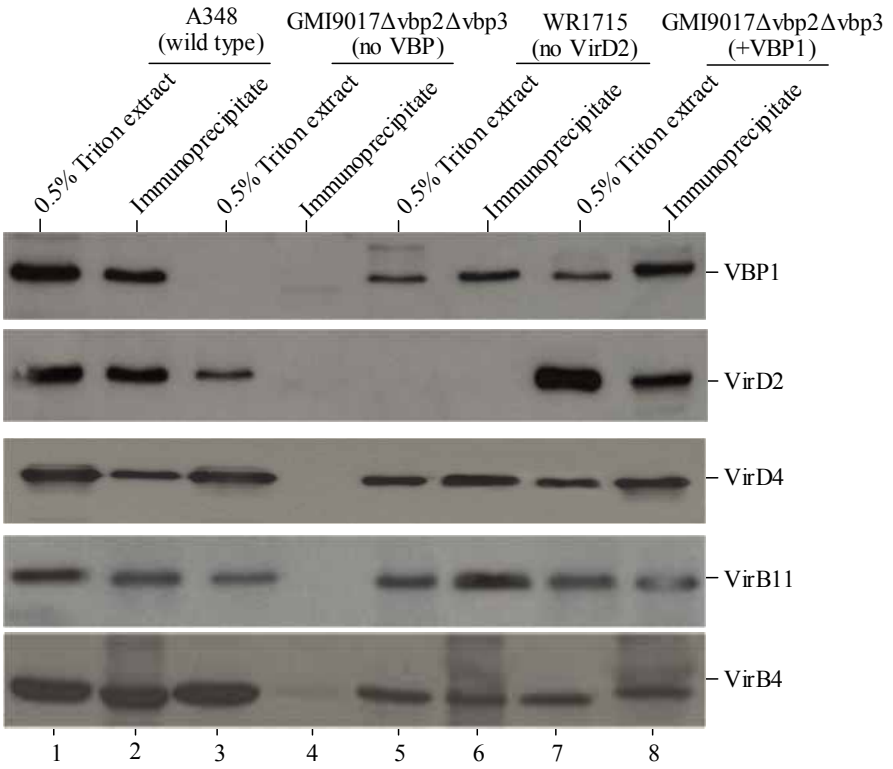

Fig. 4.19. Verification of specific co-immunoprecipitation of T4SS components by anti-VBP1 antiserum. To test if the co-immunoprecipitation is specific, pre-cleared 0.25% Triton extracts from four *A. tumefaciens* strains were co-immunoprecipited with anti-VBP1 antiserum respectively. Strains: A348 is a wild type strain; GMI9017Δvbp2Δvbp3 is a *vbp* mutant in which all three *vbp* genes were mutated; WR1715 is a *virD2*-deletion mutant; GMI9017Δvbp2Δvbp3 (+VBP1) is the GMI9017Δvbp2Δvbp3 mutant producing VBP1 from plasmid pCBvbp1C. Co-immunoprecipitated complexes from these four strains were analyzed by Western blot (lanes 2, 4, 6, 8). Crude pre-cleared 0.25% Triton extracts from these four strains were used as positive blotting controls and were loaded on to lanes 1, 3, 5, and 7 respectively.

immunoprecipitated (lane 8 in Fig. 4.19), indicating that co-immunoprecipitation of VirD2, VirD4, VirB4 and VirB11 by anti-VBP1 antiserum is VBP1-specific. In a *virD2*-deletion mutant WR1715, VirD4, VirB4 and VirB11 can also be co-immunoprecipitated (lane 6 in Fig. 4.19), implying that the co-immunoprecipitation of VirD4, VirB4 and VirB11 by anti-VBP1 antiserum is independent on VirD2. These results suggested that VBP1 interacts with VirD2 and T4SS components possibly by two different domains and thus supported a hypothesis that VBP1 help the T-complex (VirD2) to recognize the T4SS transport site.

VirD4, VirB11 and VirB4 are three energetic components of T4SS. Recent study showed that VirD4 strongly interacts with both VirB11 and VirB4 (Atmakuri *et al*., 2004). We thus assayed whether the co-immunoprecipitation of VirB11 and VirB4 is dependent on each other. We used *virB11* and *virB4* mutants, A348ΔB11 and A348ΔB4, to carry out the co-immunoprecipitation. As shown in Fig. 4.20 (lanes 3 and 4), the co-immunoprecipitation of VirB11 and VirB4 by anti-VBP1 antiserum is independent on each other.

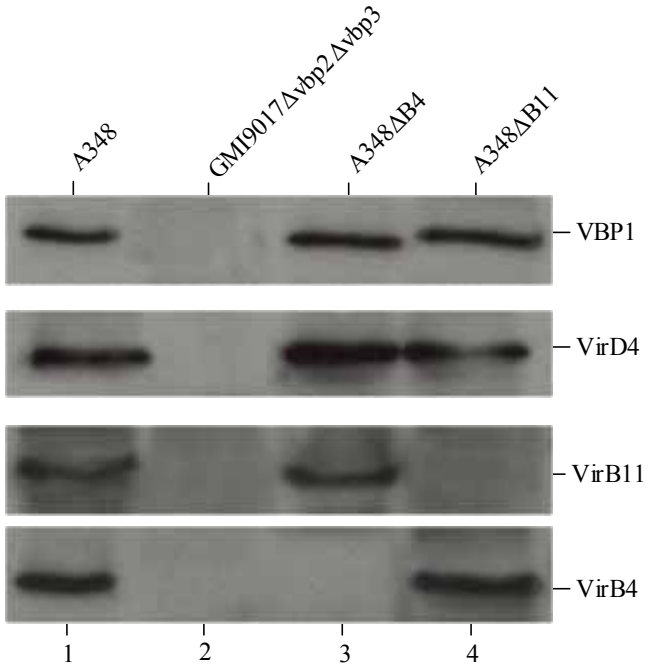

Fig. 4.20. Co-immunoprecipitation of VirB4 and VirB11 is independent of each other. Pre-cleared 0.25% Triton extracts from four *A. tumefaciens* strains were co-immunoprecipited with anti-VBP1 antiserum respectively. Strains: A348 is a wild type strain; GMI9017Δvbp2Δvbp3 is a *vbp* mutant in which all three *vbp* genes were mutated; A348ΔB4 is a *virB4*-deletion mutant; A348ΔB11 is a *virB11*-deletion mutant. Co-immunoprecipitates from these four strains were analyzed by Western blot. VirB4 can be co-immunoprecipitated from A348ΔB11 mutant (lane 4) and VirB11 can be co-immunoprecipitated from A348ΔB4 mutant (lane 3).

Chapter 5 The Role of VirD2-binding Protein in Conjugal DNA Transfer

Previous studies (Beijersbergen *et al*., 1992; Buchanan-Wollaston *et al*., 1987; Cook and Farrand, 1992; Chen *et al*., 2002) demonstrated that *A. tumefaciens* is capable of transferring the IncQ plasmid RSF1010 into eukaryotic and bacterial cells. Plasmid RSF1010 was also shown to reduce T-DNA transfer (Binns *et al*., 1995), presumably because it competes with transferred substrates at the transport pore (Stahl *et al*., 1998). In this study, we have demonstrated that *vbp* triple mutant highly attenuates the tumorigenicity of *A. tumefaciens* and VBP proteins interact with both VirD2 and VirD4. It is conceivable that the influence of *vbp* mutants on the mobilization frequency of RSF1010 by VirB/D4 T4SS would be sophisticated.

5.1. VBP Proteins Affect the Conjugal Transfer of pML122 Mediated by *A. tumefaciens* Conjugal System

We next want to know whether *vbp* mutants would affect other DNA transfer system in *A. tumefaciens*. RSF1010 has been shown to be mobilized by *A. tumefaciens* strains without VirB/D4 T4SS transport pore (Cook and Farrand, 1992; Chen *et al*., 2002), indicating that RSF1010 can be mobilized by other *A. tumefaciens* DNA transfer system. So, we introduced a derivate of RSF1010, pML122, into different *A. tumefaciens* strains (Table 5.1; for the characteristics of strains, please see Table 2.1; for the plasmid characteristics, please see Table 2.2) by electroporation. Since RSF1010 has been shown to compete the same VirB/D4 T4SS transport pore with T-complex (Stahl *et al*., 1998), we assayed the conjugal transfer of pML122 in *A. tumefaciens* under non-inducing

Table 5.1. Effect of *vbp* mutation on the mobilization of a RSF1010 derivative pML122 from *Agrobacterium* to *E. coli* (MT607) under non-inducing conditions

Donor Strains	Number of input donors (10^9)	Number of transconjugants	Frequency /per input donor ± SD (10^{-8})
A348	1.1	97	9.6 ± 4.9
A348Δvbp2	1.1	86	7.8 ± 5.0
A348Δvbp2Δvbp3	1.0	96	9.2 ± 1.3
GMI9017	0.9	64	5.7 ± 2.1
GMI9017Δvbp2	0.9	46	5.5 ± 5.2
GMI9017Δvbp2Δvbp3	1.0	0	$<10^{-9}$
A348ΔB4	1.0	87	7.8 ± 4.4
A348ΔB11	1.1	49	8.5 ± 9.8
GMI9017Δvbp2Δvbp3 (pCBvbp1C)	0.9	79	6.0 ± 6.0
GMI9017Δvbp2Δvbp3 (pCBvbp2C)	0.9	31	5.2 ± 5.1
GMI9017Δvbp2Δvbp3 (pCBvbp3C)	1.0	29	3.4 ± 3.1

Numbers of input donors and transconjugants are the data from a representative experiment. Frequency data represent the means of triplicates (±SD) from a single experiment. Two independent experiments were performed. Although absolute numbers varied between two individual experiments, the relative frequencies among the mutant strains showed the same tendencies in two experiments.

conditions, in order to reduce the interference of T-DNA transfer to pML122 transfer. We used *E. coli.* as recipient. The mobilization frequencies of pML122 in different *A. tumefaciens* strains were shown in Table 5.1. The transfer frequencies in two *virB* mutants, A348ΔB4 and A348ΔB11, are similar to wild type strain A348, indicating that the mobilization of pML122 in *A. tumefaciens* under non-inducing conditions was mediated by other *A. tumefaciens* DNA transfer system not by VirB/D4 T4SS. Without VirB/D4 T4SS, the mobilization frequency of RSF1010 in *A. tumefaciens* is very low, which is consistent with previous observations (Cook and Farrand, 1992; Chen *et al*., 2002). However, the results in Table 5.1 showed that the *vbp* triple mutant GMI9017Δvbp2Δvbp3 reduced the mobilization frequency of pML122 at least several decade-fold. When any of these three *vbp* genes was reintroduced into the *vbp* triple mutant GMI9017Δvbp2Δvbp3 by another replicon (pCBvbp1C, pCBvbp2C, and pCBvbp3C), the mobilization frequency of pML122 was restored to the level of *vbp* wild type. These results indicated that VBP proteins affect the RSF1010 mobilization by other *A. tumefaciens* conjugal system.

We also assayed the mobilization frequencies of pML122 in these *A. tumefaciens* strains with a helper, *E. coli*. MT616 strain. MT616 harbors plasmid pRK600, which was used to mobilize the megaplasmids via *oriT*. Plasmid pRK600 does not replicate in *A. tumefaciens*, but it evidently persists for a sufficient period of time to express the RK2 transfer genes (Finan *et al*., 1988). So, MT616 can help *A. tumefaciens* to mobilize pML122. Under the help of MT616, the mobilization frequency of pML122 in *A. tumefaciens* was increased to $4.4 \sim 8.2 \times 10^{-4}$ transconjugants per input donor, but *vbp* mutants did not affect the mobilization frequency of pML122 mediated by the RK2

transfer genes (data not shown), indicating that VBP proteins were not involved in the RK2 DNA transfer system.

5.2. VBP Proteins Interact with pML122

VBP proteins affected the pML122 mobilization mediated by *A. tumefaciens* conjugal system, implying that VBP protein might interact with plasmid pML122 in a way or another. Thus, we used anti-VBP1 antiserum to incubate with the non-induced cell extract of *A. tumefaciens* strains that harbor plasmid pML122 to determine whether plasmid pML122 could be co-immunoprecipitated by anti-VBP1 antiserum. We introduced plasmid pML122 to three *A. tumefaciens* strains, A348, GMI9017Δvbp2Δvbp3, and GMI9017Δvbp2Δvbp3 harboring pCBvbp1C. These three pML122-harboring strains were grown in MG/L liquid medium under non-inducing conditions. The non-induced cell extracts from these three strains were used to perform the co-immunoprecipitation. The co-immunoprecipitates were used as the template to amplify the pML122 fragment and the pCBvbp1C fragment. The PCR amplification result was shown in Fig. 5.1. Plasmid pML122 could be co-immunoprecipitated by anti-VBP1 antiserum from A348 extract (lane 2 in Fig. 5.1), but not from GMI9017Δvbp2Δvbp3 extract (lane 4 in Fig. 5.1), in which no VBP protein was expressed. However, when the plasmid pCBvbp1C was introduced to GMI9017Δvbp2Δvbp3, plasmid pML122 could be co-immunoprecipitated (lane 6 in Fig. 5.1). To test whether the plasmid pCBvbp1C could also be co-immunoprecipitated by anti-VBP1 antiserum from strain GMI9017Δvbp2Δvbp3 harboring pCBvbp1C, two primers, PvbpCS1 and PvbpCS2, were used to amplify the pCBvbp1C fragment. The results showed that pCBvbp1C fragment couldn't be amplified from the co-

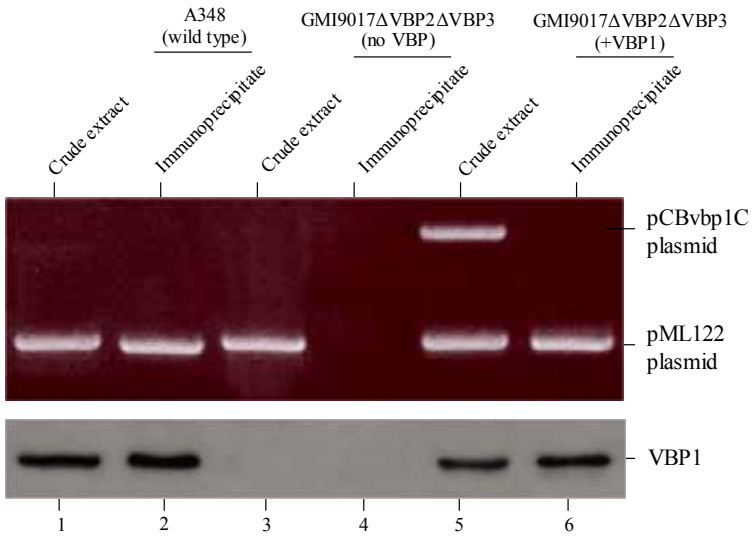

Fig. 5.1. Co-immunoprecipitation of plasmid pML122 by anti-VBP1 antiserum. Plasmid pML122 was introduced into A348, GMI9017Δvbp2Δvbp3 and GMI9017Δvbp2Δvbp3 (+VBP1) respectively. Non-induced cell crude extracts from these three pML122-harboring strains were pre-cleared by protein A-Sepharose and preimmune serum to reduce the background of nonspecific proteins. The pre-cleared crude extracts were incubated with protein A-Sepharose and anti-VBP1 antiserum at 4°C for 4 h with rocking. The co-immunoprecipitates bound to Sepharose beads were washed five times and then eluted from the beads by incubation at 96°C for 20 min with small amount of buffer. Proteins in the co-immunoprecipitates were detected by SDS-PAGE and Western blot (lower panel). DNA in the co-immunoprecipitates was detected by PCR amplification and gel electrophoresis (upper panel). Strains: A348 is a wild type strain; GMI9017Δvbp2Δvbp3 is a *vbp* mutant in which all three *vbp* genes were mutated; GMI9017Δvbp2Δvbp3 (+VBP1) is the GMI9017Δvbp2Δvbp3 mutant producing VBP1 from plasmid pCBvbp1C. Plasmid pML122 was immunoprecipitated from A58 (lane 2) and GMI9017Δvbp2Δvbp3 (+VBP1) (lane 6), whereas, plasmid pCBvbp1C was not co-immunoprecipitated from GMI9017Δvbp2Δvbp3 (+VBP1) (lane 6).

immunoprecipitate of strain GMI9017Δvbp2Δvbp3 harboring pCBvbp1C (lane 6), although the pCBvbp1C fragment could be amplified from the crude extract (lane 5). This demonstrated that VBP proteins specifically interact with plasmid pML122 in some way and thus confirmed that VBP proteins affect the conjugal transfer of pML122 mediated by *A. tumefaciens* conjugal system.

Chapter 6 Definition of Recruiting Proteins in Nucleoprotein Complex Transfer

Using MBP-VirD2 fusion protein as an affinity ligand to perform the pull-down assay, we isolated a VirD2-binding protein, designated VBP1. No proteins with known function are homologous to VBP1. Thus, VBP1 is a novel protein and the function of VBP1 remains unclear. Recombinant protein His-VBP1 was shown to be able to pull down VirD2. Further analysis suggested that the binding between VirD2 and VBP1 is highly specific. Homology analysis showed that *Agrobacterium tumefaciens* has two additional homologous genes, *vbp2* and *vbp3*. VBP2 and VBP3 can also bind VirD2 just like VBP1. To determine the biological function of *vbp* genes, we conducted the mutation of *vbp* genes in *A. tumefaciens*. The *vbp* triple mutant GMI9017Δvbp2Δvbp3, in which no fully functional *vbp* gene exists, exhibited highly attenuated virulence. This strongly supports that VBP1 is involved in the T-DNA transfer. Our results also showed that VBP proteins could pull down the VirD2-T-strand-VirE2 complex from AS-induced *A. tumefaciens* extract and specifically bind with some T4SS components. These pull-down results were further confirmed by co-immunoprecipitation. Anti-VBP1 antiserum can co-immunoprecipitate VirD2-T-strand-VirE2 complex as well as T4SS components: VirD4, VirB11 and VirB4. In addition, VBP proteins were shown to affect the conjugal transfer of plasmid pML122 mediated by *A. tumefaciens* non-T4SS DNA transfer system and to interact with this plasmid in some ways. However, the biochemical function of VBP1 is still not clear.

6.1. VBP is Possibly an Auxiliary Protein of Relaxosome, the T-DNA Processing Complex

BLAST searches revealed that all three VBP proteins have a putative nucleotidyltrasferase motif and a putative HEPN domain. Nucleotidyltrasferases are classified into more than 10 distinct superfamilies. The member proteins catalyze the same chemical reaction: the coupling of nucleoside triphosphates to a free hydroxyl group via elimination of pyrophosphate. Nucleotidyltransferases are involved in diverse biological functions that range from DNA repair, telomere maintenance, immunoglobulin gene rearrangement to regulation of biosynthetic pathways and signal transduction. It is known that protein nucleotidyltransferases, such as protein uridylyl transferases (GlnD) and protein adenylyl transferases (GlnE), could catalyze the nucleotidylation of specific proteins to regulate the functions of the modified proteins (Aravind and Koonin, 1999). Therefore, it is possible that the identified VBP1 might be involved in the T-DNA transfer because VBP1 could possess putative nucleotidyltransferase activity that may be involved in diverse biological functions.

To know more about the biochemical function of VBP, we analyzed the functions of genes adjacent to *vbp*. All three predicted proteins encoded by the ORFs in the upstream of *vbp1* are hypothetical proteins of unknown function. The first predicted protein encoded by the ORF in the downstream of *vbp1* is an aminotransferase and the second predicted protein is a two-component response regulator. We did not find any informative relationship among these proteins. However, we found some interesting genes adjacent to the two homologous genes, *vbp2* and *vbp3*. The predicted proteins encoded by the ORFs adjacent to *vbp2* and *vbp3* are shown in Fig. 6.1. The gene

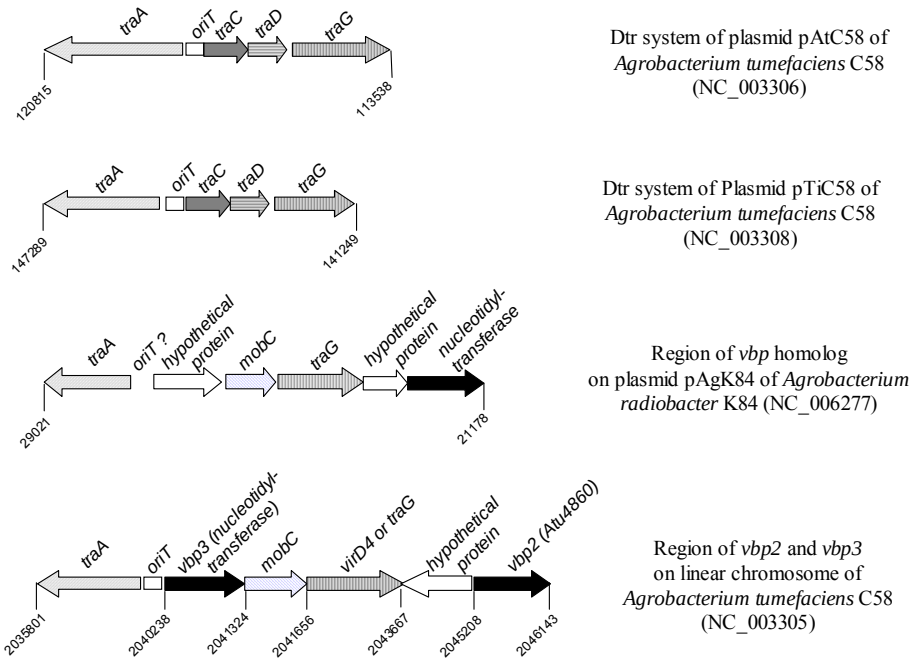

Fig. 6.1. Comparison of gene organization in the regions of *vbp* homologs with Dtr systems in *Agrobacterium*. Gene organization of the region between *vbp2* and *vbp3* on the linear chromosome of *Agrobacterium tumefaciens* C58 is shown at the bottom. A *vbp* homologous gene (*nucleotidyltransferase* gene) is also found on the plasmid pAgK84 from *Agrobacterium radiobacter* K84. Genes with predicted amino acid sequence similarity are shaded similarly. Genes whose predicted amino acid sequences are not similar are filled with blank. The numeric indicates the position of nucleotides in linear chromosome or plasmids. Sequence of *Agrobacterium tumefaciens* C58 was cited from the genome version of University of Washington.

organization of *vbp3* region is very similar for the RP4 *tra* regions (Leloup *et al*., 2002). A similar gene organization in the region of a *vbp* homolog was also found to exist in the plasmid pAgK84 of *Agrobacterium radiobacter* K84. Comparison of the gene organization of these identified or putative *tra* regions (Farrand *et al*., 1996; Chen *et al*., 2002) in *Agrobacterium* revealed that VBP or its homologous protein is most likely to be a subunit of DNA transfer and replication (Dtr) system (Fig. 6.1).

6.2. VBP may also be Involved in the Recruitment of T-complex to T4SS Transport Site

The processing of T-DNA and its transfer from *Agrobacterium* to plants is similar to the interbacterial conjugal transport of a variety of plasmids (Lessl and Lanka, 1994). In both processes, transferred DNA was cleaved at specific *cis*-acting sits (conjugation at *oriT* and T-DNA transfer at T-border) and transferred in a single-stranded form. Moreover, the protein that catalyzes the T-DNA scission remains bound to the 5′-end of the T-strand molecule. Plasmid conjugation conceptually can be divided into two function systems: the DNA transfer and replication (Dtr) system and the mating pair formation (Mpf) system. In the Dtr system, relaxase and auxiliary proteins, which can be host- or plasmid- encoded, assemble at *oriT* to form a nucleoprotein complex called the relaxosome. In many cases, a protein (normally called coupling protein) is needed to couple the Dtr to the Mpf. The most direct evidence that the mechanisms of T-DNA transfer and conjugation are functionally related is the extensive sequence similarities between *Agrobacterium virB*-encoded type IV secretion system (T4SS) proteins and IncN plasmid pKM101-encoded Mpf system proteins (Lessl *et al*., 1992). The observation that the conjugal intermediate of plasmid RSF1010 inhibits *Agrobacterium* virulence by

competing with the VirD2-T strand and/or VirE2 for a common export site (Stahl *et al*., 1998) demonstrates that *Agrobacterium virB*-encoded type IV secretion system (T4SS) has the capacity to mobilize other relaxosome. VirD4 sequence is highly similar to TraG of RP4 and behaves as a coupling protein, linking the T-DNA processing system and the mating channel. Coupling proteins determine the recognition between relaxosome and Mpf (Hamilton *et al*., 2000; Liosa *et al*., 2003). In plasmid conjugal system, several coupling protein (CP)-relaxase interactions have been demonstrated by *in vitro* studies. The $TraG_{RP4}$ CP interacts with $TraI_{RP4}$ relaxase/helicase (Schroder *et al*., 2002) and with Mob relaxase of the mobilizable plasmid pBHR1 (Szpirer *et al*., 2000). The $TrwB_{R388}$ CP interacts with $TrwC_{R388}$ relaxase/helicase, and the $TraD_F$ CP interacts with $TraM_F$, a Dtr protein that participates in processing by binding at sites near the F plasmid *oriT* sequence (Disque-Kochem and Dreiseikelmann, 1997).

In *Agrobacterium* T-DNA transfer system, VirE2 was demonstrated to be a substrate of T4SS and to interact with VirD4 coupling protein, but it was estimated only 5% of VirE2 was recruited to cell poles and less than 1% of VirE2 formed the VirE2-VirD4 complex. Most of VirE2 was believed to serve as a reservoir of this recruitment substrate (Atmakuri *et al*., 2003). If T-strand moves in the form of VirD2-T-strand-VirE2 complx, VirE2 may help the VirD2-T-strand-VirE2 complex to be recruited to the T4SS transport sites. However, in order to guarantee that the VirD2-T-strand-VirE2 complex to be recruited to the T4SS transporter sites in a 5′ to 3′ direction, the leading 5′-end of the VirD2-T-strand-VirE2 complex requires a protein that possesses high affinity to VirD4 or related T4SS components, otherwise, the VirD2-T-strand-VirE2 complex would be recruited to the transport sites in disorder. If T-strand moves in the form of VirD2-T-

strand complex and VirE2 is transported separately, we do not know how the VirD2-T-strand complex moves to the transport site and whether the movement of VirD2-T-strand complex is active or passive. It is conceivable that the recruitment of VirD2-T-strand complex to the T4SS transporter site is more difficult than the recruitment of single VirE2 molecule to the T4SS transporter site because *A. tumefaciens* cell does not have a reservoir of VirD2-T-strand complex to serve for the recruitment of this complex to T4SS and the VirD2-T-strand complex molecule is much bigger than VirE2 molecule. In this case, a protein that possesses high affinity to VirD4 is also required to help the recruitment of VirD2-T-strand complex to the transport sites. However, so far, only week interaction between VirD2 (T-strand) and VirD4 was observed in an *in vivo* study (Cascales and Christie, 2004). No evidence showed that VirD2 strongly interacts with VirD4 CP and could be recruited to the T4SS transport sites. Therefore, an additional protein that can strongly interact with both VirD2 and VirD4 (or other inner membrane T4SS components) will efficiently enhance the recruitment of T-complex to T4SS.

VBP1 can specifically and strongly bind VirD2, coupling protein VirD4 and two T4SS component proteins VirB4, VirB11. VirD4 plays an important role in recognizing T4SS translocating substrate (Atmakuri *et al*., 2003; Kumer and Das, 2002; Cascales and Christie, 2003). VirB11 is the first VirB protein that contacts with the VirD2-T-strand complex, just following the coupling protein VirD4 (Cascales and Christie, 2004). Structural studies on VirB11 have shown that VirB11 ATPases assemble as structurally dynamic, homohexameric rings with central channels large enough to accommodate DNA or unfolded polypeptides (Savvides *et al*., 2003). VirB11 is proposed to function as a gating molecular of T4SS at the inner membrane and to drive substrate export (Cascales

and Christie, 2003; Savvides *et al*., 2003). Like VirB11, VirB4 contains a conserved Walker A nucleotide-binding motif and the purified VirB4 also shows week ATPase activity (Dang *et al.*, 1999). VirB4 is an inner membrane protein and possesses two domains that embed into, or protrude across, the cytoplasmic membrane, possibly forming contacts with machine subunits across the inner membrane (Cascales and Christie, 2003; Dang *et al.*, 1999). VirB4 also shows interaction with VirB11 (Ward *et al*., 2002). Recent study (Atmakuri *et al*., 2004) showed VirD4 could form complex with VirB11 and VirB4. Nucleoside triphosphate binding site (Walker A motif) mutations of VirD4, VirB11 and VirB4 do not disrupt VirD4 substrate binding or transfer to VirB11, suggesting that these early reactions proceed independently of ATP binding or hydrolysis served by T4SS components. This observation may support a hypothesis that additional proteins may serve for these early reactions. VBP1 contains a putative nucleotidyltransferase motif and a putative higher eukaryotes and prokaryotes nucleotide-binding (HEPN) domain. So, it may serve for the early binding of T-complex to VirD4 or transfer to VirB11. Study on the cell fraction of *Agrobacterium* showed that no VBP1 protein was detected by Western blot in the membrane fraction, indicating that VBP1 protein is a cytoplasmic protein (data not shown). In detailed analyzing the amino acid sequences of three VBP proteins, we found three VBP proteins contain clusters of positively charged residues at their C-termini (Fig. 6.2), which share an important common feature with type IV secretion substrates (Christie, 2004; Vergunst *et al*., 2005). The positive charge clusters were believed to be the transport signals of type IV secretion substrates and to mediate the interactions between the secretion substrate and the VirD4 CP (Christie, 2004; Vergunst *et al*., 2005). Therefore, we speculate that the cytoplasmic

Verified VirB/D4 T4SS substrates

VirE2 ----**K**LPSDAAQLLAEPSD**R**YS**R**AFV**R**PEPALPPISDS**RR**TYES**R**P**R**SQSVNSF

VirE3 ----NSEQQALLNELLSVPLPGPLP**K**AD**H**E**R**P**R**VLESS**R**S**R**E**R**SMSGGLSL

VirF ----GGPNAVGLLTTNESFE**K**NINEVYN**R**T**R**AELDASS**R**D**R**SRSGLS**R**

VirD2 ----ATDSLSATA**H**LQQ**RR**GVLS**KR**P**R**EDDDGEPSE**RKR**E**R**DE**R**S**K**DG**R**GGN**RR**

MobA-RSF1010 ----ALA**R**PDATDN**R**G**R**LDLAALGGPM**K**ND**R**TLQAIG**R**QL**K**AMGCE**R**

Relaxases verified to bind with coupling proteins

TraI-F ----L**R**EPQ**R**V**R**EAV**R**EIA**R**ENLLQE**R**LQQME**R**DMV**R**DLQ**K**E**K**TLGGD

TraI-RP4 ----LL**RK**ENDEILVLPVD**K**ATVQ**R**M**KR**LAIGDPVTVTP**R**GSL**K**TT**R**G**R**S**R**

VBP proteins

VBP1 ----AYV**K**A**R**YSSQY**K**ISQEALDWIGE**R**ATLLLSLVGEVC**R**D**H**ISALE**R**DAG**R**EIAEQGAAEE

VBP2 ----AYV**K**A**R**YS**KH**FEISEEALGWLGE**R**TA**H**LLELV**K**VVCDE**H**IE**K**VDCGV**R**MGGSESSQ

VBP3 ----AYV**K**A**R**YS**KR**FEVSEEALTWLQE**R**TAEL**HK**LVETLC**R**E**H**IE**K**LE**H**AAGQAANSSD

Fig. 6.2. Three VBP proteins contain clusters of positively charged amino acid residues at their C termini. Positively charged residues, Arg (R), Lys (K), and His (H) were bolded and underlined. This positive charge bias of VBP proteins shares an important common feature with type IV secretion substrates. The charge bias in the C-termini of type IV secretion substrates was postulated to be the type IV secretion signal recognized by the coupling protein (CP) component of the type IV secretion system and to mediate the interactions between CP and substrates (Christie, 2004; Vergunst *et al*., 2005). Vir and VBP proteins were encoded by *A. tumefaciens* C58.

VirD2 binding protein, VBP1, may mediate the recruitment of VirD2 to type IV secretion system. As *vbp* triple mutant also affected the conjugal transfer of plasmid pML122 in *A. tumefaciens* and pML122 can be co-immunoprecipitated by anti-VBP1 antiserum, implying that VBP proteins may involved in the recruitment of some plasmid conjugation intermediates to the membrane transport sites, we defined the VBP proteins as a new class of protein; recruiting protein that can recruit the DNA transfer intermediate to the membrane transport sites.

Chapter 7 Conclusions and Future Prospects

7.1. Conclusions

A VirD2-binding protein (VBP1) was identified in this study by using a pull-down assay and peptide-mass-fingerpriting. VBP1 protein is encoded by an agrobacterial AT plasmid gene. This gene was designed *vbp1* gene. Homology analysis showed that two *vbp1* homologous genes were located on the agrobacterial linear chromosome DNA and their positions were close to each other. These two *vbp1* homologous genes were designed *vbp2* and *vbp3*. All three VBP proteins do not show homology to any protein of known function, but possess a putative nucleotidyltransferase motif in their N-termini and a putative higher eukaryotes and prokaryotes nucleotide-binding (HEPN) domain in their C-termini. All these indicated that a novel VirD2-binding protein was identified.

Three *vbp* genes were cloned to pRSET vectors and expressed as His-tagged fusion proteins. All three VBP proteins showed high expression level in *E. coli*. By using these three His-VBP fusion proteins as the affinity ligands, all three VBP proteins were demonstrated to be able to bind VirD2 specifically. To determine the biological functions of three *vbp* genes, we conducted the mutations of *vbp2* and *vbp3* in two *A. tumefaciens* strains A348 and GMI9017. A348 is a wild type strain and contains all three *vbp* genes. In GMI9017 strain, AT plasmid was cured, so, GMI9017 strain only contains *vbp2* and *vbp3* genes. Four *vbp* mutants were obtained in this study. These four *vbp* mutants were designed as A348Δvbp2, A348Δvbp2Δvbp3, GMI9017Δvbp2 and GMI9017Δvbp2Δvbp3 and were used to determine the effects of *vbp* mutations on the

tumorigenesis of *A. tumefaciens*. The results showed that *vbp* genes were involved in the tumorigenesis and these three *vbp* genes could complement each other functionally.

We used His-VBP1 as an affinity ligand to conduct the pull down assay and found that a large amount of VirE2 was pulled down compared with VirD2. The pull down results from four different *A. tumefaciens* strains demonstrated that VirE2 was pulled down in the form of VirD2-T-strand-VirE2 complex and the T-strand could also be amplified from the pulled down samples. Data in this study strongly supported that the T-complex existed in the *A. tumefaciens* extract in the form of VirD2-T-strand-VirE2 complex. This conclusion agreed with an early observation (Christie *et al*., 1988). Co-immunoprecipitation with anti-VBP1 antiserum verified that native VBP1 could bind VirD2-T-strand-VirE2 complex and further confirmed that VirD2-T-strand-VirE2 complex exists in *A. tumefaciens* extract.

Both pull-down and co-immunoprecipitation results showed that VBP1 specifically and strongly interacts with VirD4 as well as two T4SS components, VirB4 and VirB11. Like VBP1, both VBP2 and VBP3 could pull down VirB11. This further confirmed that all three VBP proteins have similar functions.

By analyzing the functions of genes adjacent to the two *vbp1* homologous genes *vbp2* and *vbp3* as well as comparing the T-DNA processing complex with the relaxosomes in conjugal plasmids, VBP1 was supposed to be an auxiliary protein of T-DNA processing nucleoprotein complex.

Based on the observations that VBP1 specifically and strongly interacts with VirD2 and VirB/D4 T4SS components: VirD4, VirB4 and VirB11, as well as *vbp* triple mutant highly attenuates the tumorigenesis of *A. tumefaciens*, VBP proteins were suggested to be

involved in the recruitment of T-complex to the T4SS transporter site. *Vbp* triple mutant was also shown to affect the conjugal transfer of a RSF1010 derivate in *A. tumefaciens* and the RSF1010 derivate can be co-immunoprecipitated by anti-VBP1 antiserum from *A. tumefaciens* extract, suggesting that VBP proteins may be involved in some plasmid conjugation systems. So, we defined VBP proteins as a new class of proteins: recruiting proteins that could recruit the DNA transfer intermediate to the membrane transport sites.

7.2. Future Prospects

In this study, VBP proteins were demonstrated to be involved in the tumorigenesis of *A. tumefaciens* and some plasmid conjugation systems. The redundancy of three homologs for one VirD2-binding function indicated that VBP might play an important role in the T-DNA transfer. However, the precise biochemical function of VBP proteins remained unclear although VBP proteins were defined as a new class of proteins: recruiting proteins. To fully understand the biochemical function of VBP proteins, further studies are required and should be focused on the following three aspects.

The first is the effect of VBP proteins on the T-strand production. If VBP proteins serve as an auxiliary protein of T-DNA processing nucleoprotein complex, the deletion of three *vbp* genes would affect the T-strand production. So, the establishment of quantitative assay of T-strand level in *A. tumefaciens* is very important for the further study of the VBP functions. In this study, four different *vbp* mutation strains were obtained. After the quantitative assay of T-strand level in *A. tumefaciens* is established, the T-strand level in different *vbp* mutation strains can be easily assayed.

The second is the subcellular location of VBP proteins. Although we have testified that VBP1 protein was a cytoplasmic protein we do not know whether VBP proteins were

co-localized with T-strand movement. If VBP proteins help T-complex to move and to recognize the T4SS transporter site, VBP would be co-localized with T-complex and localized at the T4SS transporter site.

The third is the identification of any enzymatic activity of VBP proteins. All three VBP proteins possess the conserved domain of nucleotidyltransferase. Undoubtedly, identification of any enzymatic activity of VBP protein would be very useful to the understanding of the precise biochemical functions of VBP proteins. However, nucleotidyltransferase is a superfamily that includes more than 10 distinct sub-superfamilies. So, the identification of any enzymatic activity of VBP protein is still a challenge to further studies of VBP functions.

References

Albright, L.M., Yanofsky, M.F., Leroux, B., Ma, D., and Nester E.W. (1987) Processing of the T-DNA of *Agrobacterium tumefaciens* generates border nicks and linear, single-stranded T-DNA. *J Bacteriol* **169:** 1046-1055.

Alonso, J.M., Stepanova, A.N., Leisse, T.J., Kim, C.J., Chen, H., Shinn, P., Stevenson, D.K., Zimmerman, J., and Barajas, P. *et al*. (2003) Genome-wide insertional mutagenesis of *Arabidopsis thaliana*. *Science* **301:** 653-657.

Anderson, L.B., Hertzel, A.V., and Das, A. (1996) *Agrobacterium tumefaciens* VirB7 and VirB9 form a disulfide-linked protein complex. *Proc Natl Acad Sci USA* **93:** 8889-8894.

Aravind, L., and Koonin, E.V. (1999) DNA polymerase β-like nucleotidyltransferase superfamily: identification of three new families, classification and evolutionary history. *Nucleic Acids Res* **27:** 1609-1618.

Ashby, A.M., Watson, M.D., Loake, G.Y. and Shaw, C.H. (1988) Ti plasmid-specified chemotaxis of *Agrobacterium tumefaciens* C58C^{1} toward *vir*-inducing phenolic compounds and soluble factors from monocotyledonous and dicotyledonous plants. *J Bacteriol* **170:** 4181-4187.

Atmakuri, K., Cascales, E, and Christie, P.J. (2004) Energetic components VirD4, VirB11 and VirB4 mediate early DNA transfer reactions required for bacterial type IV secretion. *Mol Microbiol* **54:** 1199-1211.

Atmakuri, K., Ding, Z., and Christie, P.J. (2003) VirE2, a type IV secretion substrate, interacts with the VirD4 transfer protein at cell poles of *Agrobacterium tumefaciens*. *Mol Microbiol* **49:** 1699-1713.

Bachand, F., Yao, X.-J., Hrimech, M., Rougeau, N., and Cohen, E.A. (1999) Incorporation of Vpr into human immunodeficiency virus type 1 requires a direct interaction with the p6 domain of the p55 Gag precursor. *J Biol Chem* **274:** 9083-9091.

Bako, L., Umeda, M., Tiburcio, A.F., Schell, J., and Koncz, C. (2003) The VirD2 pilot protein of *Agrobacterium*-transferred DNA interacts with the TATA box-binding

protein and a nuclear protein kinase in plants. *Proc Natl Acad Sci USA* **100:** 10108-10113.

Ballas, N., and Citovsky, V. (1997) Nuclear localization signal binding protein from *Arabidopsis* mediates nuclear import of *Agrobacterium* VirD2 protein. *Proc Natl Acad Sci USA* **94:** 10723-10728.

Banta, L.M., Bohne, J., Lovejoy, S.D., and Dostal, K. (1998) Stability of the *Agrobacterium tumefaciens* VirB10 protein is modulated by growth temperature and periplasmic osmoadaption. *J Bacteriol* **180:** 6597-6606.

Baron, C., Llosa, M., Zhou, S., and Zambryski, P.C. (1997) VirB1, a component of the T-complex transfer machinery of *Agrobacterium tumefaciens*, is processed to a C-terminal secreted product, VirB1*. *J Bacteriol* **179:** 1203-1210.

Bash, R., and Matthysse, A.G. (2002) Attachment to roots and virulence of a *chvB* mutant of *Agrobacterium tumefaciens* are temperature sensitive. *Molecular Plant-Microbe Interactions* **15:** 160-163.

Beaupre, C.E., Bohne, J., Dale, E.M., and Binns, A.N. (1997) Interactions between VirB9 and VirB10 membrane proteins involved in movement of DNA from *Agrobacterium tumefaciens* into plant cells. *J Bacteriol* **179:** 78-89.

Beijersbergen, A., Dulk-Ras, A.D., Schilperoort, R.A., and Hooykaas, P.J.J. (1992) Conjugative transfer by the virulence system of *Agrobacterium tumefaciens*. *Science* **256:** 1324-1327.

Beijersbergen, A., Smith, S., and Hooykaas, P.J. (1994) Localization and topology of VirB proteins of *Agrobacterium tumefaciens*. *Plasmid* **32:** 212-218.

Bevan, M. (1984) Binary *Agrobacterium* vectors for plant transformation. *Nucleic Acids Res* **12:** 8711-8721.

Binns, A.N., Beaupre, C.E., and Dale, E.M. (1995) Inhibition of VirB-mediated transfer of diverse substrates from *Agrobacterium tumefaciens* by the InQ plasmid RSF1010. *J Bacteriol* **177:** 4890-4899.

Bi, X., and Liu, L.F. (1996) A replicational model for DNA recombination between

direct repeats. *J Mol Biol* **256:** 849-858.

Bolton, G.W., Nester, E.W., and Gordon, M.P. (1986) Plant phenolic compounds induce expression of the *Agrobacterium tumefaciens* loci needed for virulence. *Science* **232:** 983-985.

Bourret, R., Borkovich, K., and Simon, M. (1991) Signal transduction pathways involving protein phosphorylation in prokaryotes. *Annu Rev Biochem* **60:** 401-441.

Braun, A.C. (1947) Thermal studies on the factors responsible for the tumor initiation in crown gall. *Am J Bot* **34:** 234-240.

Braun, A.C., and Mandle, R.J. (1948) Studies on the inactivation of the tumor-inducing principle in crown gall. *Growth* **12:** 255-269.

Britt, A.B. (1999) Molecular genetics of DNA repair in higher plants. *Trends Plant Sci* **4:** 20-25.

Brunaud, V., Balzeergue, S., Dubreucq, B., Aubourg, S., Samson, F., Chauvin, S., Bechtold, N. Cruaud, C., and DeRose, R. *et al*. (2002) T-DNA integration into the Arabidopsis genome depends on sequences of pre-insertion sites. *EMBO Rep* **3:** 1152-1157.

Buchanan-Wollaston, V., Passiatore, J.E., and Cannon, F. (1987) The mob and oriT mobilization functions of a bacterial plasmid promote its transfer to plants. *Nature* **328:** 172-175.

Burns, D.L. (2003) Type IV transporters of pathogenic bacteria. *Current Opinion in Microbiology* **6:** 29-34.

Burridge, K., Fath, K., Kelly, T., Nuckolls, G., and Turner, C. (1988) Focal adhesions: transmembrane junctions between the extracellular matrix and the cytoskeleton. *Annu Rev Cell Biol* **4:** 487-525.

Cangelosi, G.A., Ankenbauer, R.G., and Nester, E.W. (1990) Sugars induce the *Agrobacterium* virulence genes through a periplasmic binding protein and a transmembrane signal protein. *Proc Natl Acad Sci USA* **87:** 6708-6712.

Cangelosi, G.A., Best, E.A., Martinetti, G., and Nester, E.W. (1991) Genetic analysis of

Agrobacterium. *Methods Enzymol* **204:** 384-397.

Cangelosi, G.A., Hung, L., Puvanesarajah, V., Stacey, G., Ozga, D.A., Leigh, J.A., and Nester, E.W. (1987) Common loci for *Agrobacterium tumefaciens* and *Rhizobium meliloti* exopolysaccharide synthesis and their roles in plant interactions. *J Bacteriol* **169:** 2086-2091.

Cangelosi, G.A., Martinetti, A.G., Leigh, J.A., Lee, C.C., Theines, C., and Nester, E.W. (1989) Role of *Agrobacterium tumefaciens* ChvA protein in export of β-1,2-glucan. *J Bacteriol* **171:** 1609-1615.

Cascales, E., and Christie, P.J. (2003) The versatile bacterial type IV secretion system. *Nature Rev Microbiol* **1:** 137-149.

Cascales, E., and Christie, P.J. (2004) Definition of a bacterial type IV secretion pathway for a DNA substrate. *Science* **304:** 1170-1173.

Cascales, E., and Christie, P.J. (2004b) *Agrobacterium* VirB10, an ATP energy sensor required for type IV secretion. *Proc Natl Acad Sci USA* **101:** 17228-17233.

Chang, C.-H., and Winans, S.C. (1992) Functional roles assigned to the periplasmic, linker, and receiver domains of the *Agrobacterium tumefaciens* VirA protein. *J Bacteriol* **174:**7033-7039.

Charles, T.C., and Nester, E.W. (1993) A chromosomally encoded two-component sensory transduction system is required for virulence of *Agrobacterium tumefaciens*. *J Bacteriol* **175:** 6614-6625.

Chen, L., Chen, Y., Wood, D.W., and Nester, E.W. (2002) A new type IV secretion system promotes conjugal transfer in *Agrobacterium tmefaciens*. *J Bacteriol* **184:** 4838-4845.

Chen, L., Li, C.M., and Nester, E.W. (2000) Transferred DNA (T-DNA)-associated proteins of *Agrobacterium tumefaciens* are exported independently of *virB*. *Proc Natl Acad Sci USA* **97:** 7545-7550.

Chilton, M.-D. (1993) *Agrobacterium* gene transfer: Progress on a "poor man's vector" for maize. *Proc Natl Acad Sci USA* **90:** 3119-3120.

Chilton, M.-D., Drummond, M.H., Merlo, D.J., and Sciaky, D. (1978) Highly conserved DNA of Ti plasmids overlaps T-DNA maintained in plant tumors. *Nature* **275:** 147-149.

Chilton, M.-D., Drummond, M.H., Merlo, D.J., Sciaky, D., Montoya, A.L., Gordon, M.P., and Nester, E.W. (1977) Stable incorporation of plasmid DNA into higher plant cells: the molecular basis of crown gall tumorigenesis. *Cell* **11:** 263-271.

Christie, P.J. (1997) *Agrobacterium tumefaciens* T-complex transport apparatus: a paradigm for a new family of multifunctional transporters in eubacteria. *J Bacteriol* **179:** 3085-3094.

Christie, P.J. (2001) Type IV secretion: intercellular transfer of macromolecules by systems ancestrally related to conjugation machines. *Mol Microbiol* **40:** 294-305.

Christie, P.J. (2004) Type IV secretion: the *Agrobacterium* VirB/D4 and related conjugation systems. *Biochim Biophys Acta* **1694:** 219-234.

Christie, P.J., and Vogel, J.P. (2000) Bacterial type IV secretion: conjugation systems adapted to deliver effector molecules to host cells. *Trends in Microbiology* **8:** 354-360.

Christie, P.J., Ward, J.E., Winans, S.C., and Nester, E.W. (1988) The *Agrobacterium tumefaciens virE2* gene product is a single-stranded-DNA-binding protein that associates with T-DNA. *J Bacteriol* **170:** 2659-2667.

Citovsky, V., De Vos, G., and Zambryski, P. (1988) Single-stranded DNA binding protein encoded by the *virE* locus of *Agrobacterium tumefaciens*. *Science* **240:** 501-504.

Citovsky, V., Guralnick, B., Simon, M.N., and Wall, J.S. (1997) The molecular structure of *Agrobacterium* VirE2-single stranded DNA complexes involved in nuclear import. *J Mol Biol* **271:** 718-727.

Citovsky, V., Wong, M.L., and Zambryski, P. (1989) Cooperative interaction of *Agrobacterium* VirE2 protein with single stranded DNA: implications for the T-DNA transfer process. *Proc Natl Acad Sci USA* **86:** 1193-1197.

Citovsky, V., Zupan, J., Warnick, D., and Zambryski, P. (1992) Nuclear localization of

Agrobacterium VirE2 protein in plant cells. *Science* **256:** 1802-1805.

Cook, D.M., and Farrand, S.K. (1992) The *oriT* region of the *Agrobacterium tumefaciens* Ti plasmid pTiC58 shares DNA sequence identity with the transfer origins of RSF1010 and RK2/RP4 and with T-region borders. *J Bacteriol* **174:** 6238-6246.

Dang, T.A.T., and Christie, P.J. (1997) The VirB4 ATPase of *Agrobacterium tumefaciens* is a cytoplasmic membrane protein exposed at the periplasmic surface. *J Bacteriol* **179:** 453-462.

Das, A. (1998) DNA transfer from *Agrobacterium* to plant cells in crown gall tumor disease. *Subcellular Biochemistry: Plant-Microbe Interactions* **29:** 343-363.

Das, A., Anderson, L.B., and Xie, Y.H. (1997) Delineation of the interaction domains of *Agrobacterium tumefaciens* VirB7 and VirB9 by use of the yeast two-hybrid assay. *J Bacteriol* **179:** 3404-3409.

Das A., and Xie Y.-H. (1998). Construction of transposon *Tn3phoA*: Its application in defining the membrane topology of the *Agrobacterium tumefaciens* DNA transfer proteins. *Mol Microbiol* 27: 405-414.

Das, A., and Xie, Y.-H. (2000) The *Agrobacterium* T-DNA transport pore proteins VirB8, VirB9, and VirB10 interact with one another. *J Bacteriol* **182:** 758-763.

De Buck, S., Jacobs, A., Van Montagu, M., and Depicker, A. (1999) The DNA sequences of T-DNA junctions suggest that complex T-DNA loci are formed by a recombination process resembling T-DNA integration. *Plant J* **20:** 295-304.

De Iannino, N.I., and Ugalde, R.A. (1989) Biochemical characterization of avirulent *Agrobacterium tumefaciens chvA* mutants: synthesis and excretion of β-(1,2)glucan. *J Bacteriol* **171:** 2842-2849.

De la Riva, G.A., Gonzalez-Cabrera, J., Vazquez-Padron, R., and Ayra-Pardo, C. (1998) *Agrobacterium tumefaciens*: a natural tool plant transformation. *EJB Electronic Journal of Biotechnology* **1:** 118-133.

Deng, W., Chen, L., Peng, W.-T., Liang, X., Sekiguchi, S., Gordon, M.P., Comai, L., and Nester, E.W. (1999) VirE1 is a specific molecular chaperone for the exported single-

stranded-DNA-binding protein VirE2 in *Agrobacterium*. *Mol Microbiol* **31:** 1795-1807.

Deng, W., Chen, L., Wood, D.W., Metcalfe, T., Liang, X., Gordon, M.P., Comai, L., and Nester, E.W. (1998) *Agrobacterium* VirD2 protein interacts with plant host cyclophilins. *Proc Natl Acad Sci USA* **95:** 7040-7045.

Depicker, A., Van Montagu, M., and Schell, J. (1978) Homologous sequences in different Ti plasmids are essential for oncogenicity. *Nature* **275:**150-152.

Dingwall, C., and Laskey, R.A. (1991) Nuclear targeting sequences-A consensus? *Trends Biochem Sci* **16:** 478-481.

Douglas, C.J., Halperin, W., and Nester, E.W. (1982) *Agrobacterium tumefaciens* mutants affected in attachment to plant cells. *J Bacteriol* **152:** 1265-1275.

Douglas, C.J., Staneloni, R.J., Rubin, R.A., and Nester, E.W. (1985) Identification and genetic analysis of an *Agrobacterium tumefaciens* chromosomal virulence gene. *J Bacteriol* **161:** 850-860.

Dumas, F., Duckely, M., Pelczar, P., van Gelder, P., and Hohn, B. (2001) An *Agrobacterium* VirE2 channel for transferred-DNA transport into plant cells. *Proc Natl Acad Sci USA* **98:** 485-490.

Durrenberger, F., Crameri, A., Hohn, B., and Koukolikova-Nicola, Z. (1989) Covalently bound VirD2 protein of Agrobacterium tumefaciens protects the T-DNA from exonucleolytic degradation. *Proc Natl Acad Sci USA* **86:** 9154-9158.

Edwards, R.A., Keller, L.H., and Schifferli, D.M. (1998) Improved allelic exchange vectors and their use to analyze 987P fimbria gene expression. *Gene* **207:** 149-157.

Eisenbrandt, R., Kalkum, M., Lai, E.M., Lurz, R., Kado, C.I., and Lanka, E. (1999) Conjugative pili of IncP plasmids and the Ti plasmid T pilus are composed of cyclic subunits. *J Biol Chem* **274:** 22548-22555.

Engstrom, P., Zambryski, P., Montagu, M.V., and Stachel, S. (1987) Charaterization of *Agrobacterium tumefaciens* virulence proteins induced by the plant factor acetosyringone. *J Mol Biol* **197:** 635-645.

Enriquez-Obregon, G.A., Vazquez-padron, R.I., Prieto-sansonov, D.L., de la Riva, G.A., and Selmon-Housein, G. (1998) Herbicide resistant sugarcane (*Saccharum officinarum* L.) plants by *Agrobacterium*-mediated transformation. *Planta* **206:** 20-27.

Escobar, M.A., and Dandekar, A.M. (2003) *Agrobacterium tumefaciens* as an agent of disease. *TRENDS in Plant Science* **8:** 380-386.

Farrand, S.K., Hwang, I., and Cook, D.M. (1996) The *tra* region of the nopaline-type Ti plasmid is a chimera with the elements related to the transfer systems of RSF1010, RP4, and F. *J Bacteriol* **178:** 4233-4247.

Fernandez, D., Dang, T.A., Spudich, G., Zhou, X.-R., Berger, B., and Christie, P. (1996a) The *Agrobacterium tumefaciens virB7* gene product, a proposed component of the T-complex transport apparatus, is a membrane-associated lipoprotein exposed at the periplasmic surface. *J Bacteriol* **178:** 3156-3167.

Fernandez, D., Spudich, G., Zhou, X.-R., and Christie, P. (1996b) The *Agrobacterium tumefaciens* VirB7 lipoprotein is required for stabilization of VirB proteins during assembly of the T-complex transport apparatus. *J Bacteriol* **178:** 3168-3176.

Filichkin, S.A., and Gelvin, S.B. (1993) Formation of a putative relaxation intermediate during T-DNA processing directed by the *Agrobacterium tumefaciens* VirD1 and VirD2 endonuclease. *Mol Microbiol* **8:** 9159-926.

Finan, T.M., Kunker, B., Vos, G.F., and Signer, E.R. (1988) Second symbiotic megaplasmid in *Rhizobium meliloti* carrying exopolysaccharide and thiamine synthesis genes. *J Bacteriol* **167:** 66-72.

Francia, M.V., Varsaki, A., Garcillan-Barcia, M.P., Latorre, A., Drainas, C., and Cruz, F. (2004) A classification scheme for mobilization regions of bacterial plasmids. *FEMS Microbiology Reviews* **28:** 79-100.

Gelvin, S.B. (2000) *Agrobacterium* and plant genes involved in T-DNA transfer and integration. *Annu Rev Plant Physiol Plant Mol Biol* **51:** 223-256.

Gelvin, S.B. (2003) *Agrobacterium*-mediated plant transformation: the biology behind the "gene-jockeying" tool. *Microbiol Mol Biol Rev* **67:** 16-37.

Ghai, J., and Das, A. (1989) The *virD* operon of *Agrobacterium tumefaciens* Ti plasmid encodes a DNA-relaxing enzyme. *Proc Natl Acad Sci USA* **86:** 3109-3113.

Gheysen, G., Van Montagu, M., and Zambryski, P. (1987) Integration of *Agrobacterium tumefaciens* transfer DNA (T-DNA) involves rearrangements of target plant DNA sequences. *Proc Natl Acad Sci USA* **84:** 6169-6173.

Gilmour, M.W., Gunton, J.E., Lawley, T.D., and Taylor, D.E. (2003) Interaction between the InchI1 plasmid R27 coupling protein and type IV secretion system: TraG associates with the coiled-coil mating pair formation protein TrhB. *Mol Microbiol* **49:** 105-116.

Gomis-Ruth, F.X., Moncalian, G., de la Cruz, F., and Coll, M. (2002) Conjugative plasmid protein TrwB, an integral membrane type IV secretion system coupling protein. Detailed structural features and mapping of the active site cleft. *J Biol Chem* **277:** 7556-7566.

Gooder, B., Hinkle, G., Gattung, S., Miller, N., Blanchard, M., Qurollo, B., Goldman, B.S., Cao, Y., Askenazi, M., and Halling, C. *et al*. (2001) Genome sequence of the plant pathogen and biotechnology agent *Agrobacterium tumefaciens* C58. *Science* **294:** 2323-2328.

Groot, M.J.A., Bundock, P., Hooykaas, P.J., and Beijersbergen, A.G.M. (1998) *Agrobacterium tumefaciens*-mediated transformation of filamentous fungi. *Nature Biotechnology* **16:** 839-842.

Hamilton, C.L., Lee, H., Li, P-L., Cook, D.M., Piper, K.R., Bodman, S.B., Lanka, E., Ream, W., and Farrand, S.K. (2000) TraG from RP4 and TraG and VirD4 from Ti plasmids confer relaxosome specificity to the conjugal transfer system of pTiC58. *J Bacteriol* **182:** 1541-1548.

Hansen, G., Shillito, R.D., and Chilton, M.D. (1997) T-strand integration in maize protoplasts after codelivery of a T-DNA substrate and virulence genes. *Proc Natl Acad Sci USA* **94:** 11726-11730.

Hawes, M.C., and Smith, L.Y. (1989) Requirement for chemotaxis in pathogenicity of Agrobacterium tumefaciens on roots of soil-grown pea plants. *J Bacteriol* **171:** 5668-

5671.

Hoang, T.T., Karkhoff-Schweizer, R.R., Kutchma, A.J., and Schweizer, H.P. (1998) A broad-host-range Flp-FRT recombination system for site-specific excision of chromosomally-located DNA sequences: application for isolation of unmarked Pseudomonas aeruginosa mutants. *Gene* **212:** 77-86.

Hooykaas, P.J., and Schilperoort, R.A. (1992) *Agrobacterium* and plant genetic engineering. *Plant Mol Biol* **19:** 15-38.

Howard, E., and Citovsky, V. (1990) The emerging structure of the *Agrobacterium* T-DNA tansfer complex. *Bioessays* **12:** 103-108.

Howard, E.A., Zupan, J.R., Citovsky, V., and Zambryski, P.C. (1992) The VirD2 protein of *Agrobacterium tumefaciens* contains a C-terminal bipartite nuclear localization signal: Implications for nuclear uptake of DNA in plant cells. *Cell* **68:** 109-118.

Howard, M.T., Nelson, W.C., and Matson, S.W. (1995) Stepwise assembly of a relaxosome at the F plasmid origin of transfer. *J Biol Chem* **270:** 28381-28386.

Ilyina, T., and Koonin, E. (1992) Conserved sequence motifs in the initiator proteins for rolling circle DNA replication encoded by diverse replicons from eubacteria, eucaryotes and archaebacteria. *Nucleic Acids Res* **20:** 3279-3285.

Jakubowski, S.J., Krishnamoorthy, V., and Christie, P.J. (2003) *Agrobacterium tumefaciens* VirB6 protein participates in formation of VirB7 and VirB9 complexes required for type IV secretion. *J Bacteriol* **185:** 2867-2878.

Jakubowski, S.J., Krishnamoorthy, V., Cascales, E., and Christie, P.J. (2004) *Agrobacterium tumefaciens* VirB6 domain direct the ordered export of a DNA substrate through a type IV secretion system. *J Mol Biol* **341:** 961-977.

Jasper, F., Koncz, C., Schell, J., and Steinbiss, H-H. (1994) *Agrobacterium* T-strand production *in vitro*: sequence-specific cleavage and 5' protection of single-stranded DNA templates by purified VirD2 protein. *Proc Natl Acad Sci USA* **91:** 694-698.

Jayaswal, R.K., Veluthambi, K., Gelvin, S.B., and Slightom, J.L. (1987) Double stranded T-DNA cleavage and the generation of single stranded T-DNA molecules in E. coli by

a *virD*-encoded border-specific endonuclease from *A. tumefaciens*. *J Bacteriol* **169:** 5035-5045.

Ji, J.M., Martinez, A., Dabrowski, M., Veluthambi, K., Gelvin, S.B., and Ream, W. (1988) The *overdrive* enhancer sequence stimulates production of T-strands from the *Agrobacterium tumefaciens* tumor-inducing plasmid. UCLA Symp. *Mol Cell Biol* **101:** 19-31.

Jin, S., Roitsch, T., Ankenbauer, R.G., Gordon, M.P., and Nester, E.W. (1990) The VirA protein of *Agrobacterium tumefaciens* is autophosphorylated and essential for *vir* gene induction. *J Bacteriol* **172:** 525-530.

Jin, S., Song, Y., Pan, S.Q., and Nester, N.W. (1993) Characterization of a virG mutation that confers constitutive virulence gene expression in *Agrobacterium tumefaciens*. *Mol Microbiol* **7:** 555-562.

Jones, A.L., Lai, E.M., Shirasu, K., and Kado, C.I. (1996) VirB2 is a processed pilin-like protein encoded by the *Agrobacterium tumefaciens* Ti plasmid. *J Bacteriol* **178:** 5706-5711.

Jones, A.L., Shirasu, K., and Kado, C.I. (1994) The product of the *virB4* gene of *Agrobacterium tumefaciens* promotes accumulation of VirB3 protein. *J Bacteriol* **176:** 5255-5261.

Joos, H., Inze, D., Caplan, A., Sormann, M., Van Montagu, M., and Schell, J. (1983) Genetic analysis of T-DNA transcripts in nopaline crown gall. *Cell* **32:** 1057-1067.

Judd, P.K., Kumar, R.B., and Das, A. (2005) The type IV secretion apparatus protein VirB6 of *Agrobacterium tumefaciens* localizes to a cell pole. *Mol Microbiol* **55:** 115-124.

Kamoun, S., Cooley, M.B., Rogowsky, U.M., and Kado, C.I. (1989) Two chromosomal loci involved in production of exopolysaccharide in *Agrobacterium tumefaciens*. *J Bacteriol* **171:** 1755-1759.

Kennedy, B.W. (1980) Estimates of U.S. crop losses to prokaryote plant pathogens. *Plant Dis* **64:** 674-676.

Krall, L., Wiedemann, U., Unsin, G., Weiss, S., Domke, N., and Baron, C. (2002) Detergent extraction identifies different VirB protein subassemblies of the type IV secretion machinery in the membranes of *Agrobacterium tumefaciens*. *Proc Natl Acad Sci USA* **99:** 11405-11410.

Kumar R.B., and Das, A. (2002). Polar location and functional domains of the *Agrobacterium tumefaciens* DNA transfer protein VirD4. *Mol Microbiol* **43:** 1523-1532.

Kunik, T., Tzfira, T., Kapulnik, Y., Gafni, Y., Dingwall, C., and Citovsky, V. (2001) Genetic transformation of HeLa cells by *Agrobacterium*. *Proc Natl Acad Sci USA* **98:** 1871-1876.

Labes, M., Puhler, A., and Simon, R. (1990) A new family of RSF1010-derived expression and *lac*-fusion broad-host-range vectors for Gram-negative bacteria. *Gene* **89:** 37-46.

Lai, E.-M., Chesnokova, O., Banta, L.M., and Kado, C.I. (2000) Genetic and environmental factors affecting T-Pilin export and T-pilus biogenesis in relation to flagellation of *Agrobacterium tumefaciens*. *J Bacteriol* **182:** 3705-3716.

Lai, E.-M., and Kado, C.I. (2000) The T-pilus of *Agrobacterium tumefaciens*. *Trends in Microbiology* **8:** 361-369.

Lee, Y., Jin, S., Sim, W., and Nester, E.W. (1996) The sensing of plant signal molecules by *Agrobacterium*: genetic evidence for direct recognition of phenolic inducers by the VirA protein. *Gene* **179:** 83-88.

Leloup, L., Lai, E.-M., and Kado, C.I. (2002) Identification of a chromosomal *tra*-like region in *Agrobacterium tmefaciens*. *Mol Genet Genomics* **267:** 115-123.

Lessl, M., Balzer, D., Pansegrau, W., and Lanka, E. (1992) Sequence similarities between the RP4 Tra2 and the Ti VirB region strongly support the conjugation model for T-DNA transfer. *J Biol Chem* **267:** 20471-20480.

Lessl, M., and Lanka, E. (1994) Common mechanisms in bacterial conjugation and Ti-mediated T-DNA transfer to plant cells. *Cell* **77:** 321-324.

Lippincott, B.B., and Lippincott, J.A. (1969) Bacterial attachment to a specific wound site as an essential stage in tumor initiation by *Agrobacterium tumefaciens*. *J Bacteriol* **97:** 620-628.

Llosa, M., Gomis-Ruth, F.X., Coll, M., and Cruz, F. (2002) Bacterial conjugation: a two-step mechanism for DNA transport. *Mol Microbiol* **45:** 1-8.

Llosa, M., and O'Callaghan, D. (2004) Euroconference on the biology of type IV secretion processes: bacterial gates into the outer world. *Mol Microbiol* **53:** 1-8.

Llosa, M., Zupan, J., Baron, C., and Zambryski, P. (2000) The N- and C-terminal portions of the *Agrobacterium* protein VirB1 independently enhance tumorigenesis. *J Bacteriol* **182:** 3437-3445.

Llosa, M., Zunzunegui, S., and Cruz, F. (2003) Conjugative coupling proteins interact with cognate and heterologous VirB10-like proteins while exhibiting specificity for cognate relaxosomes. *Proc Natl Acad Sci USA* **100:** 10465-10470.

Loake, G.J., Ashby, A.M., and Shaw, C.M. (1988) Attraction of *Agrobacterium tumefaciens* C58C^{1} towards sugars involves a highly sensitive chemotaxis system. *J Gen Microbiol* **134:** 1427-1432.

Lopatin, M.I. (1939) Influence of bacterial root canter on the development of the cherry tree in the orchard. *Plant Prot* **18:**167-173.

Luban, J., Bossolt, K.A., Franke, E.K., Kalpana, G.V., and Goff, S.P. (1993) Human immunodeficiency virus type 1 Gag protein binds to cyclophilines A and B. *Cell* **73:** 1067-1078.

Matthysse, A.G., and McMahan, S. (1998) Root colonization by *Agrobacterium tumefaciens* is reduced in *cel*, *attB*, *attD*, and *attR* mutants. *Applied and Environmental Microbiology* **64:** 2341-2345.

Matthysse, A.G., and McMahan, S. (2001) The effect of the Agrobacterium tumefaciens attR mutation on attachment and root colonization differs between legumes and other dicots. *Applied and Environmental Microbiology* **67:** 1070-1075.

Matthysse, A.G., Yarnall, H., Boles, S.B., and McMahan, S. (2000) A region of the

Agrobacterium tumefaciens chromosome containing genes required for virulence and attachment to host cells. *Biochimica et Biophysica Acta* **1490:** 208-212.

Mayerhofer, R., Koncz-Kalman, Z., Nawrath, C., Bakkeren, G., Crameri, A., Angelis, K., Redei, G.P., Schell, J., Hohn, B., and Koncz, C. (1991) T-DNA integration: A model of illegitimate recombination in plants. *EMBO J* **10:** 697-704.

Middleton, R., Sjolander, K., Krishnamurthy, N., Foley, J., and Zambryski, P. (2005) Predicted hexameric structure of the *Agrobacterium* VirB4 C terminus suggests VirB4 acts as a docking site during type IV secretion. *Proc Natl Acad Sci USA* **102:** 1685-1690.

Miller, J.F., Mekalanos, J.J., and Falkow, S. (1989) Coordinate regulation and sensory transduction in the control of bacterial virulence. *Science* **243:**916-922.

Miller, V.L., and Mekalanos, J.J. (1988) A novel suicide vector and its use in construction of insertion mutation: osmoregulation of outer membrane proteins and virulence determinants in *vibrio cholerae* requires *toxR*. *J Bacteriol* **170:** 2575-2583.

Minnemeyer, S.L., Lightfoot, L.R., and Matthysse, A.G. (1991) A semi-quantitative bioassay for relative virulence of *Agrobacterium tumefaciens* strains on *Bryophyllum daigremontiana*. *J Bacteriol*. **173:** 7723-7724.

Mushegian, A.R., Fullner, K.J., Koonin, E.V., Nester, E.W. (1996) a family of lysozyme-like virulence factors in bacterial pathogens of plants and animals. *Proc Natl Acad Sci USA* **93:** 7321-7326.

Mysore, K.S., Bassuner, B., Deng, X., Darbinian, N.S., Motchoulski, A., Ream, W., and Gelvin, S.B. (1998) Role of the *Agrobacterium tumefaciens* VirD2 protein in T-DNA transfer and integration. *Molecular Plant-Microbe Interactions* **11:** 668-683.

Nam, J., Matthysse, A.G., Gelvin, S.B., (1997) Differences in susceptibility of *Arabidopsis* ecotypes to crown gall disease may result from a deficiency in T-DNA integration. *Plant Cell* **9:** 317-333.

Nam, J., Mysore, K.S., Zheng, C., Knue, M.K., and Matthysse, A.G., *et al*. (1999) Identification of T-DNA tagged *Arabidopsis* mutants that are resistant to transformation by *Agrobacterium*. *Mol Gen Genet* **261:** 429-438.

Narasimhuhu, S.B., Deng, X.-B., Sarria, R., and Gelvin, S.B. (1996) Early transcription of *Agrobacterium* T-DNA genes in tobacco and maize. *Plant Cell* **8:** 873-886.

Newton, J.A., and Fray, R.G. (2004) Integration of environmental and host-derived signals with quorum sensing during plant-microbe interactions. *Cellular Microbiology* **6:** 213-224.

Nilsson, J., Stahl, S., Lundeberg, J., Uhlen, M., and Nygren, P. (1997) Affinity fusion strategies for detection, purification and immobilization of recombinant proteins. *Protein Expression and Purification* **11:** 1-16.

Nixon, B.T., Ronson, C.W., and Ausubel, F.M. (1986) Two-component regulatory systems responsive to environmental stimuli share strongly conserved domains with the nitrogen assimilation regulatory genes *ntrB* and *ntrC*. *Proc Nat Acad Sci USA* **83:** 7850-7854.

O'Connell, K.P., and Handelsman, J. (1989) *chvA* locus may be involved in export of neutral cyclic β-1,2 linked D-glucan from *Agrobacterium tumefaciens*. *Mol Plant-Microbe Interact* **2:** 11-16.

Ohata, S., Mita, S., Hatori, T., and Nakmura, K. (1990) Construction and expression in tobacco of a β-glucuronidase (GUS) reporter gene containing an intron within the coding sequence. *Plant Cell Physiol* **31:** 805–813.

Ooms, G., Bakker, A., Molendijk, L., Wullems, G.J., Gordon, M.P., Nester, E.W., and Schilperoort, R.A. (1982) T-DNA organization in homogeneous and heterogeneous octopine-type crown gall tissues of *Nicotiana tabacum*. *Cell* **30:** 589–597.

Otten, L., DeGreve, H., Leemans, J., Hain, R., Hooykass, P., and Schell, J. (1984) Restoration of virulence of *vir* region mutants of *A. tumefaciens* strain B6S3 by coinfection with normal and mutant *Agrobacterium* strains. *Mol Gen Genet* **195:** 159-163.

Pansegrau, W., Balzer, D., Kruft, V., Lurz, R., and Lanka, E. (1990) *In vitro* assembly of relaxosomes at transfer origin of plasmid RP4. *Proc Natl Acad Sci USA* **87:** 6555-6559.

Pansegrau, W., Schoumacher, F., Hohn, B., and Lanka, E. (1993) Site-specific cleavage and joining of single-stranded DNA by VirD2 protein of *Agrobacterium tumefaciens* Ti plasmids: analogy to bacterial conjugation. *Proc Natl Acad Sci USA* **90:** 11538-11542.

Pan, S.Q., Jin, S., Boulton, M.I., Hawes, M., Gordon, M.P., and Nester, E.W. (1995) An *Agrobacterium* virulence factor encoded by a Ti plasmid gene or a chromosomal gene is required for T-DNA transfer into plants. *Mol Microbiol* **17:** 259-269.

Parke, D., Ornston, L.N., and Nester, E.W. (1987) Chemotaxis to plant phenolic inducers of virulence genes is constitutively expressed in the absence of the Ti plasmid in *Agrobacterium tumefaciens*. *J Bacteriol* **169:** 5336-5338.

Peralta, E.G., Hellmiss, R., and Ream, L.W. (1986) Overdrive, a T-DNA transmission enhancer on the *A. tumefaciens* tumor-inducing plasmid. *EMBO J* **5:** 1137-1142.

Peralta, E.G., and Ream, L.W. (1985) T-DNA border sequence required for crown gall tumorigenesis. *Proc Natl Acad Sci USA* **82:** 5112-5116.

Perwez, T., and Meyer, R.J. (1999) Stabilization of the relaxosome and stimulation of conjugal transfer are genetically distinct function of the R1162 protein MobB. *J Bacteriol* **181:** 2124-2131.

Piers, K.L., Heath, J.D., Liang, X., Stephens, H.M., and Nester, E.W. (1996) *Agrobacterium tumefaciens*-mediated transformation of yeast. *Proc Nat Acad Sci USA* **93:** 1613-1618.

Planet, P.J., Kachlany, S.C., DeSalle, R., and Figurski, D.H. (2001) Phylogeny of genes for secretion NTPases: Identification of the widespread *tadA* subfamily and development of a diagnostic key for gene classification. *Proc Natl Acad Sci USA* **98:** 2503-2508.

Porath, J. (1992) Immobilized metal ion affinity chromatography. *Protein Expression and Purification* **3:** 263-281.

Ream, W. (1989) *Agrobacterium tumefaciens* and interkingdom genetic exchange. *Annu Rev Phytopathol* **27:** 583-618.

Regensburg-Tuink, A.J., and Hooykaas, P.J. (1993) Transgenic *N. glauca* plants expressing bacterial virulence gene *virF* are converted into hosts for nopaline strains of *A. tumefaciens*. *Nature* **363:** 69-71.

Reuhs, B.L., Kim, J.S., and Matthysse, A.G. (1997) Attachment of *Agrobacterium tumefacins* to carrot cells and *Arabidopsis* wound sites is correlated with the presence of a cell-associated, acidic polysaccharide. *J Bacteriol* **179:** 5372-5379.

Riker, A.J., Berbee, J.G., and Smalley, E.B. (1959) Effects of crown gall and hairy root on the growth of apple trees. *Phytopathology* **49:** 88-90.

Robbins, J., Dilworth, S.M., Laskey, R.A., and Dingwall, C. (1991) Two ieterdependent basic domains in nucleoplasmin nuclear targeting sequence: identification of a class of bipartite nuclear targeting sequence. *Cell* **64:** 615-623.

Robertson, J.L., Holliday, T., and Matthysse, A.G. (1988) Mapping of *Agrobacterium tumefaciens* chromosomal genes affecting cellulose synthesis and bacterial attachment to host cells. *J Bacteriol*. **170:** 1408-1411.

Rosenberg, C., and Huguet, T. (1984) The pAtC58 plasmid of *Agrobacterium tumefaciens* is not essential for tumour induction. *Mol Gen Genet* **196:** 533-536.

Rossi, L., Hohn, B., and Tinland, B. (1993) The VirD2 protein of *Agrobacterium tumefaciens* carries nuclear localization signals important for transfer of T-DNA to plants. *Mol Gen Genet* **239:** 345-353.

Rossi, L., Hohn, B., and Tinland, B. (1996) Integration of complete transferred DNA units is dependent on the activity of virulence E2 protein of *Agrobacterium tumefaciens*. *Proc Natl Acad Sci USA* **93:** 126-130.

Sambrook, J.F., Fritsch, E.F., and Maniatis, T. (1989) *Molecular Cloning: A Laboratory Manual*. Cold Spring Harbor, NY: Cold Spring Harbor Laboratory Press.

Sambrook, J.F., and Russell, T. (2001) *Molecular Cloning: A Laboratory Manual (3rd edition)*. Cold Spring Harbor, NY: Cold Spring Harbor Laboratory Press.

Sanders, L., Wang, C.-O., Walling, L., and Lord, E. (1991) A homolog of the substrate adhesion molecule vitronectin occurs in four species of flowering plants. *Plant Cell* **3:**

629-635.

Savvides, S., Yeo, H.-J., Beck, M.R., Blaesing, F., Lurz, R., Lanka, E., Buhrdorf, R., Fischer, W., Haas, R., and Waksman, G. (2003) VirB11 ATPases are dynamic hexameric assemblies: new insights into bacterial type IV secretion. *EMBO J* **22:** 1969-1980.

Scheiffele, P., Pansegrau, W., and Lanka, E. (1995) Initiation of *Agrobacterium tumefaciens* T-DNA processing: purified protein VirD1 and VirD2 catalyze site- and strand-specific cleavage of superhelical T-border DNA in vitro. *J Biol Chem* **270:** 1269-1276.

Schilperoort, R.A., Veldstra, H., Warnaar, S.Q. Mulder, G., and Cohen, J.A. (1967) Formation of complexes between DNA isolated from tobacco crown gall tumours and complementary to Agrobacterium tumefaciens DNA. *Biochim Biophys Acta* **145:** 523-525.

Schmidt-Eisenlohr, H., Domke, N., Angerer, C., Wanner, G., Zambryski, P.C., and Baron, C. (1999) Vir proteins stabilize VirB5 and mediate its association with the T pilus of *Agrobacterium tumefaciens*. *J Bacteriol* **181:** 7485-7492.

Schrammeijer, B., Dulk-Ras, A., Vergunst, A.C., Jacome, E.J., and Hooykaas, P.J.J. (2003) Analysis of Vir protein translocation from *Agrobacterium tumefaciens* using *Saccharomyces cerevisiae* as a model: evidence for transport of a novel effector protein VirE3. *Nucleic Acids Research* **31:** 860-868.

Schrammeijer, B., Risseeuw, E., Pansegrau, W., Regensburg-Tuink, T.J.G., Crosby, W.L., and Hooykaas, P.J.J. (2001) Interaction of the virulence protein VirF of *Agrobacterium tumefaciens* with plant homologs of the yeast Skp1 protein. *Curr Biol* **11:** 258-262.

Schroth, M.N., Mccain, A.H., Foott, J.H., and Huisman, O.C. (1988) Reduction in yield and vigor of grapevine caused by crown gall disease. *Plant Dis* **72:** 241-246.

Shamaei-Tousi, A., Cahill, R., and Frankel, G. (2004) Interaction between protein subunits of the type IV secretion system of *Bartonella henselae*. *J Bacteriol* **186:** 4796-4801.

Shaw, C.H.J., Watson, M.D., Carter, G.H., and Shaw, C.H. (1984) The right hand copy of the nopaline Ti plasmid 25 bp repeat is required for tumor formation. *Nucleic Acids Res* **12:** 6031-6041.

Shaw, C.H.J., Ashby, A.M., Brown, A., Royal, C., Loake, G.J., and Shaw, C.H. (1989) VirA and G are necessary for acetosyringone chemotaxis in *Agrobacterium tumefaciens*. *Mol Microbiol* **2:** 413-417.

Sheng, J., and Citovsky, V. (1996) *Agrobacterium*-plant cell DNA transport: Have virulence proteins, will travel. *The Plant Cell* **8:** 1699-1710.

Shurvinton, C.E., Hodge, L., and Ream, W. (1992) A nuclear localization signal and the C-terminal omega sequence in the *Agrobacterium tumefaciens* VirD2 endonuclease are important for tumor formation. *Proc Natl Acad Sci USA* **89:** 11837-11841.

Silver, P.A. (1991) How proteins enter the nucleus. *Cell* **64:** 489-497.

Simone, M., McCullen, C.A., Stahl, L.E., and Binns, A.N. (2001) The carboxy-terminus of VirE2 from *Agrobacterium tumefaciens* is required for its transport to host cells by the *virB*-encoded type IV transport system. *Mol Microbiol* **41:** 1283-1293.

Smith, E.F., and Townsend, C.O. (1907) A plant-tumor of bacterial origin. *Scince* **24:** 671-673.

Stachel, S.E., Messens, E., Van Montagu, M., and Zambryski, P. (1985) Identification of the signal molecules produced by wounded plant cells that activate T-DNA transfer in *Agrobacterium tumefaciens*. *Nature* **318:** 624-629.

Stachel, S.E., and Nester, E.W. (1986) The genetic and transcriptional organization of the *vir* region of the A6 Ti plasmid of *Agrobacterium tumefacins*. *EMBO J* **5:** 1445-1454.

Stachel, S.E., Nester, E.W., and Zambryski, P.C. (1986) A plant cell factor induces *Agrobacterium tumefaciens vir* gene expression. *Proc Natl Acad Sci USA* **83:** 379-383.

Stachel, S.E., Timmerman, B., and Zambryski, P. (1986b) Generation of single-stranded T-DNA molecules during the initial stages of T-DNA transfer for *Agrobacterium tumefaciens* to plant cells. *Nature* **322:** 706-712.

Stachel, S.E., Timmerman, B., and Zambryski, P. (1987) Activation of *Agrobacterium*

tumefaciens vir gene expression generates multiple single-stranded T-strand molecules from the pTiA6 T-region: Requirement of 5' virD gene products. *EMBO J* **6:** 857-863.

Stachel, S.E., and Zambryski, P.C. (1986) *Agrobacterium tumefaciens* and the susceptible plant cell: a novel adaptation of extracellular recognition and DNA conjugation. *Cell* **47:** 155-157.

Stahl, L.E., Jacobs, A., and Binns, A.N. (1998) The conjugal intermediate of plasmid RSF1010 inhibits *Agrobacterium tumefaciens* virulence and virB-dependent export of VirE2. *J Bacteriol* **180:** 3933-3939.

Steck, T.R., Close, T.J., and Kado, C.I. (1989) High levels of double-stranded transferred DNA (T-DNA) processing from an intact nopaline Ti plasmid. *Proc Natl Acad Sci USA* **86:** 2133-2137.

Sundberg, C., Meek, L., Carroll, K., Das, A., and Ream, W. (1996) VirE1 protein mediates export of the single-stranded DNA binding protein VirE2 from *Agrobacterium tumefaciens* into plant cells. *J Bacteriol* **178:** 1207-1212.

Sundberg, C.D., and Ream, W. (1999) The *Agrobacterium tumefaciens* chaperone-like protein, VirE1, interacts with VirE2 at domains required for single-stranded DNA binding and cooperative interaction. *J Bacteriol* **181:** 6850-6855.

Swart, S., Logman, T.J., Smit, G., Lugtenberg, B.J., and Kijne, J.W. (1994) Purification and partial characterization of a glycoprotein from pea (*Pisum sativum*) with receptor activity for rhicadhesin, an attachment protein of *Rhizobiaceae*. *Plant Mol Biol* **24:** 171-183.

Thomashow, M.F., Karlinsey, J.E., Marks, J.R., and Hurlbert, R.E. (1987) Identification of a new virulence locus in *Agrobacterium tumefaciens* that affects polysaccharide composition and plant cell attachment. *J Bacteriol* **169:** 3209-3216.

Tinland, B., Koukolikova-Nicola, Z., Hall, M.N., and Hohn, B. (1992) The T-DNA-linked VirD2 protein contains two distinct functional nuclear localization signals. *Proc Natl Acad Sci USA* **89:** 7442-7446.

Tinland, B., Schoumacher, F., Gloeckler, V., Bravo-Angel, A.M., and Hohn, B. (1995) The *Agrobacterium tumefaciens* virulence D2 protein is responsible for precise

integration of T-DNA into the plant genome. *EMBO J* **14:** 3585-3595.

Toro, N., Datta, A., Carmi, O.A., Young, C., Prusti, R.K., and Nester, E.W. (1989) The *Agrobacterium tumefaciens virC1* gene product binds to overdrive, a T-DNA transfer enhancer. *J Bacteriol* **171:** 6845-6849.

Turk, S.C.H.J., Van Lange, R.P., Regensburg-Tuink, Tonny, J.G., and Hooykaas, P.J.J. (1994) Localization of the VirA domain involved in acetosyringone-mediated *vir* gene induction in *Agrobacterium tumefaciens*. *Plant Mol Biol* **25:** 899-907.

Tzfira, T., and Citovsky, V. (2000) From host recognition to T-DNA integration: function of bacterial and plant genes in the *Agrobacterium*-plant cell interaction. *Mol Plant Pathol* **1:** 201-212.

Tzfira, T., and Citovsky, V. (2002) Partners-in-infection: host proteins involved in the transformation of plant cells by *Agrobacterium*. *TRENDS in Cell Biology* **12:** 121-129.

Tzfira, T., Vaidya, M., and Citovsky, V. (2001) VIP1, an *Arabidopsis* protein that interacts with *Agrobacterium* VirE2, is involved in VirE2 nuclear import and *Agrobacterium* infectivity. *EMBO J* **20:** 3596-3607.

Tzfira, T., Vaidya, M., and Citovsky, V. (2002) Increasing plant susceptibility to *Agrobacterium* infection by overexpression of the *Arabidopsis* nuclear protein VIP1. *Proc Natl Acad Sci USA* **99:** 10435-10440.

Van Larebeke, N., Enbler, G., Holsters, M., Van Den Elsacker, S., Zaenen, I., Schilperoort, R.A., and Schell. J. (1974) Large plasmid in *Agrobacterium tumefaciens* essential for crown gall-inducing ability. *Nature* **252:** 169-170.

Vanlentine, L. (2003) *Agrobacterium tumefaciens* and the plant: the David and Goliath of modern genetics. *Plant Physiol* **133:** 948-955.

Veluthambi, K., Jayaswal, R.K., and Gelvin, S.B. (1987) Virulence genes A, G, and D mediate the double stranded border cleavage of T-DNA from the *Agrobacterium* Ti plasmid. *Proc Natl Acad Sci USA* **84:** 1881-1885.

Veluthambi, K., Ream, W., and Gelvin, S.B. (1988) Virulence genes, borders, and overdrive generate single-stranded T-DNA molecules from the A6 Ti plasmid of

Agrobacterium tumefaciens. *J Bacteriol* **170:** 1523-1532.

Vergunst, A.C., Lier, M.C.M., Dulk-Ras, A.D., and Hooykaas P.J.J. (2003) Recognition of the *Agrobacterium tumefaciens* VirE2 translocation signal by the VirB/D4 transport system does not require VirE1. *Plant Physiol* **133:** 978-988.

Vergunst, A.C., Lier, M.C.M., Dulk-Ras, A.D., Stuve, T.A.G., Ouwehand, A., and Hooykaas P.J.J. (2005) Positive charge is an important feature of the C-terminal transport signal of the VirB/D4-translocated proteins of *Agrobacterium*. *Proc Natl Acad Sci USA* **102:** 832-837.

Vergunst, A.C., Schrammeijer, B., Dulk-Ras, A., Vlaam, C.M.T., Regensburg-Tuink, T.J.G., and Hooykaas, P.J.J. (2000) VirB/D4-dependent protein translocation from *Agrobacterium* into plant cells. *Science* **290:** 979-982.

Vogel, A.M., and Das, A. (1992) Mutational analysis of *Agrobacterium tumefaciens* VirD2: tyrosine 29 is essential for endonuclease activity. *J Bacteriol* **174:**303-308.

Vogel, A.M., and Das, A. (1994) Mutational analysis of *Agrobacterium tumefaciens* pTiA6 *virD1*: identification of functionally important residues. *Mol Microbiol* **12:** 811-817.

Vogel, A.M., Yoon, J., and Das, A. (1995) Mutational analysis of a conserved motif of *Agrobacterium tumefaciens* VirD2. *Nucleic Acids Res* **23:** 4087-4091.

Wagner, V.T., and Matthysse, A.G. (1992) Involvement of a vitronectin-like protein in attachment of *Agrobacterium tumefaciens* to carrot suspension culture cells. *J Bacteriol* **174:** 5999-6003.

Wang, K., Genetello, C., Van Montagu, M., and Zambryski, P. (1987) Sequence context of the T-DNA border repeat element determines its relative activity during T-DNA transfer to plant cells. *Mol Gen Genet* **210:** 338-346.

Wang, K., Herrera-Estrella, A., and Van Montagu, M. (1990) Overexpression of *virD1* and *virD2* genes in *Agrobacterium tumefaciens* enhances T-complex formation and plant transformation. *J Bacteriol* **172:** 4432-4440.

Wang, K., Herrera-Estrella, L., Van Montagu, M., and Zambryski, P. (1984) Right 25 bp

terminus sequences of the nopaline T-DNA is essential for and determines direction of DNA transfer from *Agrobacterium* to the plant genome. *Cell* **38:** 35-41.

Wang, K., Stachel, S.E., Timmerman, B., Van Montagu, M., and Zambryski, P. (1987b) Site-specific nick in the T-DNA border sequence as a result of *Agrobacterium vir* gene expression. *Science* **235:** 587-591.

Ward, D.V., Draper, O., Zupan, J.R., and Zambryski, P.C. (2002) Peptide linkage mapping of the *Agrobacterium tumefaciens vir*-encoded type IV secretion system reveals protein subassemblies. *Proc Natl Acad Sci USA* **99:** 11493-11500.

Wattiau, P., Woestyn, S., and Corenelis, G.R. (1996) Customized secretion chaperones in pathogenic bacteria. *Mol Microbiol* **20:** 255-262.

Watt, V.M., Ingles, C.J., Urdea, M.S., Rutter, W.J. (1985) Homology requirements for recombination in *Escherichia coli*. *Proc Natl Acad Sci USA* **82:** 4768-4772.

White, P.R., and Braun, A.C. (1941) Crown gall production by bacteria-free tumor tissues. *Science* **94:** 239-241.

Winans, S.P. (1992) Two-way chemical signaling in Agrobacterium-plant interactions. *Microbiol Rev* **56:** 12-31.

Wood, D.W., Setubal, J.C., Kaul, R., Monks, D.E., Kitajima, J.P., Okura, V.K., Zhou, Y., Chen, L. *et al*. (2001) The genome of the natural genetic engineer *Agrobacterium tumefaciens* C58. *Science* **294:** 2317-2323.

Xiang, C., Han, P., Lutziger, I., Wang, K., and Oliver, D.J. (1999) A mini binary vector series for plant transformation. *Plant Mol Biol* **40:** 711-717.

Xu, X.Q., Li, L.P., and Pan, S.Q. (2001) Feedback regulation of an *Agrobacterium* catalase gene *katA* involved in *Agrobacterium*-plant interaction. *Molecular Microbiology* **42:** 645-657.

Yanofsky, M.F., Porter, S.G., Young, C., Albright, L.M., Gordon, M.P., and Nester, E.W. (1986) The *virD* operon of *Agrobacterium tumefaciens* encodes a site-specific endonuclease. *Cell* **47:** 471-477.

Yusibov, V.M., Steck, T.R., Gupta, V., and Gelvin, S.B. (1994) Association of single-

stranded transferred DNA from *Agrobacterium tumefaciens* with tobacco cells. *Proc Natl Acad Sci USA* **91:** 2994-2998.

Zaenen, I., Van Larebeke, N., Teuchy, H., Van Montagu, M., and Schell, J. (1974) Supercoiled circular DNA in crown-gall inducing *Agrobacterium* strains. *J Mol Biol* **86:** 109-127.

Zambryski, P. (1992) Chronicles from the *Agrobacterium*-plant cell DNA transfer story. *Annu Rev Plant Phys Plant Mol Biol* **43:** 465-490.

Zambryski, P., Joos, P.H., Genetello, C., Leemans, J., Van Montagu, M., and Schell, J. (1983) Ti plasmid vector for the intriduction of DNA into plant cells without alteration of their normal regeneration capacity. *EMBO J* **2:** 2143-2150.

Zhao, Z.M., Sagulenko, E., Ding, Z.Y., Christie P.J. (2001) Activities of *virE1* and the VirE1 secretion chaperone in export of the multifunctional VirE2 effector via an *Agrobacterium* type IV secretion pathway. *J Bacteriol* **183:** 3855-3865.

Zhu, J., Oger, P.M., Schrammeijer, B., Hooykaas, P.J.J., Farrand, S.K., and Winans, S.C. (2000) The bases of crown gall tumorigenesis. *J Bacteriol* **182:** 3885-3895.

Zhu, Y., Nam, J., Humara, J.M., Mysore, K.S., Lee, L.Y., Cao, H., Valentine, L., Li, J., Kaiser, A.D., and Kopecky, A.L., *et al*. (2003) Identification of *Arabidopsis rat* mutants. *Plant Physiol* **132:** 494-505.

Ziemienowicz, A. (2001) Odyssey of *Agrobacterium* T-DNA. *Acta Biochimica Polonica* **48:** 623-635.

Ziemienowicz, A., Gorlich, D., Lanka, E., Hohn, B., and Rossi, L. (1999) Import of DNA into mammalian nuclei by proteins originating from a plant pathogenic bacterium. *Proc Natl Acad Sci USA* **96:** 3729-3733.

Ziemienowicz, A., Merkle, T., Schoumacher, F., Hohn, B., and Rossi, L. (2001) Import of *Agrobacterium* T-DNA into plant nuclei: two distinct functions of VirD2 and VirE2 proteins. *The Plant Cell* **13:** 369-383.

Zorreguieta, A., and Ugalde, R.A. (1986) Formation in *Rhizobium* and *Agrobacterium* spp. of a 235-kilodalton protein intermediate in β-D-(1-2)glucan synthesis. *J Bacteriol*

167: 947-951.

Zupan, J., Muth, T.R., Draper, O., and Zambryski, P. (2000) The transfer of DNA from *Agrobacterium tumefaciens* into plants: a feast of fundamental insights. *The Plant Journal* **23:** 11-28.

Zupan, J., and Zambryski, P. (1995) Transfer of T-DNA from *agrobacterium* to plant cell. *Plant Physiol* **107:** 1041-1047.

Zupan, J., and Zambryski, P. (1997) The *Agrobacterium* DNA transfer complex. *Critical Reviews in Plant Sciences* **16:** 279-295.